Physiological Role of Prolylcarboxypeptidase

Dissertation

zur Erlangung des akademischen Grades
doctor rerum naturalium
(Dr. rer. nat.)

eingereicht an der
Mathematisch-Naturwissenschaftlichen Fakultät I
Humboldt-Universität zu Berlin

von
Dipl. Biologin **Ines Claudia Schadock**

Präsident der Humboldt-Universität zu Berlin:
Prof. Dr. Jan-Hendrik Olbertz
Dekan der Mathematisch-Naturwissenschaftlichen Fakultät I :
Prof. Dr. Andreas Herrmann

Gutachter/in: 1. Prof. Dr. rer. nat. Michael Bader

2. Prof. Dr. rer. nat. Nobert Hübner

3. Prof. Dr. rer. nat. Achim Leutz

Datum der mündlichen Prüfung: 20.06.2011

ABSTRACT

Prolylcarboxypeptidase (PRCP, EC3.4.16.2) is an enzyme specifically cleaving the last carboxy-terminal amino acid from substrates containing a penultimate proline. Its known potential substrates are linked to cardiovascular and metabolic phenomenon. To analyse the *in vivo* function of this enzyme a PRCP knockout mouse was generated. Homozygous knockout mice are viable but show tendency of decreased life span. In mice *prcp* expression is present in all tissues tested with very specific localizations of *prcp* promotor activity to distinct brain areas within the cortex, hippocampus, hypothalamus and the brain stem.

The metabolic phenotype of PRCP deficient mice is characterized by low body weight even when feeding the animals a high fat diet. The increased plasma leptin levels and elevated expression of proopiomelanocortin gene (*pomc*) found in knockout hypothalami suggests an involvement of PRCP in the regulation of food intake and energy homeostasis. One of the gene products of *pomc* is α-melanocortin stimulating hormone that is terminating feeding when released from hypothalamic POMC neurons. Its carboxy-terminal structure is fitting the cleavage preferences of PRCP. *Prcp* promotor activities are localized in arcuate nucleus and paraventricular nucleus, brain areas of known αMSH signalling, supporting a role of PRCP in the degradation of central αMSH.

The impact of PRCP on angiotensin II (AngII) metabolism was studied by determining the level of AngII and its degradation product Ang1-7 in blood and tissues. But instead of increased AngII levels due to the missing degradation enzyme in knockout mice, the breakdown product Ang1-7 was found increased in kidney and white adipose tissue. These results were explainable by the increased activity of angiotensin converting enzyme 2 (ACE2) found in kidney. Probably ACE2 is compensating the lack of PRCP in the knockout mouse. Nevertheless, blood pressure and heart rate of PRCP knockout mice was increased. The mild hypertension was accompanied by mild hypertrophy of the hearts. *Prcp* promotor activity was found in brain stem areas im-

portant for regulation of blood pressure and heart rate suggesting that central PRCP regulates blood pressure.

Keywords:

prolylcarboxypeptidase, angiotensin II, alpha-melanocortin stimulating hormone, hypertension, obesity

ZUSAMMENFASSUNG

Die Namen-gebende Hauptcharakteristik von Prolylcarboxypeptidase (PRCP, EC3.4.16.2) ist spezifisch die letzte carboxyterminale Aminosäure von Substraten abzuspalten, deren vorletzte Aminosäure ein Prolin ist. Seine bisher publizierten Substrate Angiotensin II (AngII) und α-Melanocortin Stimulierendes Hormone (αMSH) legen eine Rolle von PRCP in der Entwicklung von kardiovaskulären und metabolischen Krankheiten nahe. Um die in vivo Funktion von PRCP zu studieren, wurde eine Knockout Maus generiert. Die homozygoten Tiere dieser Linie zeigten von Geburt an keine offensichtlichen Beeinträchtigungen. Allerdings beschreibt eine Langzeitstudie der Tiere eine Tendenz verkürzter Lebenserwartung im Vergleich zu Kontrolltieren. Die Expression von *prcp* in der Maus ist in allen getesteten Organen vorhanden, wobei die höchste Expression im Gehirn gefunden wurde. Hier wurde zudem *prcp* Promotoraktivität in eng begrenzten Bereichen von Cortex, Hippocampus, Hypothalamus und Hirnstamm lokalisiert.

PRCP Knockoutmäuse wiesen generell ein reduziertes Körpergewicht auf, selbst wenn sie über Monate mit einer Hochfettdiät versorgt wurden. Erhöhte Plasmaleptin Werte und Proopiomelanocortin (*pomc*) Expression in knockout Hypothalami wiesen auf eine wichtige Rolle von PRCP in der Regulation von Futteraufnahme und Energiehomöostase hin. Eines der Genprodukte von *pomc* ist αMSH, welches bei Freisetzung im Hypothalamus die Futteraufnahme terminiert. Die carboxyterminale Struktur dieses Neuropeptids erfüllt alle Voraussetzungen, um von PRCP gespalten zu werden. Zudem konnte *prcp* Promotoraktivität in den selben Hirnstrukturen gezeigt werden, in denen auch αMSH-Wirkung beschrieben wurde. Eine mögliche Funktion von PRCP wäre somit die Inaktivierung des Appetitzüglers αMSH im Hypothalamus.

Der Einfluß von PRCP auf den AngII Metabolismus, sollte durch Analyse von Peptidkonzentrationen ermittelt werden. Dabei stellte sich heraus, daß AngII Werte in PRCP Knockoutmäusen unverändert waren. Hingegen konnten paradoxerweise erhöhte Niveaus des Degradationsproduktes Ang1-7 in Niere und weißem Fettgewebe gezeigt werden. Die Entdeckung einer erhöhten Enzymaktivität von Angiotensin Converting

Enzyme 2 (ACE2) in Knockout Nieren, bot einen Erklärungsansatz für diese Ergebnisse. Es wird davon ausgegangen, daß ACE2 die fehlende PRCP Aktivität in knockout Mäusen kompensiert. Trotzdem sind Blutdruck und Herzrate in PRCP Knockoutmäusen erhöht. Die milde Hypertension resultiert zusätzlich in einer leichten Herzhypertrophie. Da die spezifische *prcp* Promotoraktivität in Hirnnuclei gefunden wurde, die in die Kontrolle der Herzfrequenz und des Blutdrucks involviert sind, wird eine regulatorische Funktion von Hirnstamm-PRCP auf Herzrhytmus und Blutdruck vermutet.

Schlagwörter:

Prolylcarboxypeptidase, Angiotensin II, alpha-Melanocortin Stimmulierendes Hormon, Hypertension, Obesitas

ACKNOWLEDGEMENT

Mein besonderer Dank gilt Prof. Michael Bader für die Möglichkeit, dieses Thema zu bearbeiten, die stets ausgezeichnete Betreuung meiner Arbeit und für die erstklassigen Arbeitsbedingungen in seinem Labor. Dank seiner konstruktiven Kritik und Anregung war die Anfertigung dieser Arbeit erst möglich.

Für die Möglichkeit, mein Methodenspektrum zu erweitern und etablierte Versuchsanordnungen nutzen zu können, möchte ich mich bei Prof. R.A.S. Santos (Peptidmessungen, UFMG, Belo Horizonte, Brasilien), Dr. W.E. Siems (ACE2 und NEP Enzymaktivitätsbestimmungen, FMP, Berlin), Prof. G. Lewin (Aktivitätsmessung von Mäusen, MDC, Berlin) sowie Dr. Arndt Heuser und Martin Taube (Echokardiographie und Kleintier Körperkompositions Scan, MDC, Berlin) bedanken.

Ein großes Dankeschön gilt meinen Arbeitskollegen der AG Bader. Namentlich erwähnen möchte ich Sabine Grüger und Manfred Ströhmann für die tatkräftige Unterstützung im Tierhaus; Andrea Müller, Susanne de Costa Goncalves, Anne Köhn und Sonja Kumsteller, die den Laboralltag so reibungslos organisieren, dass man jederzeit gern dort arbeitet; Natalia Alenina, Fatimunissa Qadri (alias Sayeeda), Mihail Todiras, Ralf Plehm und Irina Lapidous, die mir mit Rat und Tat zu wissenschaftlichen Methodiken den Rücken gestärkt haben.

Bei meiner Familie und bei meinen Freunden möchte ich mich für das große Verständnis und die immerwährende Unterstützung bedanken, auch wenn sie viel auf meine Person verzichten mußten.

CONTENT

LIST OF FIGURES

LIST OF TABLES

1 INTRODUCTION

1.1 What is Prolylcarboxypeptidase?

In 1968 Erdös and coworkers discovered that the carboxy-terminal bond between proline (Pro) and phenylalanine (Phe) of des-Arg9-Bradykinin, which is usually resistant to carboxypeptidases, was cleaved by a kidney extract. Because angiotensin II (AngII) has the same carboxy-terminal structure (-Pro-Phe) it was tested and found to be a substrate of the same enzyme, which was initially named angiotensinase C [1]. Showing, that the enzyme cleaves a variety of -Pro-X bonds led to its renaming into prolylcarboxypeptidase (PRCP, EC.3.4.16.2; [2]).

Comparing the sequence around the putative active residue of enzymes indicates that PRCP is related to both the serine carboxypeptidase and prolylendopeptidase families of serine proteases. Although cDNA has low sequence identity to other enzymes, 114 residues in the active-site region of the protein show highest similarity with human deamidase (*ctsa*) and human prolylendopeptidase (*prep*) [3]. The human as well as the mouse gene encompass nine exons with the 5'end of the first exon encoding the signal peptide and a propeptide region. Exon 4 to 9 encode the catalytic domain of the molecule [4].

Given its main characteristic to cleave small peptides only when the penultimate residue is a proline, PRCP is one of ten known enzymes that are able to cleave a proline bond [5]. Proline, the only mammalian imino acid, is believed to be important in the process of protein folding. Unlike other amino acids, proline can introduce structural heterogeneity, since the X-Pro bond can adapt either the stereoisomeric cis or trans conformation [6]. Up to date many peptides are known that achieve physiological activity when being transformed into a particular three-dimensional structure. Additionally, the presence of proline was published to hinder non-specific proteolytic degradation [7] but also serves as recognition site for peptidases with restricted specificity to proline-containing substrates like PRCP and prolylendopeptidase [8].

Moreover, PRCP has an acidic pH optimum (≈5.0) when hydrolysing short synthetic peptide substrates [3,9], but also retain significant activity in the neutral range with longer naturally occurring peptides [10]. Besides pH optimum and peptide length, experiments with purified PRCP from human kidneys revealed preferences for aliphatic amino acids to be removed by the enzyme. Alanine and valine were cleaved with approximately 4 and 3-fold higher efficiency then phenylalanine, the amino acid present in des-Arg9-bradykinin and AngII. Then again glycine showed only 6% of the hydrolysation rate seen with phenylalanine [9].

Recently the crystal structure of human PRCP was clarified shedding light on cleaving specificity of the enzyme. Consistent with the biochemical properties of PRCP in solution a dimerization interface was observed [11]. The arrangement of the catalytic triad of amino acids in the active site (Ser179, Asp430 and His455) was identified as a classical constellation seen in other serine α/β hydrolases [12]. Unique for PRCP, an apparent charge-relay system within the active site of the enzyme was described. The authors suggest this structure to explain the acidic pH optimum of PRCP [13].

Next to des-Arg9-bradykinin and AngII, more substrates fitting the cleavage characteristic of PRCP are discussed today. An overview of already published and possible substrates is given in Table 1.In 1978 it was speculated that lysosomal PRCP could be responsible for intracellular cleavage of angiotensin III (AngIII), regulating angiotensin levels in kidney and elsewhere [9]. 2002 Schmaier and colleagues presented PRCP as the prekallikrein activator initiating the cascade to liberate bradykinin from its precursor high molecular weight kininogen [14]. Interactions of the renin angiotensin system with the kallikrein kinin system are diverse, wherefore research in actions of PRCP was focused for years on these topics (reviewed in [15]). However, recently the peptide hormone alpha melanocortin stimulating hormone (αMSH) was added to the list of PRCP's substrates [16] and will be further introduced in chapter 1.2.

Table 1: Potential PRCP substrates.

potential substrate	*gene*	aa	aa - COOH
angiotensin II	*agt*	8	DRVYIHPF
apelin 13	*apel*	13	QRPRLSHKGPMPF
agouti related peptide (N-terminal splice product)	*agrp*	44	-PEFPG
des-Arg9-bradykinin	*kng1*	8	RPPGFSPF
ghrelin (growth hormone releasing peptide)	*ghrl*	28	-KESKKPPAKLQPR
gonadoliberin (lhrh)	*gnrh1*	10	HWSYGLRPG
a-melanocortin stimulating hormone	*pomc*	13	SYSMEHFRWGKPV
neuropeptide EI	*pmch*	13	EIGDEENSAKFPI
a neoendorphin	*pdyn*	10	YGGFLRKYPK

PRCP was found in a variety of organs with highest expression in human placenta, lung and liver [3], but also in different cell types like leucocytes (Kumamoto et al. 19981), fibroblasts [17] and alveolar macrophages [18]. And even in body fluids like urine [19], synovial fluid [20] and thoracic lymph [9] it is present. In cell culture the highest expression was found in human umbilical vein endothelial cells (HUVEC; [17,20]). The sub cellular localization of the enzyme was reported in lysosomes, but also extracellular as a result from lysosome fusion with the cell membranes [20]. The discovery of PRCP on the cell surface of macrophages was followed by a detailed description of PRCP co-localization with cytokeratin 1, urokinase plasminogen activator receptor, gC1qR, and lysosomal associated membrane protein 1 [10,21].

Due to its properties to cleave AngII different studies consider PRCP as candidate gene for essential hypertension [22,23]. Cleaving AngII, PRCP turns the ligand for angiotensin receptor 1 (AT1) into Ang1-7, the ligand activating Mas [24]. Mas is thought to oppose most of the actions of AT1 initiating nitric oxide and prostaglandin generation [25]. Data about other enzymes able to cleave AngII like angiotensin converting enzyme 2 (ACE2), do not necessarily negate the role of PRCP as an additional switch that transforms Ang II from a vasoconstrictor to a vasodilator [4]. As the AngII metabolism is one of the topics this study is focusing on, chapter 2.2 gives an overview about the renin angiotensin system.

Several authors also proposed that PRCP might be a risk factor for inflammation, suggesting it is a prerequisite for healing and scar formation [26]. Evidences were pub-

lished specifically associating PRCP with rheumatoid arthritis and tonsillitis [20,27]. The link how PRCP might be involved in inflammation processes is the kallikrein kinin system (KKS). PRCP is believed to activate prekallikrein, therefore starting the cascade to liberate bradykinin [14,28]. Bradykinin binds to the constitutive bradykinin B2 receptor which leads to nitric oxide and PGI2 formation. Additionally, tissue plasminogen activator is released, which converts plasminogen to plasmin and therefore inhibits platelet aggregation, thrombus formation and promotes fibrinolysis [29]. Further confirming the involvement of PRCP in the KKS is that transfection of endothelial cells with an antisense oligonucleotide to PRCP blocks prekallikrein activation, whereas a sense oligonucleotide is ineffective [21]. Recently, the potential cleavage site on the C-terminus of prekallikrein has been reported [30]. Furthermore, PRCP is cleaving the kinin B1 receptor agonist des-Arg9-bradykinin, which additionally put the enzyme into an ideal position to modulate KKS activity [1].

1.2 Hormonal Control of Food Intake

Food intake and energy expenditure are complex mechanisms that are regulated by a number of hormones. Interestingly in the Table 1 of potential PRCP substrates there are three hormones known to play essential roles in metabolism. These are agouti related peptide (AGRP), ghrelin (GHRL) and alpha melanocortin stimulating hormone (αMSH). To construct a theory in which metabolic processes PRCP could be involved this chapter will give a short overview about the function of these three molecules.

Ghrelin (GHRL)

The name of the hormone ghrelin is an acronym generated from growth hormone release inducing (GHRL). The orexigenic 28 amino acid peptide is produced and secreted by enteroendocrine cells in the oxyntic glands of the stomach and upper intestine in response to negative energy balance [31]. Its G-protein coupled receptor growth hormone secretagogue receptor (GHSR) is highly expressed in the hypothalamus, mainly in the ARC but also in other brain regions like the VTA. In the arcuate nucleus of the hypothalamus (ARC) GHRL is believed to activate NPY/AGRP neurons while inhibiting the anorexigenic POMC neurons [32]. The concentration of the hormone secreted from the stomach into circulation is rising with the time passed since the last meal. Thus, stimulating NPY/AGRP neurons causes the liberation of NPY and AGRP to stimulate appetite (Figure 1).

The counter player of GHRL is leptin. Leptin is produced by adipocytes and is released into circulation in levels corresponding to the amount of adipocytes. A high level of plasma leptin stimulates POMC neurons, which are collocated with AGRP/NPY neurons in the same hypothalamic regions [33]. Activation of POMC neurons forces the liberation of αMSH into the synaptic cleft where AGRP and αMSH are competing for the same receptor binding sites at melanocortin receptor 3 and 4 (MC3R, MC4R). Leptin receptors have also been found on AGRP/NPY neurons suggesting an inhibitory effect on secretion of AGRP [34,35,36].

Along with leptins anorectic effects in the hypothalamus its pleiotropic actions include reproductive functions [37], regulation of the hypothalamic-pituitary-adrenal (HPA)-axis

[38], glucose and insulin metabolism (reviewed by [39]), as well as lipolysis [40], contribution to the sympathetic nerve activity [41], hematopoiesis [42], angiogenesis [43,44] and immune response [45].

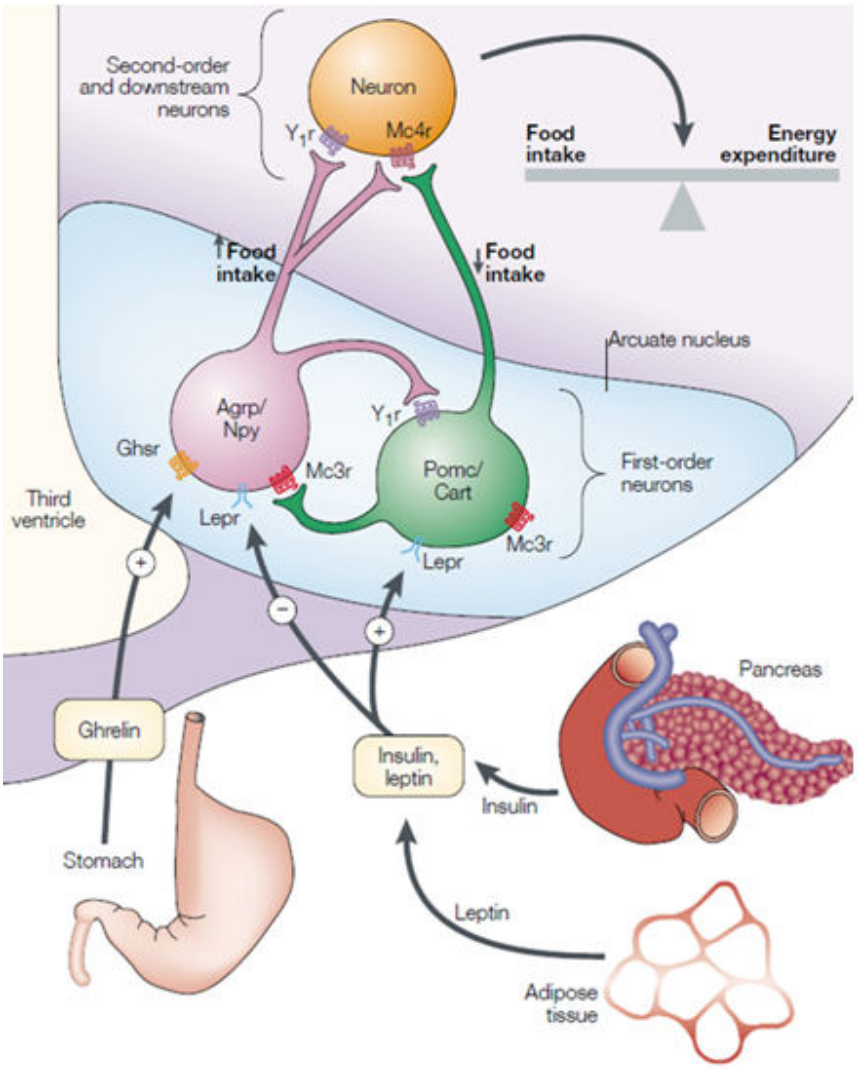

Figure 1: Control of energy homeostasis by arcuate nucleus (ARC) neurons.

Two sets of neurons in the ARC – AGRP/NPY and POMC/CART neurons – are regulated by circulating hormones. The neuropeptides AGRP and NPY stimulate food intake and energy expenditure, whereas αMSH (post-translational derivate of *pomc*) and CART are neuropeptides that inhibit food intake and increase energy expenditure. Insulin and leptin circulate in proportions to body adipose stores. They inhibit AGRP/NPY neurons and stimulate adjacent POMC/CART neurons. Lower insulin and leptin levels are predicted to activate AGRP/NPY neurons, while inhibiting POMC/CART neurons. The circulating peptide ghrelin is secreted from the stomach and can activate AGRP/NPY neurons and stimulate appetite. AGRP agouti related peptide, NPY neuropeptide Y, POMC proopiomelanocortin, CART cocaine- and amphetamine-regulated transcript, αMSH α-melanocortin stimulating hormone, Ghsr growth hormone secretagogue receptor, Lepr leptin receptor, MC3R / MC4R menalocortin ¾ receptor, Y_1r neuropeptide Y1 receptor [46].

Agouti related peptide (AGRP)

One of the oldest known genetic models of obesity is the agouti mouse. Overexpression of this peptide leads to a phenotype characterized by hyperphagia, hyperinsulinemia, hypometabolism and increased linear growth (reviewed by [47]). In 1997 a hypothalamic protein with high sequence homology was discovered by two scientific groups in parallel [48,49], suggesting an important role of this protein in the regulation of energy homeostasis (Figure 1).

Besides its production in hypothalamus, it was shown to a lower extent in peripherally organs like the adrenal gland, testis, kidney and lung [49]. Because of its specific synthesis only in neuropeptide Y (NPY) containing cells of the ventromedial part of the ARC within the hypothalamus these neurons got the name AGRP/NPY neurons. Following activation by GHRL, AGRP and NPY are released from intracellular secretory granules and function as appetite stimulators. Especially AGRP has been described as one of the most potent and long-lasting stimulators of appetite [50]. As an inverse agonist of αMSH AGRP blocks the melanocortin receptors MC3R and MC4R and therefore restrain αMSH signaling [48].

Reported circulating levels of AGRP described the protein as a biomarker for the transition between the fed and fasted state [51]. In both, a short term (2h) and a long-term fasting study (6d) plasma AGRP levels rose in human as well as in rodent [52,53]. In rodents, AGRP is normally suppressed by leptin, and the release of this suppression during fasting leads to an increase in AGRP mRNA in the hypothalamus and a resultant increase in food intake [54]. Similarly, AGRP mRNA has been shown to increase in the adrenal gland as a result of fasting in rodents [55], where leptin receptors have also been identified [56]. Therefore it was speculated that in response to fasting, falling leptin levels regulate AGRP secretion from either the hypothalamus or probably the adrenal gland and other organs [52]. Consequently, it was already hypothesized in the year 2004 that AGRP signaling from the periphery might regulate central control of energy balance [52]. In support of this, AGRP has been shown to cross the blood brain barrier into the brain [57]. The exact source of circulating AGRP and its function are to date still unknown.

α-Melanocortin Stimulating Hormone (αMSH)

To terminate feeding the action of the hormone αMSH in the hypothalamus is necessary. αMSH is one of the gene products of proopiomelanocortin (*pomc*). Therefore the neurons producing αMSH in the brain are called POMC neurons. The activation of these neurons is triggered by leptin and insulin binding to their receptors located at POMC neurons in the ARC. The subsequently released αMSH is able to bind to several melanocortin receptors in the brain with melanocortin receptor 3 (MCR3) and 4 (MCR4) being the specialized subtypes to translate a high αMSH signaling into sensation of satiety (Figure 1).

Genetic deletions of MC4R in human and mice results in severe hyperphagic obesity [58]. Up to 5% of cases of severe childhood obesity and between 0.5% and 2.5% of adult obesity can be lead back to MC4R mutations [59,60]. As the function of hypothalamic MC4R was related mainly to regulation of food intake [61] the role of MC3R next to MC4R is not completely understood yet. MC3R knockout mice exhibit a less dramatic phenotype than mice lacking MC4R, connecting MC3R to functions in feed efficiency (weight gain per kcal consumed) and partitioning of fuel stores into fat [58].

The signaling of the satiety hormone αMSH is an interplay with the neurotransmitter AGRP. As an inverse agonist specifically for MC3R and MC4R, AGRP is antagonizing the actions of αMSH. Thus, the balance between AGRP and αMSH in hypothalamus is critical to signal appetite or satiety. Increased AGRP levels shift the balance to robust appetite stimulation, whereas POMC neuron activation by high plasma leptin and insulin levels is inducing αMSH liberation from neuron terminals and in parallel inhibits AGRP/NPY neurons.

1.3 Renin Angiotensin System

The most important mechanisms to control arterial blood pressure as well as water and salt balance is the Renin Angiotensin System (RAS) [62]. This system is composed of the active angiotensin peptides and their receptors. Figure 2A is illustrating the classical so called 'circulating RAS' in which angiotensin I (AngI) is the first peptide released from its precursor angiotensinogen (AGT) by the action of renin. Once present in the blood AngI is rapidly converted by angiotensin converting enzyme (ACE) to angiotensin II (AngII). As described by Guyton and Hall, AngII is a powerful vasoconstrictor that in as little as 1 millionth of a gram can increase the arterial pressure of a human being 50 mmHg or more [63].

AngII then is activating its G-protein coupled receptors angiotensin receptor type 1 (AT1) and type 2 (AT2) in the vasculature and peripheral organs. Most of its effects AngII produces when binding to the AT1. In rat and mice two AT1 receptor subtypes are known, the AT1a and AT1b [64,65,66]. Derived from two different genes (*agt1ra* and *agt1rb*) the receptors are pharmacologically identical but they differ in their distribution and expression patterns. While At1a is the most prominent receptor in most organs, At1b is mainly produced in adrenal gland and hypophysis [67,68]. AngII stimulated AT1 activation leads to vasoconstriction, to aldosterone and adrenaline liberation in the adrenal gland and vasopressin release in the hypophysis [69]. In the kidney AT1 actions lead to sodium and water retention and a decrease in glomerular filtration rate.

AngII binding to AT2 was shown to produce opposing effects to that mediated by AT1. AT2 activation induces vasodilation, cell apoptosis and natriuresis, mediated by stimulation of bradykinin, nitric oxide and cyclic guanosinemonophosphate [68,70].

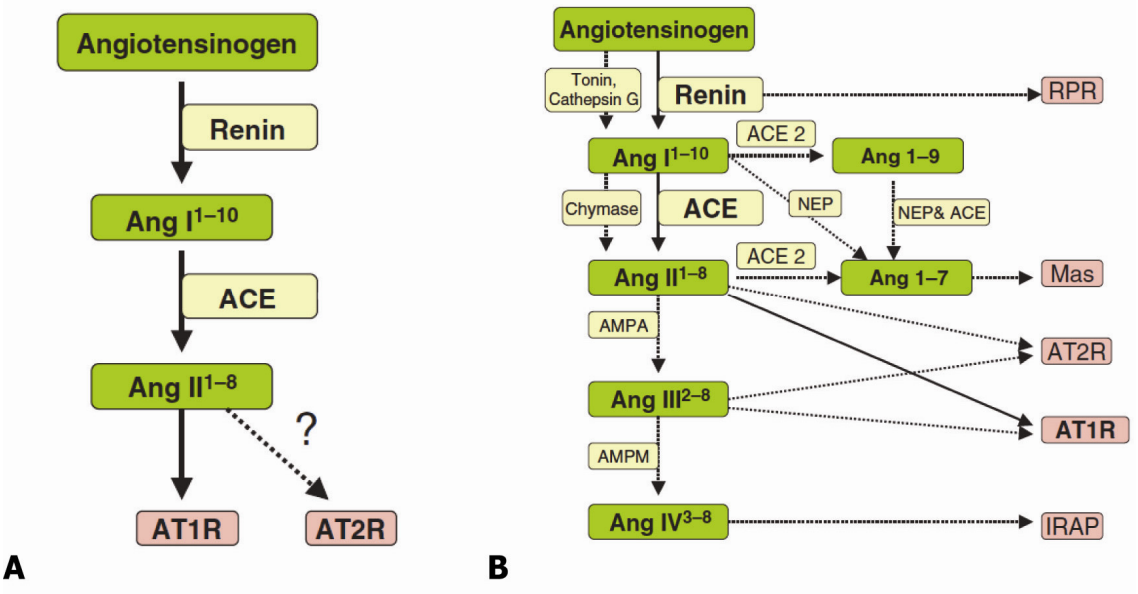

Figure 2: Scheme of the Renin Angiotensin System (RAS).
A The classic 'circulating RAS' and **B** local 'tissue RAS' [71].

After decades of studying this system, more components have been discovered expanding the view of RAS. Today it is known that there is also a local 'tissue RAS' in most organs (Figure 2B) In fact, even intracellular generation of AngII has been reported but will not be in focus of this introduction [72].

Next to the circulating RAS controlling the acute hemodynamic stability, the local tissue RAS seems to be important for sub acute and chronic modulation of hemodynamics [73]. The existence of individually functioning local RAS in different organs was reported already for the heart, brain, kidney and vessels. In this case locally produced AngII directly influences cell proliferation and differentiation, acting on cells in a paracrine as well as in a autocrine way. Furthermore, the way of AngII signalling in the brain was recently suggested to be that of a neurotransmitter [74].

When the AngII degradation peptides angiotensin2-8 (AngIII), angiotensin3-8 (AngIV) and angiotensin1-7 (Ang1-7) were shown to be biologically active molecules, the search for the corresponding receptors started [75]. Following, the Mas oncogene (Mas) as receptor for Ang1-7 [24] and the insulin-regulated aminopeptidase receptors (IRAP) binding AngIV [76,77] were described.

A special interest in the heptapeptide Ang1-7 rose when additionally to its suggested receptor, angiotensin converting enzyme 2 (ACE2) was recognized to be the major enzyme responsible for generating Ang1-7 from AngII [78]. It seems that Ang1-7 is opposing the cardiovascular effects of AngII, leading to vasodilation [79,80,81]. Alternative ways of producing Ang1-7 are the enzymes PRCP degrading AngII, and neutral endopeptidase (NEP) and prolylendopeptidase (PEP) generating the heptapeptide from AngI [82,83].

Ang III has been known since the 1970s. It is generated by the action of aminopeptidase A from AngII and causes vasoconstriction and release of aldosterone. Exerting its action via AT1 and AT2, it principally works similar to Ang II. Even though it was suggested that AngIII may be equally or even more important in some actions mediated by AT1 receptors [84], Ang II is still considered the main effector of RAS. Finally, the metabolic clearance rate of AngIII was five times that of AngII [85], indicating that AngII plays a dominant role as an effector of the classical 'circulating RAS' [71].

2 AIMS OF THE STUDY

During the last years prolylcarboxypeptidase (PRCP) attracted attention when it was discovered that its action on plasma prekallikrein is pivotal to initiate the liberation of bradykinin. The role of other potential PRCP substrates, like des-Arg9-bradykinin and AngII have not been explored extensively, even though the described cleavage characteristics of the enzyme predicted even more possible substrates.

This study aimed to investigate the physiological role of PRCP using a PRCP knockout mouse. To this purpose, a homozygous PRCP-/- line on pure genetic background has to be established and characterized. This line should also allow the localization of PRCP in mouse tissues. In order to limit the broad spectrum of potential substrates, this study concentrates on peptides involved in the control of energy homeostasis and on the regulation of blood pressure.

As potential PRCP substrates creating a possible body weight phenotype ghrelin, agouti related peptide and α melanocortin stimulating hormone were chosen. Methods to determine protein content and mRNA levels of the three candidate peptides should be applied. The body weight of homozygous PRCP-/- mice should be monitored while feeding the animals standard chow and high fat diet. Additionally, MRT-based body composition scans should be used to show the distribution of fat, water and lean mass in the knockout mouse.

The importance of PRCP in cleaving AngII should be further established by measuring angiotensin peptides in PRCP-/- tissues and blood, and measurements of blood pressure and heart rate. The in vitro analysis of RAS components like AT1, Mas and ACE2 should give further evidence about the mechanisms by which PRCP participates in the control of blood pressure.

3 MATERIAL & METHODS

3.1 Chemicals

Table 2: List of used chemicals.

Chemicals	Producer and Location
Acetic Acid	Roth, Karlsruhe
ACN (acetonitril)	Roth, Karlsruhe
Acrylamid/Bisacrylamid 19:1	Roth, Karlsruhe
Acrylamid-/Bisacrylamid 37,5:1	Roth, Karlsruhe
Agarose	Sigma, Gibco
Ampicillin	Serva, Heidelberg
Angiotensin I and II	Bachem, Weil am Rhein
AngI and AngII tracer	NEN
Aprotinin	Phoenix Pharmaceuticals. Inc. Burlingame, USA
APS (ammoniumperoxydisulfate)	Sigma, Steinheim
Bactoagar	Difco Microbiology
Bactotrypton	Difco Microbiology
Bestatin	Sigma, Steinheim
Boric Acid	Sigma, Steinheim
Bradford Reagent	Sigma, Steinheim
Bradykinin	Bachem, Weil am Rhein
Brij-35	Sigma, Steinheim
Bromphenoleblue	Sigma, Steinheim
BSA (bovine serum albumin)	Sigma, Steinheim
Buffer A and B	Phoenix Pharmaceuticals. Inc. Burlingame, USA
Chlorophorm	Roth, Karlsruhe
Coal Norit A	Serva, Heidelberg
Complete Protease Inhibitor Cocktail Tablets	Roche, Mannheim
C18-SEP columns	Phoenix Pharmaceuticals. Inc. Burlingame, USA
DALEK (D-Ala2,Leu5)-Enkephalin	Biosynthan, Berlin
DEPC	Serva, Heidelberg
Dextran T-70	Amersham Bioscience, NJ, USA
DMF (dimethylformamide)	Sigma, Steinheim
DMSO (dimethylsulfoxide)	Sigma, Steinheim
DNaseI	Boehringer Mannheim, Mannheim
dNTPs	Amersham Bioscience, NJ, USA
DTT	Sigma, Steinheim
EDTA	Sigma, Steinheim
Eosin-Y	Sigma, Steinheim
EGTA	Sigma, Steinheim
Ethanol	Roth, Karlsruhe
Ethidiumbromide	Sigma, Steinheim
Eukitt	O. Kindler GmbH & Co, Germany
$Fe(NH_4)_2(SO_4)_2$	Sigma, Steinheim
Glucose	Sigma, Steinheim
Glycerol	Roth, Karlruhe
Guanidinethiocyanate	Sigma, Steinheim
H_2O_2	Sigma, Steinheim
HCl	Roth, Karlruhe

Heparine	Sigma, Steinheim
HFBA (heptafluorobutyric acid)	Merck, Darmstadt
Histo-Clear	Roth, Karlruhe
p-hydroxymercuribenzoic acid	Sigma, Steinheim
Humalog Insulin	Lilly, USA
IGEPAL CA-630	Sigma, Steinheim
IPTG	Fermentas, Burlington, CDN
Insulin	Sigma, Steinheim
Isoflurane	Curamed Pharma, Darmstadt
Isopropanol	Roth, Karlsruhe
Kanamycin	Sigma, Steinheim
KCl	Sigma, Steinheim
Ketavet	Pharmazeutische Handelsgeselschaft, Grabsen
KH_2PO_4	Merck, Darmstadt
$K_3Fe(CN)_6$	Sigma, Steinheim
$K_4Fe(CN)_6$*$3H_2O$	Sigma, Steinheim
Lisinopril	Sigma, Steinheim
Mca-APK(Dnp)	Biosynthan, Berlin
Mca-AP	Biosynthan, Berlin
Methanol	Roth, Karlsruhe
2-Methylbutane	Roth, Karlsruhe
MES (2-Morpholinoethanesulfonic acid)	Sigma, Steinheim
$MgCl_2$	Merck, Darmstadt
Milk Powder	Roth, Karlruhe
Na_2HPO_4	Roth, Karlruhe
NaCl	Roth, Karlruhe
NaOH	Roth, Karlruhe
neomycin	Invitrogen, Darmstadt
NP-40 (Nonidet)	Sigma, Steinheim
NTPs	Promega, Madison, WI, USA
Paraffin	Roth, Karlruhe
Pepstatin A	Sigma, Steinheim
PFA (paraformaldehyde)	Roth, Karlruhe
pGEM®-Teasy	Promega, Madison, WI, USA
1,10-phenantroline monohydrate	Sigma, Steinheim
phenylmethanesulfonylfluorude	Sigma, Steinheim
Proteinase K	Merck, Darmstadt
Random Hexamer Primer	Boehringer, Mannheim
RIPA buffer	Pierce, Rockford, IL
Rompun	Bayer AG, Leverkusen
RNasin	Promega, Madison, WI, USA
Roti-Block	Roth, Karlruhe
Roti-HistolR	Roth, Karlruhe
Roti-Load	Roth, Karlruhe
Saccharose	Merck, Darmstadt
SDS (sodium dodecyl sulfate)	Serva, Heidelberg
TEMED (tetramethylethylendiamin)	Sigma, Steinheim
Tris	Roth, Karlruhe
Tissue-TekR OCT	Sakura, Japan
Triton X-100	Sigma, Steinheim
TRIZOL	Invitrogen, Darmstadt
Tween-20	Sigma, Steinheim
Urea	Sigma, Steinheim
[α-32P] UTP	PerkinElmer, Meriden, CT, USA
Vectashield	Vector Lab, Peterborough, UK
Xylol	Roth, Karlsruhe

X-Gal	Fermentas, St. Leon-Rot
$ZNSO_4$	Sigma, Steinheim
β-Mercaptoethanol	Sigma, Steinheim

3.2 Kits, Enzymes and Markers

Table 3: Used Kits, enzymes and Markers.

Components	Producer and Location
DekadeTM Marker System Kit	Ambion, Austin, TX, USA
DNA Polymerase kit (Cat. No. 10342-046)	Invitrogen, Darmstadt
DNaseI	Promega, Madison, WI, USA
ECL™ Western Blotting Analysis System	Promega, Madison, WI, USA
JetStar Plasmid Purification MAXI Kit 2.0 Restore	Genomed GmbH, Löhne
Mouse Adipokine Panel MADPK-71K	Millipore, Schwalbach/ Ts.
Mouse Ghrelin EIA kit	Phoenix Pharmaceuticals. Inc. Burlingame, USA
Mouse Leptin ELISA kit	RayBiotech, Inc., Norcross GA
Mouse αMSH EIA kit	Phoenix Pharmaceuticals. Inc. Burlingame, USA
M-MLV Reverse Transcriptase	Invitrogen, Darmstadt
Normal donkey serum	Merck, Darmstadt
Precision Blue Protein™ Standard All Blue	BioRad Laboratories Richmond, USA
Proteinase K	Invitrogen, Darmstadt
QIAquick® Gel Extraction Kit	Qiagen, Hilden
QuantiTect SYBR Green PCR Kit	Qiagen, Hilden
QuickSpin Columns for radiolabeled RNA	Roche, Mannheim
Restriction enzymes	New England Biolabs, Ipswich, MA
RNasin	Promega, Maddison, WI, USA
Roti-Block	Roth-Karlsruhe
Roti-Load	Roth-Karlsruhe
RPA II Kit Ambion	AMS Biotechnology, Whitney, UK
Saccharose	Merck, Darmstadt
S b PierceGE	GE Healthcare, Buckinghamshire, UK
SeeBlue®Plus2 Pre-stained Protein Standard	Invitrogen, Darmstadt
SP6-RNA-Polymerase	Promega, Madison, WI, USA
SuperSignaling® West Dura Extended Duration	Rockford, IL, USA
TaqDNA Polymerase	Invitrogen, Darmstadt
TM Plus Western Blot Stripping Buffer	Pierce, Rockford, IL, USA
T4-DNA-Ligase	Promega, Madison, WI, USA
T7-RNA-Polymerase	Promega, Madison, WI, USA
T3-RNA-Polymerase	Promega, Madison, WI, USA
Wizard® SV Gel and PCR Clean-up System	Roche, Mannheim
λ DNA/EcoRI + HindIII Marker, 3	Fermentas, St. Leon-Rot
Φ174 DNA/BsuRI (HaeIII) Marker, 9	Fermentas, St. Leon-Rot

3.3 Lab Instruments, Machines and other Material

Table 4: Labaratory instruments, machines and other material.

Instrument, machine, material	Producer and Location
Accu Check Sensor Comfort	Roche, Mannheim
Accu Check Sensor Comfort Stripes	Roche, Mannheim
Automatic Pipette Witoped XP Witeg	Labortechnik GmbH, Wertheim
Balance 440-43N	Kern & Sohn GmbH, Baldingen-Frommern
Benchtop 3.3 / Vacu-Freeze	VirTiz, New York, USA
Capacitance Extender	BioRad Laboratories Richmond, USA
Cell Culture Incubator Heracell	GFL, Hannover
Celluloseacetat Filter (0,2 µm(	Whatman® GmbH Schleicher & Schuel, Dassel
Centrifuge Sigma 3K12	Sigma, Osterode am Harz
Centrifuge Sorvall®PC5C Plus	Kendro, Hanau
Centrifuge Megafuge 1.0R	Heraeus Instuments GmbH, Düsseldorf
Centrifuge 5415D	Eppendorf, Hamburg
8-channel-Pipette M300	Biohit, Rosbach v. d. Höhe
Digital Balance	Sartorius Research, Göttingen
Electroporator 2510	Eppendorf, Hamburg
Falcon Tubes TPP®	Trasadingen, Schweiz
FastPrep®	MP Biomedicals, Illkrich, France
GenePulse® Kuvetts	BioRad Laboratories Richmond, USA
Gel Electrophoresis Chamber (vertical)	Biometra, Göttingen
Hybond™-ECL™ nitrocellulose membrane	Amersham Bioscience
iQ5 Cycler	BioRad Laboratories, München
Fujifilm LAS-1000/ Intelligent Dark Box	Fujifilm, Japan
Laminair®HB2448	Heraeus Instuments GmbH, Düsseldorf
Leica DMI 6000B Microscope	Leica, Wetzlar
Leica CM3050S Cryotom	Leica, Wetzlar
Liquid Scintillation Analyzer Tri-Carb 1900 TR	PerkinElmer, Meriden, CT, USA
Luminex 100/200™	Europe Luminex B.V., Oosterhout, NL
Magnetfish MR3001	Heidolph, Schwabach
MATRIX tubes	MP Biomedicals, Illkrich, France
Membran Vacuumpump	Vacumbrand GMBH+CO, Wertheim
Microfluor Mircotiter Plate (black)	Thermo Scientific, Langenselbold
Microplate Reader Infinite® M200	Tecan, Crailsheim
Microwave 8020	Privileg, Fürth
Menzel Gläser Superfrost Plus	Thermo Scientific, Waltham, USA
NanoDrop2000	Thermo Scientific, Waltham, USA
Odyssey®	Li-Cor Biosience GmbH, Bad Homburg
One-way Pipettes Discovery (2, 20, 200 µL)	Abimed, Langenfeld
Titer Plate Shaker Model 4625	LabLine Instuments, Mumbai, India
Vacuum Manifold (filtration unit)	Millipore, Schwalbach/ Ts.
Pasteur Pipettes	Roth, Karlsruhe
PCR Tubes	Biozym Scientific GmbH, Oldendorf
pH-Meter pH Level 1	WTW, Weilheim
Phosphoimager Fujix BAS2000	Fuji, Tokyo, Japan
Phosphoimagerplatte BAS-III	Fuji, Tokyo, Japan
Photometer GeneQuant pro	Amersham Bioscience, Little Chalfon, UK
Potter-ELVEHJEM	Kleinfeld Labortechnick
PVDF Membrane	Amersham Bioscience, Little Chalfon, UK
Roller Mixer SRT1	Snijders, Tilburg, NL

Power Supply PowerPac™HC	BioRad Laboratories Richmond, USA
PVDF membrane	GE Healthcare, Freiburg
Saldo Gel Dryer Model SE 1160	Hoefer Scientific Instruments, SF, USA
Save-Lock Tubes	Eppendorf, Hamburg
Scintillation counter LS600SC	Beckman, Minnesota, USA
SDS-PAGE Gel Electrophoresis Chamber	BioRad Laboratories Richmond, USA
Shaker Certomat®H B.	Braun, Melsungen
Sonificator Sonoplus	Bandelin electronic, Berlin
SpeedVac SVC100 x	Savant Instruments, Farmingdale, NY, USA
Tankblotter	BioRad Laboratories München
Thermocycler PTC-200	BioRad Laboratories München
Thermomixer 5436	Eppendorf, Hamburg
Transilluminator MultiImage™Light Cabinet	Alpha Innotech Corporation, CA, USA
Vortex Genic 2	Bender & Hobein AG, Zürich, SUI
Water Bath	GFL, Burgwedel
Whatman Paper	Whatman® International, Maidstone, UK
X-ray Retina Film	Fotochemische Werke GmbH, Berlin
X-Ray Film Processor AGFA CURIX 60	AGFA GEVAERT N.V., Mortsel, Belgium
1470 Wizard Automatic Gamma Counter	Wallac/Perkin Elmer, Massachusetts, USA

3.4 Antibodies

Table 5: List of primary and secondary antibodies.

Primery Antibody	Dilution	Blocking	Producer and Location
AT1 rabbit anti-mouse	1:500	Odyssey blocking buffer	Millipore, Schwalbach/ Ts.
ACE2 goat anti-human	1:500	Odyssey blocking buffer	R&D Systems, Wiesbaden-Nordenstadt
Mas rabbit anti-mouse	1:200	Odyssey blocking buffer	Alomone Labs, Jerusalem, Israel
αMSH rabbit anti-mouse	1:400	Normal donkey serum	Peninsula Labaratories, LLC, San Carlos, USA
T-15 goat anti-mouse	1:500 to 1:1000	chapter 3.6.3.4	Santa Cruz Biotechnology, Heidelberg, Germany
Y-15 goat anti-mouse	1:500 to 1:1000	chapter 3.6.3.4	Santa Cruz Biotechnology, Heidelberg, Germany

Secondary Antibody	Dilution	Blocking	Producer and Location
Goat anti-mouse	1:10,000	See primary antibodies	Licor Bioscience, Bad Homburg
Donkey anti-rabbit-Cy3	1:5000	1:400	Jackson Immuno, USA

3.5 Oligonucleotides

Oligonucleotides were purchased from BioTeZ GmbH (Berlin-Buch). The lyophilized primers were dissolved in ddH_2O to a concentration of 100 µM. These stock solutions were kept frozen at -20°C until usage, diluting them again to 5 µM working concentrations. The primers used for DNA genotyping, ribonuclease protection assay and quantitative real time PCR are listed in Table 6.

Table 6: Collection of mouse oligonucleotides used for genotyping PCR, primer walking, qPCR and RPA.

primer	**Sequence (5'-3')**	**Annealing temperature**	***gene,* method**
PRCP1 (10µM)	GTTCCCACTTCTAAGGAGG	60°C	*prcp*
PRCP2 (10µM)	GTGTCTCTGGTTTTATGTGAAG	60°C	primer waling
PRCP3 (10µM)	GTTGGCTACTGGTTTGCTG	60°C	primer waling
PRCP4 (10µM)	GAGGCACTCAGAGCTATGAG	60°C	primer waling
PRCP5 (10µM)	TTGTTCCCGTTCTTGTATTGG	60°C	primer waling
PRCP6 (10µM)	ATGATGGTGAGTGGTCTTGG	60°C	*prcp*
PRCP8 (10µM)	CAGCCACCGAATTCACTTTT	60°C	DNA-
GW1 (10µM)	CCATACAGTCCTCCTCACATCCATGCT	60°C	genotyping
AgRP_fw1 (10µM)	CCTGGCTACAGGAAGCAGTC	60°C	*agrp*
AgRP_rv1 (10µM)	TGCTTGCTGATCTTTGCCTA	60°C	qPCR
At1_fw (5µM)	CCATTGTCCACCCGATGAAG	60°C	*agtr1a*
At1_rv (5µM)	TGCAGGTGACTTTGGCCAC	60°C	qPCR
ghrl_fw (5µM)	GAGCCCAGAGCACCAGAAAG	60°C	*ghrl*
ghrl_rv (5µM)	GCAGTTTAGCTGGTGGCTTCT	60°C	qPCR
KST (5µM)	GCCTGGTTCAGGATGAAGTATCCTC	60°C	*prcp*
PCP3 (5µM)	GCAACTTTTTGCAGCCTTTGCCTG	60°C	RPA
lep_fw1 (5µM)	TCAAGCAGTGCCTATCCAGA	64°C	*lep*
lep_rv1 (5µM)	TGAAGCCCAGGAATGAAGTC	64°C	qPCR
Mas_fw	GCCATGAATACCTCCAGCAG	60°C	*Mas1*
Mas_rv	GCTCATGATGACCCAGTGC	60°C	qPCR
POMCfw1 (5µM)	CCATAGATGTGTGGAGCTGGT	60°C	*pomc*
POMCrv (5µM)	AGCGAGAGGTCGAGTTTGCA	60°C	qPCR
PRCP_rv1 (10µM)	GTGAGCGACTGGAGACCACT	60°C	*prcp*
KST1 (10µM)	GCTCTTATGGTGGCATGCTT	60°C	qPCR
ßact_fw (5µM)	TACAATGAGCTGCGTGTG	60°C	*actb*
ßact_rv (5µM)	CACAGCCTGGATGGCTAC	60°C	qPCR
TBPf2 (10µM)	CCCTATCACTCCTGCCACACC	60°C	*tbp*
TBPr2 (10µM)	CGAAGTGCAATGGTCTTTAGGTC	60°C	qPCR

3.6 Molecular Biological Protocols

3.6.1 DNA analysis

3.6.1.1 DNA Preparation for Genotyping

DNA was prepared from tail biopsies collected in Eppendorf tubes. Two to 3mm long tail tip pieces were incubated with 50 μL proteinase K containing tail buffer (100 mM Tris-HCl, 0.3 M Na-Acetate, 0.1 mM EDTA, 1% SDS (w/v); pH 7.0) at a final concentration of 1mg/mL for several hours to over night at 55°C. After inactivation of the enzyme at 95°C for 10 min, 375 μL TE buffer (10 mM Tris-HCl, 1 mM EDTA; pH 8.0) containing 21.33 μg/mL RNase A was added. Samples were shaken vigorously (Vortex Genic 2) and stored at -20°C until use.

3.6.1.2 Polymerase Chain Reaction

Polymerase chain reaction (PCR) was carried out, following the manufacturer instructions, with the recombinant TaqDNA Polymerase by incubating the DNA sample with Taq polymerase (5U/μL), 10x PCR buffer, 50 mM Magnesiumchlorid and W-1. When ever calculated PCR products reached a size larger than 800 bp also 10% W-1 was added to the PCR reaction. W1 (Invitrogen) was used to stabilize large amplicons during long reactions. For all PCR reactions, if not indicated differently, the same cycling conditions were used (Table 7) with changes in annealing temperature (AT) and elongation time (ET).

Table 7: General PCR temperature profile. AT annealing time, AT°C annealing temperature, ET elongation time.

PCR steps	time	temperature	
Denaturation	5 min	96°C	
Denaturation	30 sec	96°C	l
Annealing	AT	AT°C	l 35x cycles
Elongation	ET	72°C	l
Final elongation	5 min	72°C	

All PCR reactions were carried out in the PCR Thermo-Cycler (DNA Machine BIORAD). In order to visualize PCR products 8-12 μL of 50 μL PCR reaction were mixed with

DNA gel loading buffer (4g sucrose, 2.5 mg bromphenol blue in 10 mL TE solution) and loaded on agarose gel. Agarose (0.7-3 %) was boiled in 1x TAE buffer and finally ethidium bromide solution was added (0.5 µg/mL).

3.6.1.3 Primer Walking

To simplify the procedure of animal genotyping the exact position of the genetrap vector within the *prcp* gene intron 4 needed to be identified. Seven forward primers (PRCP1 to PRCP7) every 1,000 bp of intron 4 and a reverse primer at the 5'-end of the gene trap (GW1) for the use at 60°C annealing temperature were designed. The PCR was carried out with genomic DNA (gDNA) prepared from mouse tail biopsies as templates. The following program was used for the thermocycler: 5 min 95°C; 35 times repeats: 1 min 95°C, 1 min 60°C, 1 min 72°C; and final elongation for 10 min at 72°C. The analysis of the reaction product by electrophoresis in agarose gel allowed to define the best primers for genotyping.

3.6.1.4 DNA Extraction from Agarose Gels

PCR fragments used for cloning, were extracted from agarose gels using QIAquick Gel Extract Kit (Qiagen®). The extraction procedures recommended by the manufacturer were followed.

3.6.1.5 Measurement of Nucleic Acid Concentration

The quality and quantity of DNA were measured by comparison of band-intensity on ethidium bromide stained agarose gels. The DNA molecular weight marker was used as a standard. Alternatively, photometrically measuring absorption of the samples at 260 nm was carried out (NanoDrop2000, Thermo Scientific). DNA quality (i.e. contamination with salt or proteins) was checked by the measurements at 260, 280, and 320 nm. The concentration was calculated according to the formula:

$C = (E\ 260 - E\ 320) \times f \times c$

with C standing for the concentration of sample (µg/µL), E the absorption at 260 nm and 320 nm and f for the dilution factor. The value of c has to be chosen for the ex-

act sample type used (c = 0.05 µg/µL for double stranded DNA, c = 0.04 µg/µL for RNA, c = 0.03 µg/µL for single stranded DNA).

3.6.1.6 DNA Sequencing

The DNA samples were submitted to automatic sequencing using the thermo sequenase fluorescent-labeled primer reaction. The sequencing was performed by the company Invitek (Berlin-Buch, Germany).

3.6.1.7 Cloning

3.6.1.7.1 Ligation

The products from primer walking PCRs were assayed with 2 % agarose gel electrophoresis and isolated from agarose gel for further cloning. Taq and other polymerases have a terminal transferase activity that results in the nontemplated addition of a single nucleotide to the 3'-ends of PCR products. In the presence of all 4 dNTPs, dA is preferentially added. This terminal transferase activity is the basis of the TA-cloning strategy. For the cloning of PCR products the pGEM-T Easy Vector was used.

The ligation of an insert into a vector was carried out in the following reaction mix: 50 ng vector DNA, 100-300 ng insert DNA, 1 µL ligation buffer (10x), 1 µL T4 DNA ligase (5 U/µL) in a total volume of 10 µL, adjusted with DNAse free water (provided with the kit). The ligation reaction was carried out at 16°C overnight or at room temperature for 2 hours. Alternatively a quick ligation using 2x ligation buffer was performed at room temperature for half-an-hour up to 2 hours.

3.6.1.7.2 Preparation of Electrocompetent Escherichia coli bacteria

Onehundred mL of lysogeny broth (LB) medium (Table 8)were inoculated with a single colony of *Escherichia coli* (*E. coli*, strain DH5α) and incubated overnight at 37°C for bacterial growth. Next, 1 mL overnight culture was transferred to 250 mL LB medium and grown at 37°C to optical density of 0.6. Cells were placed on ice for 15 min, than transferred to a prechilled centrifuge bottle and centrifuged at 2600 g for 15 min at 2°C. Cells were washed 2 times with 250 mL and 10 mL 10% glycerol in

water and finally resuspended in 1 mL 10% glycerol. Aliquots of 30 µL were stored at -80°C.

3.6.1.7.3 Transformation of Electrocompetent Bacteria

Electroporation of bacteria was done by gently mixing one aliquot of competent cells with 2 µL of ligation reaction or with 50 ng of pure plasmid DNA. Cells were transferred to a prechilled cuvette (0.1 cm electrode gap) and electroporated at 1350 V for 5 ms (Electroporator 2510). Immediately, 1 mL of fresh LB medium (Table 8) was added and cells were transferred to a new sterile Eppendorf tube. After shaking 60 min at 37°C, cells were spread on ampicillin-agar plates (Table 8)and supplemented with XGal and IPTG, if required. Plates were incubated overnight at 37°C. Positive clones were selected by theby the usual blue-white screening method [86].

Table 8: Composition of LB plates and medium.

LB Plates		**LB Medium**	
10-15 %	Bactoagar	5 g	Yeast extract
100 µg/L	X-Gal	10 g	Bactotrypton
80 µg/mL	IPTG	10 g	NaCl
100 µg/mL	Ampicillin in LB Medium*	100 µg/mL	Ampicillin ad. 1000 mL H_2O*

*alternatively kanamycin/chloramphenicol (15 µg/mL) or 3 µg/mL tetracycline was used

3.6.1.7.4 Analytical DNA Preparation

A single *E. coli* colony was grown in LB overnight at 37°C (Shaker Certomat). Two mL of the cell culture was centrifuged at 13,000 g for 1 min and pellets resuspended in 300 µL of solution E1. Cells were lysed by adding 300 µL of E2 solution. The same amount of E3 solution was added to the tube, and immediately mixed by inverting (E1 to E3 see Table 9). Cell debris and chromosomal DNA were pelleted by centrifugation at 13,000 g, for 5 minutes at room temperature. The supernatant was transferred into a new tube and 0.6 mL of isopropanol was added to precipitate the DNA. After centrifugation (13,000 g, room temperature, 10 min) and washing with 70% ethanol, the air-dried pellet was resuspended in 50 µL TE buffer (10:1 solution con-

tains 10mM Tris pH 8 and 1mM EDTA). Two to 5 µL of DNA was taken for control digestion. Plasmid-DNA was stored at -20°C.

Table 9: Composition of solutions for analytical DNA preparation.

E1 solution	E2 solution	E3 solution
50 mM Glucose 10 mM EDTA pH 8.0 25 mM Tris-HCl pH 8.0 0.4 mg/mL RNaseA	100 mM NaOH 0.5 % SDS	3.1 M Potassium Acetate

3.6.1.7.5 Preparative DNA Isolation

Plasmid DNA was isolated from 200 mL of overnight cell culture using JetStar Plasmide Purification MAXI Kit 2.0 according to the manufacturer's instruction. The DNA was usually dissolved in 100-400 µL TE buffer and kept at -20°C.

3.6.2 RNA Analysis

3.6.2.1 RNA Extraction

Tissues were collected in MATRIX tubes® containing lysing matrix beads (MP Biomedicals) and directly frozen in liquide nitrogen. Until RNA extraction organs were kept frozen at -80°C. For homogenization 1 mL Trizol® per 100 mg tissue was added and immediately transferred to FastPrep® homogenizer (MP Biomedicals). Depending on the tissue composition homogenization was performed either one time (adrenal gland, BAT, brain, kidney, liver, lung, spleen, salivary gland, testis, white adipose tissue) or two times (aorta, heart, muscle, small intestine, stomach) at speed level 4 for 40 seconds. Only white adipose tissue (WAT) was directly centrifuged at 15,000 rpm (Beckmann), for 30 seconds and the TRIZOL-tissue homogenate transferred into a clean Eppendorf tube, leaving any lipids behind. The separated homogenate was preceded like all other tissue homogenates: Adding 300 µL chloroform, the tubes were mixed 15 sec vigorously (Vortex Genic 2). Then the tubes were incubated for 5 min at room temperature. Following centrifugation (see above) the liquid phase (ca. 500 µL) was transferred into a new tube containing an equal amount of isopropanol.

After inverting the tubes slowly five times, the RNA was incubated 10 min at room temperature and again centrifuged. The remaining pellet was washed two times in 500 µL precooled (-20°C) Ethanol and then dried for 10 to 20 min at 37°C. Finally, the pellet was dissolved in DEPC treated ddH_2O (0.1% v/v DEPC, two times autoclaved) until the pellet was completely solved. RNA was frozen in liquid nitrogen and stored at -80°C.

RNA concentration was measured utilizing NanoDrop2000 (Thermo Scientific). If possible 30 µg of RNA was DNA-digested in the following mixture: 1 µL RNasin, 0.5 µL DNaseI and 10x DNaseI buffer (Boehringer Mannheim) and incubated first 15 min at 37°C, than heat inactivated at 75°C for 10 min. Digested RNA was stored at -80°C until use or after repeated RNA measurement used for transcription.

3.6.2.2 cDNA Synthesis and Reverse Transcription

If not mentioned different in the text than 7.5 µg DNaseI digested RNA was used for reverse transcription (RT-PCR). First a reaction mix composed of 1 µL random hexamer primer, 2 µL dNTP (5 µM mix of adenosine-, guanine-, cytosine- and tyrosine-deoxyribonucleotid-triphosphate), 4 µL 5x first strand buffer, 2 µL dethiothreitol, 0.5 µL RNasin and 1 µL Moloney Murine Leukemia Virus Reverse Transcriptase (Invitrogen) was prepared for every sample on ice. The appropriate amount of RNA and ddH_2O to a final volume of 20 µL was added and incubated for 10 min at 25°C, 40 min at 42°C, 10 min at 80°C and immediately cooled down to 4°C. Before using cDNA for any kind of procedure, always a test-PCR with a 1:10 diluted cDNA was performed.

3.6.2.3 Quantitative Real Time PCR

This method was used to quantify PCR product amounts. Before analyzing experimental groups always optimal primer concentration, cDNA dilution and the most stable "house keeping" gene for the designated tissue were tested. Realtime PCR (qPCR) approach used the SYBR green method in a 96-well plate format detecting the signal with the iQ5 cycler (BioRad). Reactions contained 7.5 mL 3x SYBR Master-Mix (Qiagen), primer (100 nM), and template in a total volume of 15 mL. The ther-

mal profile used for amplification was 95°C for 10 min, followed by 50 cycles of 95°C for 15 sec, 60°C for 20 sec, and 72°C for 40 sec. At the end of the amplification phase, a melting-curve analysis was carried out. Gene expression was normalized to chosen 'house keeping gene' mRNA expression. The method of Livak and Schmittgen[87] was applied to compare gene expression levels between groups, using the equation $2^{-\Delta\Delta CT}$.

3.6.2.4 Ribonuclease Protection Assay

Ribonuclease protection assay (RPA) is a highly sensitive method to identify individual RNA molecules in a heterogeneous RNA extract. Mixing the RNA samples with a RNA antisense probe designed for the gene of interest and a reference gene, probes hybridises with complementary strands to form double-stranded RNA. The mixture is then exposed to ribonucleases that specifically cleave only single-stranded RNA, leaving the double-stranded molecules intact. Running the digested samples on a denaturating gel presents remaining 'protected' molecules as single bands. The instruction manual of Ambion was followed.

3.6.2.4.1 DNA Probe Design and Digestion

The DNA probe was designed by cloning of a partial mRNA-sequence of the gene target and annealing oligonucleotides into the multiple cloning site of pGEMTeasy. Alternatively, oligonucleotides recognizing the T7 promoter sequence of the vector including a partial sequence of the gene target were purchased from BIOTEZ and annealed.

For RPA analysis of *prcp* mRNA, 10 µg of DNA probe was digested overnight with the enzymes NocI and SalI in a volume of 50 µL respectively. The enzymatic reaction was assayed via electrophoresis (1% agarose gel) before probe labeling.

3.6.2.4.2 Probe and Marker Labelling

The labeled antisense RNA probe was synthesized by T7 or SP6 RNA polymerase in the presence of [α-^{32}P] UTP using an RNA transcription kit (Stratagene, USA). To perform in vitro transcription 200 ng of DNA was mixed with: 1 µL 10 mM rATP, 1 µL 10

mM rCTP, 1 µL 10 mM rGTP, 5 µL 5x transcription buffer, 1 µL RNasin, 1 µL 0.2 M DTT, 3 µL [α-32P] UTP (800 Ci/mM), 1 µL of T7, or T3 or Sp6- polymerase in a final volume of 25 µL (DEPC H_2O).

After incubation at 37°C for 1 hour, 1 µL of RNase-free DNase I was added to digest the DNA template at 37°C for 15 min. To clean the probe from free unincorporated nucleotides, 25 µL of DEPC H_2O were added to the reaction (total 50 µL) and probes were purified with QuickSpin Columns for radiolabeled RNA purification, according the manufacturers protocol. The activity of the probe was measured with the scintillation counter LS600SC (Beckman, Minnesota, USA).

The DecadeTM Marker System kit (Ambion) was used to label RNA marker with radioactive dATP [γ-^{32}P] (300 Ci/mmol) as prescribed in the given protocol of the manufacturer.

3.6.2.4.3 RNA-RNA Hybridization

RNA expression via RPA was carried out using the commercially available Ambion RPA II kits. According to the manufacturer's protocol briefly, 20 µg sample RNA and 20 µg yeast control were hybridized with antisense probe at 42°C for 16 hours with 80,000 cpm followed by digestion with RNase A+T1. After RNAse inactivation and RNA precipitation, protected fragments were separated by gel electrophoresis (Table 10). Gels were dryed (Saldo Gel Dryer) and used to exposed to a X-ray Retina film. X-ray films were analyzed using the FUJIX BAS 2000 Phospho-Imager system.

Table 10: Composition of the denaturating gel and running buffer.

Urea-polyacryl gel		**TBE Buffer**	
7 M	Urea	130 mM	Tris
10x	TBE	45 mM	Boric acid
15 % (v/v)	Acrylamid-/Bis-Acrylamid 19:1	2.5 mM	EDTA
0.0008 %	(v/v) APS		
0.001 % (v/v)	TEMED		

3.6.3 Protein and Peptide Analysis

3.6.3.1 Protein Isolation

Onehundred to 200 mg of mouse tissue was homogenized (FASTPREP®) in 300-500 µL of RIPA buffer or protein lysis buffer containing protease and phosphatase inhibitors (Roche, Table 11). The tissue homogenates were sonicated for 30 sec (Bandelin electronic) and centrifugated at 13,000 g for 10 min at 4°C. The upper layer containing the proteins was transferred into a new Eppendorf tube and was stored at -20°C.

Table 11: Buffer composition for protein isolation and western blot.

RIPA Buffer		**Protein Lysis Buffer**		**PBS Buffer**	
150 mM	NaCl	20 mM	Tris-HCl pH 7.4	137 mM	NaCl
50 mM	Tris pH 8.0	150 mM	NaCl	2.7 mM	KCl
0.5 %	Na-deoxycholate	1 mM	EDTA	8.0 mM	Na_2HPO_4
0.1 %	SDS	1 mM	EGTA	1.5 mM	KH_2PO_4
1 %	Nonidet P-40	0.5 %	Triton X-100		pH 7.5
		1 mM	PMSF		
		1	tablet*		

* Complete Protease Inhibitor Cocktail, Mini, EDTA free (1 Tablet/10 mL RIPA buffer)

3.6.3.2 Measuring Concentration of Proteins

The quantity of protein was estimated spectrophotometrically at a wavelength of 595 nm (OD_{595}) as described by Bradford 1976 [88]. The procedure is based on the formation of a complex between the dye Brilliant Blue G, and proteins in solution. The protein-dye complex causes a shift in the absorption maximum of the dye from 465 to 595 nm. The extent of absorption is proportional to the amount of protein present. Samples containing known concentrations of bovine serum albumin (BSA) were used as standard.

Protein samples were diluted (usually 1:20) in PBS (Table 11) and 5 µL of each sample was mixed with 250 µL of the Bradford reagent. In parallel, different concentrations of BSA (0.1 – 1.4 µg BSA/µL) were mixed with the Bradford reagent as well. After incubation for 20 min at room temperature, samples and standards were measured for the protein concentration at 595 nm using a plate analyzer (Infinite M200).

The protein concentration was graphically calculated regarding the protein standard curve.

3.6.3.3 SDS Polyacrylamid Gel Electrophoresis

Proteins were separated depending on their molecular weight on gradient gels containing 10% polyacrylamide. If not stated differentially, 50 µg of protein were mixed with an appropriate amount of 3x Roti-load, incubated for 5 min at 95 °C and separated at 100 V (10 V/cm) in SDS-PAGE running buffer (196 mM glycine, 0.1% SDS, 50 mM Tris-HCl pH 8.4). After electrophoresis the gels were subjected to western blotting.

3.6.3.4 Western Blot

Western blotting was used to transfer proteins electrophoretically from a damageable polyacrylamide gel to a more robust support. The setup in the transfer case was as follows: sponge cloth, two pieces Whatman paper, polyacrylamid gel, Hybond-C nitrocellulose or PVDF membrane (pre-activated in methanol), Whatman paper and sponge cloth. The assembled case was inserted in the case holder and put into the transfer chamber filled with transfer buffer (25 mM Tris-HCl, 192 mM Glycine; pH 8.4). The transfer was run at 100-120 V for 2 hours.

The membrane was then incubated with blocking solution (Odyssey Blocking Reagent) for 1 hour at room temperature. In case of PRCP antibodies different blocking solutions were tested (1%, 3% and 5% milk powder, 5% BSA, Roti-Block).

The primary antibody was applied in PBS buffer (Table 11) with 0.08% Tween 20 (pH 7.4 = PBST) at a dilution of 1:100-1:1000, depending on the antibody. Incubation with the primary antibody was carried out at 4°C rolling overnight (Roller Mixer SRT1). Unspecifically bound antibody was removed by washing the membrane 3 times for 15 min in wash-buffer (50 mM Tris, pH 7.4, 150 mM NaCl with 0.08% Tween 20, pH 7.4).

Depending on the detection system used the membrane was then incubated with the peroxidase-conjugated secondary antibody at a dilution of 1:1000 or with an Odyssey

secondary antibody 1:10,000 in PBS for 1 hour at room temperature when using the Odyssey technique. After washing 4 times for 15 min with wash-buffer, the membrane was either incubated with detection solution (Super Signal West Dura Extended Duration) and bands were detected using a CCD-camera (Fujifilm LAS-1000). Or blots were directly analyzed with Odyssey® when Odyssey reagents and secondary antibodies were used.

3.6.3.5 Classical Enzyme-Linked Immunosorbend Assay

Enzyme-linked immunosorbend assays (ELISA) utilize antibodies specific to the analyte of interest, fixed at the surface of a micro titer plate. Incubation of standard samples of known protein concentrations and unknown samples leads to binding of the substrate. After washing the plate was incubated with a second antibody specific to the desired antigen. The second antibody is normally linked to an enzyme which is used by adding a specific substrate for the enzyme to cleave. The conversion of the substrate provides the detectable signal, commonly by a color change.

For detection of leptin, αMSH and GHRL in mouse plasma samples, commercially available kits were used according to manufacturers protocol. Results were calculated with the Graph Pad Prism software. For the detection of αMSH peptides first needed to be extracted from the plasma. Briefly, aprotinin treated plasma samples were acidified with an equal amount of Buffer A (PHOENIX Pharmaceuticals #RK-BA-1) mixed and centrifuged at 10,000 g, at 4°C for 20 min. C18 SEP columns were equilibrated with 1 mL of Buffer B, followed by three times washing with 3 mL buffer A. The centrifuged plasma was loaded onto the pre-treated column and slowly washed with buffer A (3 times, 3 mL). Peptide elution was carried out adding 3 mL buffer B onto the column. The eluate was collected in a polystyrene tube and lyophylized (Benchtop 3.3). Prior to use sample extracts were resuspended in assay buffer provided with the kit.

3.6.3.6 Advanced ELISA: LUMINEX

Based on the principle of ELISA, Luminex is a multi screen approach detecting several analytes at the same time. First color-coded polystyrene microspheres were

coated with a different specific antibody. Antibody-coated microspheres were applied together to the samples in a specialized 96 titer plate (provided in the kit). Detection of the multiplexed results was carried out by the Luminex system. Thereby, single beads were analyzed separately by scanning the microspheres in a thin glas capillary by two lasers. The provided Luminex software calculated the protein concentrations according to standard samples measured at the same plate.

3.6.3.7 Radioimmuno assay for AngII and Ang1-7

The measurement of AngII and Ang1-7 with radioimmuno assay (RIA) is an established standard method in the laboratory of Prof. R.A.S. Santos (Federal University of Minas Gerais, Belo Horizonte, Brazil) and was carried out as described in Velloso et al. [89]. In brief, blood and organs were collected and homogenized in guanidinium thiocyante. Samples were extracted using a C 18 bond-elut phenylsilane cartridge (500 mG/3 mL-varian) pre-activated with a mixture of 20 mL 99.9% acetonitrile (ACN)/ 0.1% heptafluorobutyric acid (HFBA, 0.1%) and 20 mL 0.1% HFBA in ultrapure water. The columns were washed sequentially with 3 mL 0.1% bovine serum albumin (0.1% BSA/0.1% HFBA), 10 mL 10% ACN/0.1% HFBA and 3 mL 0.1% HFBA. After sample application, the column was washed with 20 mL 0.1% HFBA and 3 mL 20% ACN/0.1% HFBA. The peptides were eluted with 3 mL 99.9% ACN/0.1% HFBA and the solvent was evaporated.

Angiotensin peptides were determined by radioimmunoassay (all samples in the same assay, pg/mL plasma) by the method of Neves et al. [90]. For Ang II, samples were reconstituted with 0.9% NaCl, 0.1% BSA and 0.03% acetic acid. The Ang II antibody (kindly donated by S. Prennie, Cleveland Clinic Foundation, Cleveland, OH, USA) presented 100% cross-reactivity with Ang- (2-8), Ang-(3-8), and Ang-(4-8). Cross-reactivity of less than 0.001% was observed with Ang I and Ang-(1-7). The inter- and intra-assay levels of variability were 5.2 and 6.8%, respectively [91]. Plasma Ang-(1-7) was determined using a polyclonal antibody with less than 0.08% cross-reactivity with Ang-(2-7) and Ang-(3-7), and less than 0.08% cross-reactivity with Ang-(4-7). Cross-reactivity with Ang I, Ang II, and amino-terminal fragments was

less than 0.001%. The inter- and intra-assay levels of variability were 8.6 and 4.8%, respectively.

Resuspended samples were incubated for 20 hours with the antibody in the presence of radioactive labeled I125-peptide (Ang1-7, AngII resepectively). After treatment with dextran coal (chapter 3.6.3.8) and centrifugation, supernatants were measured in an automatic gamma counter.

3.6.3.8 AngI Radioimmuno Assay

For the AngI RIA, blood was collected in a cocktail of protease inhibitors (µL/mL of blood: 50 µL 7.5% EDTA, 10 µL 1 mM phenylmethylsulfonylfluoride, 50 µL 30 mM ortho-phenanthroline, 10 µL 1 mM p-hydroxy-mercury benzoate, and 20 µL 1 mM pepstatin A). After centrifugation at 2000 g for 15 min, plasma was transferred into a new tube, shock frozen in liquide nitrogen and stored at -80°C.

The measurement of AngI required 50 µL protease-treated plasma (in triplicates). The plasma samples were incubated for 16 to 20 hours with 50 µL AngI-RIA buffer (0.1 M Tris, 1 mM EDTA, 0.5 mg/mL BSA, pH 7.4), 500 µL AngI antiserum (1:105) and 500 µL radioactively labeled tracer (6 pg/mL I^{125}-labeled AngI peptide) at room temperature. Afterwards, 300 µL Norit A coal and dextran was added (1.25 g Norit A coal, 0.25 g Dextran T 70 in 100 mL AngI-RIA buffer). Fifteen minutes later, samples were centrifuged at 4000 g for 20 min at 4°C and the supernatant discarded. Coal pellets were measured in an automatic gamma counter. A standard curve with dilutions of 10 fg/mL to 5 pg/mL was included in every measurement.

3.6.3.9 AngII Radioimmuno Assay

Samples for AngII RIA were treated according to the protocol in chapter 3.6.3.8 with the following modifications: 350 µL AngII-RIA buffer (0.1 M Tris, 0.325 mM neomycin, 0,1% Triton X-100, pH 7.4) was add to 50µL of protease treated plasma and incubated with 100 µL AngII-antiserum (1:30,000) and 100 µL radioactively labeled I^{125}-AngII peptide (40 pg/mL). Norit A coal and dextran were diluted in AngII-RIA buffer (250 mL AngII RIA buffer, 4 g Norit A coal, 1 g Dextran T70).

3.6.4 Enzyme Activity Assays

3.6.4.1 Renin

The renin activity of plasma samples was calculated from the generation rate of AngI after adding a known amount of precursor protein AGT. The concentration of AngI was monitored over time via the RIA technique described in chapter 3.6.3.8.

3.6.4.2 ACE2

The activity of ACE2 was analyzed in the laboratory of Dr. W. E. Siems at the Leibnitzinstitute for Molecular Pharmacology (FMP, Berlin-Buch) using an established standard protocol [92]. The assay based on the cleavage of a peptide based enzyme substrate linked to a chromophor – 2,4-Dinitrophenyl (Dnp). The advantage of chromogenic substrates is the facial spectrometrical detection and analysis of the reaction product. As the ACE2 specific chromogenic substrate Mca-APK(Dnp) (MAPK) was purchased from Biosythan. When the substrate is cleaved the resulting fragment Mca-AP-OH provides a detectable fluorescence signal (extinction 320 nm, emission 405 nm).

Kidney and small intestine tissue were homogenized in 30 volumes ice-cold Tris buffer (50 mM) using a Potter-ELVEHJEM homogenizer. The homogenate was filtered through a nylon gaze, the filtrate was vigourously shaken and aliquotated. Samples were frozen on dry ice and stored at -80°C. Prior to use samples were sonicated and protein concentration was measured. In a black 96-well microtiter plate 200 µL MES buffer (50 mM 2-morpholinoethanesulfonic acid, 300 mM NaCl, 10 µM $ZnSO_4$, 0.01% Brij-35, pH 6.5), 20 µL sample and 10 µL substrate (diluted in DMSO) were incubated for 1 hour at 37°C with shaking. Each sample was determined in triplicates, using 0.5 M EDTA and 0.5 M o-phenantroline to inhibit ACE2 activity. The molecular standardization was performed with Mca-AP and calculated per mg protein.

3.6.4.3 Neutral Endopeptidase

Neutral endopeptidase (NEP) activity was measured according to the ACE2 protocol with (D-Ala2,Leu5)-enkephalin (DALEK) as specific substrate. As DALEK is not a

chromogenic substrate the protocol is slightly modified as described in [93]. The degradation of DALEK leads to the formation of the peptide Tyr-D-Ala-Gly which could be detected by high performance liquide chromatography (HPLC). The data were analyzed and compared to inhibitor-treated samples (10^{24} M bestatin and 10^{26} M lisinopril).

3.7 X-Gal Staining of Cryosections

Organs were collected from mice under narcosis (Ketavet (Ketaminhydrochlorid) 100 mg/kg + Rompun (Xylazinehydrochlorid) 10 mg/kg). Animals were perfused with 10 mL saline via the left ventricle of the heart, followed by 10 mL perfusion with 4% PFA. Specimens were incubated overnight in 30% sucrosein water at 4°C (until the organ automatically dropped when inverting the tube). Next day, the solution was exchanged against 4% PFA, incubating the tissues for 20 hours at 4°C. Thereafter, organs were transferred to Tissue-TekR OCT and slowly cooled down in precooled 2-Methylbutan. Sections (10-50 µm) were taken at a cryotom (Leica CM3050S) and mounted on slices or kept in PBS as free-floating slices.

The genetrap vector of the PRCP-/- contains the full sequence of a functional β-galactosidase (*lacz*) which is expressed instead of the *prcp* gene in case of the knockout mouse. Utilizing X-Gal as a substrate for β-galactosidase on tissue slices highlights the sides of *prcp* promotor activity in blue.

After rehydratization of dryed slices with 3 changes of PBS in 15 min, slides were arranged in humidified chambers at 37°C and incubated in the dark, with fresh X-Gal solution containing 5mM $K_3Fe(CN)_6$, 5 mM $K_4Fe(CN)_6*3H_2O$, 0.01% NP 40, 1M $MgCl_2$ and 0.5 mg/mL X-Gal (dissolved in dimethylformamide). Brain slices were incubated 48 hours, than washed 2 times for 5 min in PBS and rinsed with ddH_2O. Slides were counterstained using eosin, to stains the cytoplasm. Therefore, PBS washed sections were transferred to Eosin Y (90% ethanol, 0.1% eosin) for 45 sec, rinsed with ddH_2O followed by subsequent dips into 50%, 75%, 100% ethanol. Finally, slides were transferred for 5 min into Histo-clear and mounted with Eukitt. Slides were allowed to dry for at least 48 hours.

3.8 Immunohistochemistry on Parafinsections

For paraffin sections tissue samples were fixed overnight in 4% PFA in PBS at 4°C. After fixation the samples were dehydrated through a series of graded ethnol/PBS solutions for 2 hours each step: 70%, 80%, 90%, 96% and 100% ethanol. Following dehydration, the samples were incubated 2 times for 2 hours in Roti-HistolR. The samples were preinfiltrated with paraffin for 2 hours at 67°C and finally infiltrated with fresh paraffin overnight at 67°C. The next day, the samples were embedded in molds and stored at 4°C until use. Sections (5 µm) were taken at a rotary microtome and stored at 4°C.

The paraffin-sections were removed from the fridge and allowed to equilibrate at room temperature for 10 min. Sections were deparafinized by subsequent washes: 3 times 5 min xylol, 2 times 5 min 100% ethanol, 2 times 96% ethanol, 3 min 70% ethanol and 5 min in tris buffered saline (TBS: 50 mM Tris pH 7.6 in 0.9% NaCl solution). Trypsin digestion (1 tablet in 1.5 mL ddH2O) of the sections surfaces at 37°C for 15 min, prepares the tissue for immuno-labeling. After washing 3 times 5 min with high salt TBS (50 mM Tris, 500 mM NaCl, pH 7.5), the slides were blocked for 30 min with 10% normal donkey serum at room temperature to prevent unspecific antibody binding. After washing with high salt TBS sections were incubated overnight at 4°C with the primary antibody (Table 5), and washed again. Sections were incubated for 1 hour at room temperature with the Cy3-conjugated secondary antibody in the dark. Before mounting with Vectashield, the slides were washed 3 times for 5 min in TBS.

Pictures were taken at a Leica DMI 6000B microscope equipped with phase contrast and epifluorescence dyes.

3.9 Working with Laboratory Animals

3.9.1 Animal Husbandry

Mice were kept at standard conditions according to the German animal protection act. At the Max Delbrück Centre animal facility, mice were housed in ICV cages with

free excess to food and drinking water, at constant 20°C room temperature and a daily light cycle of 12 hours light followed by 12 hours darkness (6:00 pm – 6:00 am). Not more than 6 animals of the same sex were maintained together in one stock cage, the mating system was a so-called trio (one male with 2 females). The resulting offspring was genotyped and weaned at the age of ~21 days. Unless otherwise indicated males of twelve weeks age were used for experiments described.

Strain Purity

To obtain a pure background, heterozygous mice were backcrossed into the C57Bl/6 and FVB/N lines (Charles River), named PRCP_C57Bl/6 and PRCP_FVB/N respectively. In the 8th generation (F8) *prcp* heterozygous mice were cross-bred to generate homozygous PRCP-/- and PRCP+/+ lines for both backgrounds. In the experiments carried out, the PRCP+/+ line was always used as a control.

3.9.2 Establishment of the PRCP Kockout Mouse

The commercially available embryonic stem cell line GST090 (Baygenomics®) was microinjected into blastocysts of 129P2/OlaHsd mice in the laboratory of Prof. Michael Bader. Following transplantation of these embryos into pseudopregnant C57Bl/6 foster mothers, chimeras with agouti colored fur spots were bred with C57Bl/6 mice and the resulting offspring genotyped by RT-PCR.

3.9.3 Glucose Measurement

For the glucose tolerance test, D-glucose (2 mg/g body weight) was injected intraperitoneally into overnight-fasted mice. Glucose levels from tail blood samples were monitored at 0, 15, 30, 60, and 120 min after injection using an Accu-Check glucometer. An insulin sensitivity test was performed on overnight-fed mice, after intraperitoneal injection of insulin (0.75 units/kg body weight). Tail blood samples were taken at time points 0, 15, 30, and 60 min after injection for measurement of blood glucose levels.

3.9.4 Diets

Unless otherwise indicated, mice were fed a standard diet (Snniff M-Z#V1124-300). For the body weight experiments a 45% high fat diet with 22.5% crude protein, 23.1% crude fat, 5.7% crude fiber, 5.9% crude ash, 8.6% starch and 29.4% sugar was fed (Ssniff EF/RM D12451 modified #E15744-347).

3.9.5 Metabolic Cages

To collect urine and data about water consumption, mice were housed singly in metabolic cages (UNO, NL) for three days. Water consumption was recorded daily by weighing the water bottles. Urine was collected daily, centrifuged at 5000 g (Eppendorf 5415D) and supernatant kept in a fresh tube at -20°C. The analysis of urinary sodium, potassium and albumin was carried out by Labor 28 AG (Medizinisches Vorsorgezentrum, Berlin).

3.9.6 Body Composition Scan

The body composition scan was carried out by Martin Taube at the MRI core facility of the Max Delbrück Centre. The advantage of the MRI-based body analysis is to collect non-invasively detailed data about body fat, water and muscle content, in alive animals. To ensure similar conditions for all animals, only twelve week-old male mice, housed in groups not bigger than three animals per cage, were used. Prior to measurement, all food inside the cage had to be removed for four hours. The MRI-scan always took place between 12:00 and 14:00 pm. The mice were then immobilized for five minutes in a small examination chamber. After the scan, animals had again free access to food and water.

3.9.7 Echocardiography

Echocardiography (ECG) is a non-invasive ultrasound technique to examine the heart geometry. The recorded two-dimensional ultrasonic images serve as a guideline to evaluate wall thickening and inner diameter of the left ventricle in systole and diastole of the heart. Based on the diameter the ejection fraction of the heart and fractional shortening can be calculated. Thereby the ejection fraction translates in per-

cent the fraction of blood pumped out by the ventricle during the systole. The fractional shortening translates as a ratio the change in diameter of the left ventricle between contracted and relaxed states. The ratio of diastolic left ventricular posterior wall dimension (LVPWd) and left ventricle diameter (LVd) in diastole reflects changes in heart geometry. High values indicate heart hypertrophy while low values hint at dilated ventricle walls.

Martin Taube carried out echocardiography at the MDC small animal MRI core facility. Following isofluran anesthesia (1.6 vol% isofluran/air) adhesive electrodes (Needle Electrodes (5) 29 gauge, AD Instruments) were attached to mice extremities and connected to Octal Bio Amp (AD Instruments). Like published by Royer et al. [94] ECG standard intervals were measured using six circuits. The whole procedure lasted 5 minutes per mouse and was repeated after chronic treatment with AngII (chapter 3.9.10), always between 9:00 and 12:00 am.

3.9.8 Acute Measurement of Blood Pressure

The insertion of catheters was carried out by Prof. Mihail Todiras as described by Jankowski et al. [95]. Applying aseptic techniques to anaesthetized mice (Ketavet (Ketaminhydrochlorid) 100 mg/kg + Rompun (Xylazinehydrochlorid) 10 mg/kg), catheters (4 to 5 cm length, 0.25 mm inner diameter, and 0.40 mm outer diameter) were placed in the femoral artery for the measurement of arterial pressure and in the femoral vein for injections with the peptides to test (AngI, AngII and bradykinin). The catheters were filled with sterile 0.9% NaCl solution containing heparin (10 U/mL) and tunneled subcutaneously, exteriorized at the back of the neck, and sutured in place between the scapulae. The mice were allowed to recover for 72 h before the beginning of the experiment. During the recovery period 24-48 h after surgery, catheters were flushed with heparinized saline solution (3-5 µL/gbw).

On the day of the experiment, mice were tested in a conscious, unrestrained state in their home cages. Sixty minutes after the arterial catheter had been coupled with a 23-gauge stainless steel pin with a 25-cm piece of Portex polyethylene tubing (PE-50; 0.58 mm inner diameter, 0.96 mm outer diameter) to a MLT 1050/D pressure transducer (AD Instruments, Colorado Springs, USA), baseline blood pressure and

heart rate were measured continuously for 1 hour after the coupling. All hemodynamic data were collected and analyzed on a computer using Chart software (Version 5; Powerlab; Colorado Springs, USA).

3.9.9 Chronic Blood Pressure Measurement

For long term experiments the insertion of a telemetry transducer was necessary to avoid a constantly open wound and inflammation during the whole experiment. Surgery and measurement were accomplished as described in detail by Gross et al. [96]. Mice were anesthetized with isoflurane (1.6 vol% isofluran/air). The pressure-sensing catheter of the TA11PA-C20 blood pressure device (Data Sciences International, St. Paul, MN) was introduced via the right femoral artery in the abdominal aorta, and the transmitter was placed in a subcutaneous pocket along the right flank. The mice were allowed to recover ten days from surgery before baseline blood pressure and heart rate values were recorded for three days in three sequent weeks. By this time, the mice had regained their circadian blood pressure and heart rate rhythm, and the surgery and anesthesia-dependent initial changes in mean arterial pressure (MAP) and heart rate were followed by stable values.

The data from the TA11PA-C20 device were sampled for 10 sec every 5 min continuously day and night with a sampling rate of 1000 Hz, and stored on a hard disk. Systolic and diastolic blood pressure and heart rate were recorded using the DATAQUEST software (A.R.T. 2.1; Data Sciences International). Activity was monitored as changes in transmitter signal strength resulting from murine (transmitter) locomotion.

3.9.10 Minipumps

To constantly apply a dose of 1.4 mg/kg/d AngII, micro-osmotic pumps (model 1004, Alzet, Cupertino, CA) were inserted into the mice, ten days after insertion of telemetry transducers. To fill the pump, AngII was calculated depending on the body weight of the mouse (0.12 µL/h, fill volume 98 µL).

3.9.11 Animal Activity Study

The animal home cage activity study was performed with professional equipment of the group of Prof. Lewin at the Max Delbrück Centre Berlin. Animals were housed singly over four days. The TSE ActiMot / MotTil system with home cage shaped frames detected the activity of the animals via infrared sensors. Data were saved on a hard disc and values in intervals of 20 min assembled by ACTIMOT software. The resulting table was finally analyzed using Microsoft Excel software.

4 RESULTS

The results chapter is divided into three parts starting with a general description of the studied PRCP knockout mouse. The second and third chapter present data gained from this mouse model preparing the basis of discussing the involvement of PRCP in the melanocortin system and renin angiotensin system.

4.1 Generation and Characterization of the PRCP Knockout Mouse

4.1.1 Generation of PRCP Knockout Mice

The microinjection of the Baygenomic's ® GST090 ES cell line clone into blastocysts followed by transplantation into pseudopregnant foster mothers gave rise to four chimeras, indicated by agouti coat color. When breeding these chimeras with C57Bl/6 mice, the resulting offspring confirmed germ line transmission of the vector construct, proven by RT-PCR (Figure 3B).

PRCP heterozygous mice were then bred with each other to produce the first PRCP knockout mice (PRCP-/-). To confirm the genotype, RNA gained from fresh frozen organs was used for Ribonuclease protection assay (RPA). Therefore, a probe was designed spanning exon 4 to exon 6 of the *prcp* wild type gene, covering the insertion site of the gene trap in intron 4. The RPA gel presented the predicted band at 352bp in PRCP+/+ tissues while this band was absent in PRCP-/- tissues (Figure 3C).

4.1.2 Localization of the Gene Trap Vector Insertion Side

To simplify the procedure of animal genotyping the exact position of the genetrap vector within the *prcp* gene needed to be identified. According to Baygenomics® the insertion site of the gene trap should be located between exon 4 and 5 (Figure 3A).

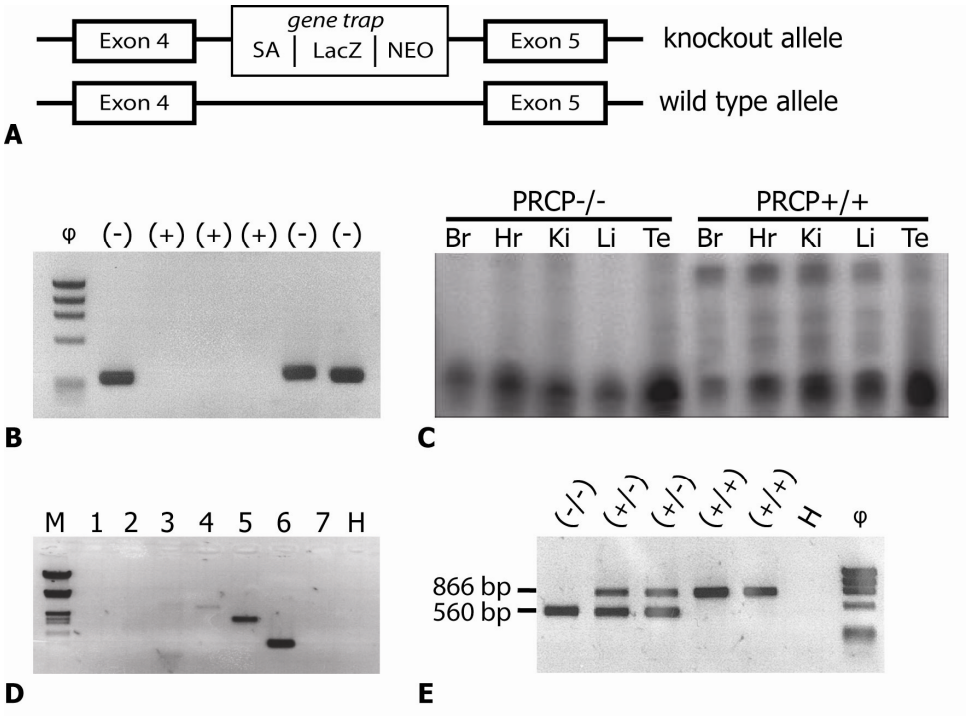

Figure 3: Localization of the gene trap insertion site in PRCP-/- mice.

A Scheme of the knockout and wild type alleles. **B** Reverse transcription PCR to identify animals carrying the gene (-). **C** Ribonuclease protection assay with RNA gained from PRCP-/- and +/+ tissues. **D** Primer walking within the *prcp* gene intron 4 using 7 primers every ~1,000 bp, indicated by the numbers. **E** Established multiplex PCR identifying wild type (866 bp) and knockout band (560 bp) in one PCR. SA splice acceptor, LacZ β-galactosidase gene, NEO neomycin resistance gene, φ NEB Marker φX174 DNA-HeaIII digest, Br brain, Hr heart, Ki kidney, Li liver, Te testis, M Fermentas λ DNA/EcoRI + HindIII Marker 3, H water control

The *prcp* intron 4 spans 7352 bp (reference number ENSMUSG00000061119) a sequence to long to be simply sequenced. That is why primer walking was used as the method of choice. Designing seven forward primers (PRCP1 to PRCP7) every 1000 bp of intron 4 and a reverse primer at the 5'-end of the gene trap (GW1) led to amplicons in the combination of the forward primers PRCP4, PRCP5, PRCP6 the reverse primer GW1 (Figure 3D).

Cloning and sequencing of the fragment PRCP6/GW1 revealed the insertion of the gene trap between base 41,825 and 41,826 within the mouse *prcp* gene. A complete sequence overview of all used primers between exon 4 and 6 is given in Figure 1. Based on this information a multiplex PCR was created amplifying a wild type (866 bp) and a knockout band (560 bp) at the same time. An example of the established genotyping PCR used further on is shown in Figure 3E.

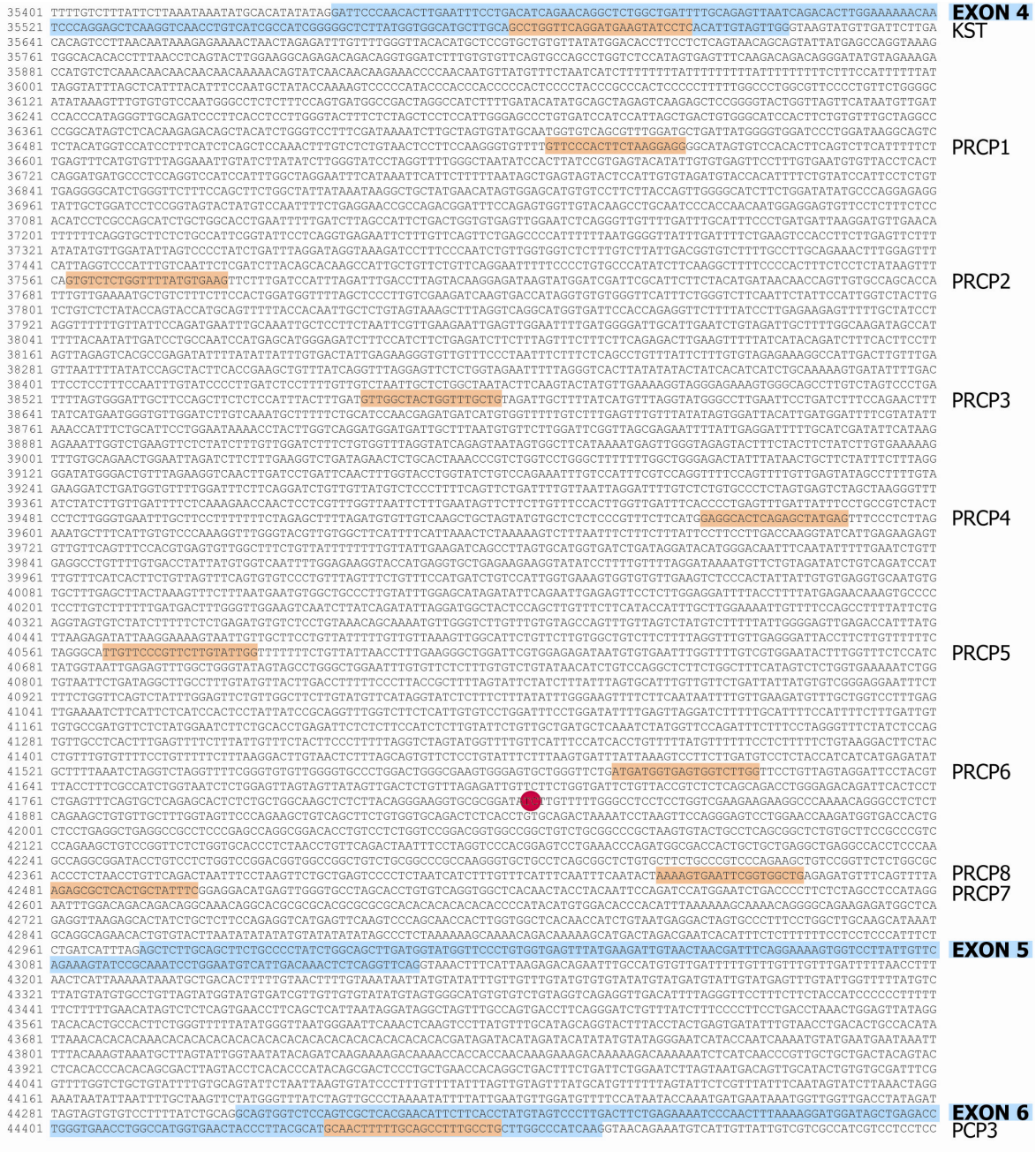

Figure 4: Insertion site of the gen trap vector in the *prcp* gene.

Primers (orange boxes, PRCP1 to PRCP7) were designed every 1000 bp between exon 4 and exon 5 of the mouse *prcp* gene (ensemble accession number ENSMUSG00000061119). The gene trap insertion site was identified by primer walking PCR between base T at position 41825 and C at position 41826 (red circle). Coding exons sequences are highlighted in blue. The primers KST and PCP were used for probe design of a *prcp*-specific ribonuclease protection probe.

4.1.3 Phenotypic Description of the PRCP Knockout Mouse

After successful generation of the PRCP knockout mouse, animals were backcrossed to guarantee working with genetically pure backgrounds. As mentioned in The Jackson Laboratory strain detail sheet of the FVB mouse lines, these mice show a good breeding performance (http://jaxmice.jax.org/support/phenotyping/FVBNJdata001800.pdf). Due to this fact the back cross with FVB/N wild type mice until the eighth generation (PRCP_FVB/N) was already finished while the back cross to C57Bl/6 wild type mice (PRCP_C57Bl/6) was still in progress. Therefore, most of the examinations were carried out using PRCP_FVB/N mice from homozygous knockout and wild type mouse breedings. If not mentioned different in the text, PRCP_FVB/N mice were used for the experiments.

Knowing that PRCP expression is highest in human placenta [3], litter size and birth rate were monitored regularly, to rule out a role of PRCP already in embryonic development. Compared to homozygous wild type mice, PRCP-/- breedings showed the same birth rate, approximately every 24 days like their controls. The average litter size was determined by comparing the fourth to sixth litter of five and six mating cages per genotype. Within a trio-breeding formation (one male + two females) PRCP+/+ had 11.8±2.7 and PRCP-/- 11.7±3.1 pups per litter.

To exclude general growth abnormalities, groups of male PRCP_C57Bl/6 mice were checked for body length. Anal-nose length of 20 weeks old, anesthetized mice was not different between PRCP-/- (8.7 cm) and PRCP+/+ (8.79 cm) and also not in twelve-week-old mice (Figure 5A). But monitoring body weight of mice starting at the age of weaning (four weeks) revealed that already one month old PRCP-/- mice are 2.9 g less heavy than age-matching wild type controls and this difference is still present until reaching adulthood with around twelve weeks (Figure 5B). This observation prompted further investigations (chapter 3.2).

Studying long-term survival, PRCP-/- and control mice with mixed genetic background and FVB/N background were followed. Even though the animals did not show any obvious impairment in terms of body shape or signs of sickness, life expectancy seems to be reduced for PRCP-/- mixed background animals. At the age of 18

months already 50% of the PRCP-/- mice had died while 77% of wild type mice were still alive (Figure 5C). The same tendency of shorter life span could be seen in a smaller group of PRCP_FVB/N mice (Figure 5D). A Kaplan Meier analysis performed on data from mixed background animals, revealed a p-value of 0.0575.

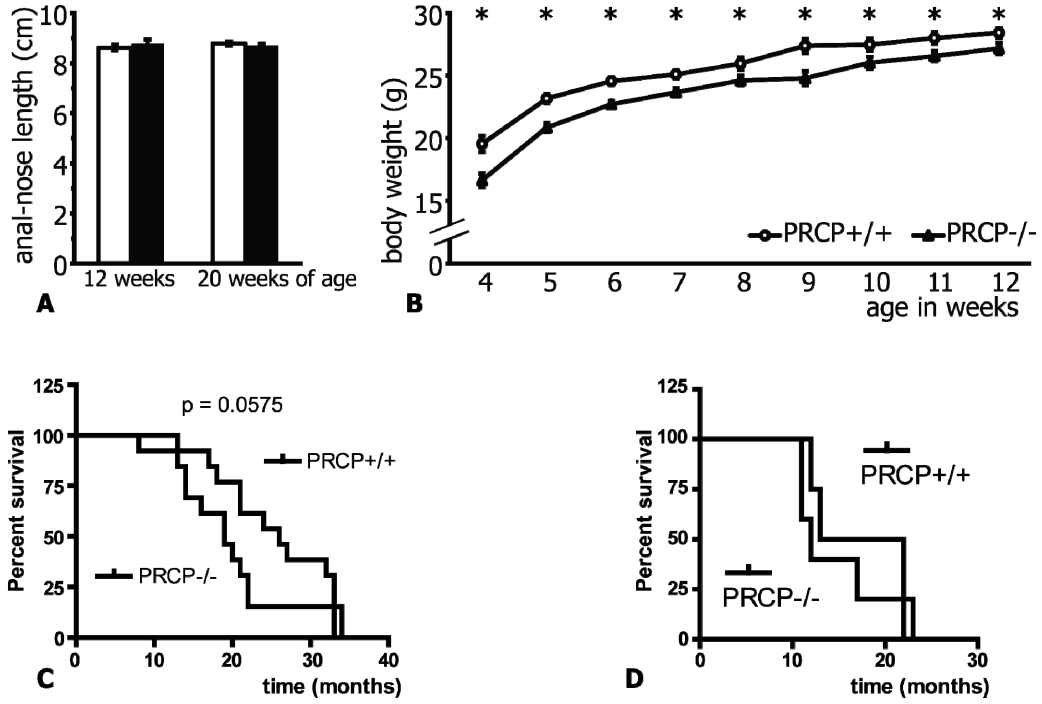

Figure 5: Body dimensions and survival of PRCP knockout mice.

A anal- nose length of two different aged groups of PRCP-/- (black bars, n=7 and 8) and PRCP+/+ mice (white bars, n=7 and 9). **B** Body weight development of mice in the age between 1 and 3 months (PRCP+/+ n=32, PRCP-/- n=25). Life expectancy of mice with **C** mixed background (n=13 each group) and **D** FVB/N background (n=5 each group). All data are mean ± SEM, *p < 0.05.

4.1.4 *Prcp* Gene Expression and Protein Content in Mouse Tissues

Different studies show PRCP presence or expression in a variety of organs, cell types and body fluids [3]. Among these publications also controversial discussions about species-specific expression of the enzyme e.g. in lung can be found [97]. Therefore a screening for basal expression of *prcp* gene in mouse wild type organs was performed using qPCR.

As the RNA content per gram tissue and even per cell may vary between individuals, different tissues and under different experimental conditions (reviewed in Pfaffl et al. [98]), the expression of *prcp* was normalized to a house keeping gene. These genes are

constitutively expressed and are required for the maintenance of the basic cellular functions. The house keeping genes used here were β-actin (*actb*) and tata box binding protein (*tbp*).

Initial studies showed that *actb* expression is highly different in wild type mouse tissues. On the other hand, the expression of *tbp* was found stable for nearly all organs tested. Only in adrenal gland and heart the C_t values were decreased for about 2 cycles. As C_t levels of *prcp* were also found to be decreased in these organs, *tbp* was kept as a standard for normalization of the whole expression study to make the data gained comparable.

Figure 6A is giving an overview about *tbp* versus *prcp* ΔC_t values. This analysis showed that *prcp* expression is highest in RNA extracts from brain, followed by white adipose tissue (WAT), kidney, lung, heart and small intestine. Calculating *prcp* expression in aorta was difficult, as the C_t values gained from RNA of two different trails of RNA preparation were found to vary strongly, seen by the high SEM given in the graphic. Furthermore, *prcp* expression is present in all other tissues tested.

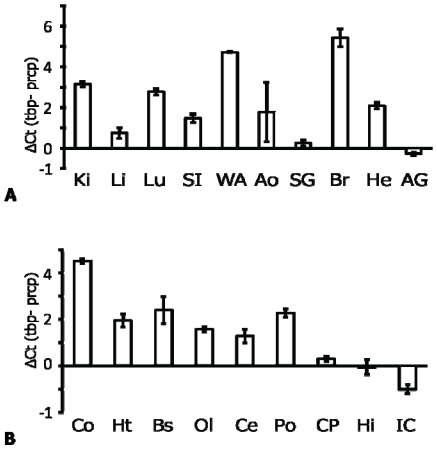

Figure 6: *Prcp* expression in mouse tissues.

Quantitative real time PCR for *prcp* in wild type mouse tissues **A** and selected brain areas **B**. Ki kidney, Li liver, Lu lung, He heart, SI small intestine, WA white adipose tissue, Ao aorta, AG adrenal gland, SG salivary gland, Br brain; Co cortex, Ht hypothalamus, Bs brain stem, Ol olfactorial bulb, Ce cerebellum, Po pons, Hi hippocampus, IC inferior colliculus, CP striatum; all data are mean ± SEM

To find out whether *prcp* expression is restricted to a particular part of the brain, qPCR of nine areas of the brain was done (Figure 6B). The evaluation of this study revealed that *prcp* gene expression was not limited to particular brain regions, but is

present all over the brain. Between these brain areas the cortex presented the highest ΔC_t followed by brainstem, pons and hypothalamus. The expression levels shown for hippocampus and inferior colliculus (IC) could not be compared directly to the rest of the brain samples, as again the *tbp* C_t in this samples was around 2 cycles decreased from that seen in the other brain parts.

For visualization of protein content in wild type organs the commercially available antibodies T-15 and Y-15 specific to PRCP were tested. Using different protocols starting with the Western blot conditions published the first time by Shariat-Madar and colleagues [21,28] it was not possible to find a specific band in the pattern appearing for wild type tissues, which was absent or at least less strong in the PRCP-/- animals (data not shown). Changing the original protocol utilizing different membrane types, different blocking solutions (milk protein, BSA, Roti-Block and Odyssey Blocking) and proteins concentrations from different organs did not allow the identification of the predicted 56kDa band.

The same antibodies were published to be applicable for immuno histochemistry. Testing both antibodies in different concentrations on brain and kidney sections did not give specific signals (data not shown). Also a closer look at structures like hippocampus or prefrontal cortex of the brain, which show *prcp* promotor activity in X-Gal stainings (chapter 4.1.5), did not turn out to be different comparing wild type and knockout slices.

4.1.5 PRCP Promotor Activity in the Brain

As immuno histostaining with the tested antibodies was inapplicable, another staining procedure using the selection markers provided by the gene trap was used. Next to the neomycin resistance gene the pGT1.8TM vector includes the β-galactosidase gene (*lacz*), which is expressed instead of the *prcp* full gene. Thus, incubating tissue slices with the β-galactosidase substrate X-Gal, turns areas of *prcp* promotor activity only in knockout tissue blue. Due to endogenous *lacz* expression in some organs tested (heart, liver, spleen, lung, kidney, salivary gland and pancreas) this method is not able to replace immuno histochemistry completely, with one exception: the brain.

Here, background staining in wild type tissue was absent even when staining for 48 hours. Therefore, *prcp* gene promotor activity presented here is restricted to the mouse brain.

Using this staining technique all brain areas exhibiting expression of *prcp* by qPCR were confirmed by specific blue stainings in the corresponding brain slices. The correlation of the stained brain nuclei to known structures of the brain was done by comparing the slices to mouse brain maps of Allen Brain Atlas (http://mouse.brain-map.org/welcome.do). In slices of the frontal lobe of the telencephalon blue staining was found in the central amygdala, arcuate nucleus (ARC), subcommissural organ (SCO), paraventricular nucleus (PVN), choroid plexus of the central ventricle, hippocampus and highly pronounced in layers of the motor cortex (Figure 7). In brain stem sections a clear staining was located to the nucleus of the solitary tract (NTS), vagus nerve, nucleus ambiguous, area postrema (AP) and the area of rostral and caudal ventrolateral medulla (RVLM, CVLM). Layers of the olfactory bulb also revealed characteristic staining patterns (Figure 8).

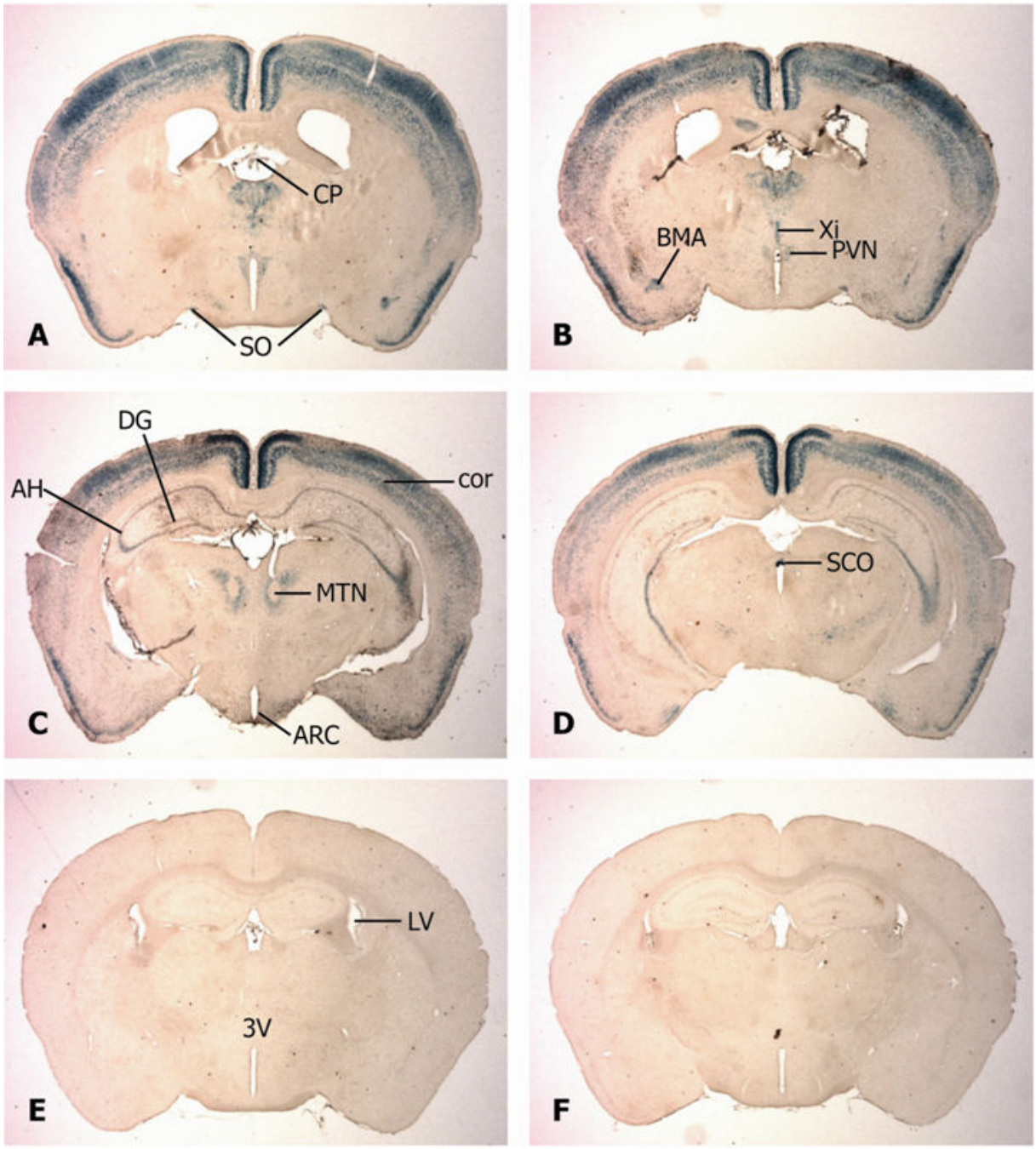

Figure 7: X-Gal staining of mouse brain slices.

Coronal sections of the telencephalon. **A** to **D** PRCP-/-, **E** and **F** PRCP+/+. Brain sections were incubated 48 hours in X-Gal staining solution (blue), followed by 30 seconds EosinY counter staining (red). AH and DG hippocampus, ARC arcuate hypothalamic nucleus, BMA basomedial amygdaloid nucleus (anterior part), CP choroid plexus, PVN paraventricular nucleus, LV lateral ventricle, MTN mediodorsal thalamic nucleus, SCO subcommissural organ, SO supraoptic nucleus, cor cortex, 3V 3rd ventricle, Xi xiphoid thalamic nucleus

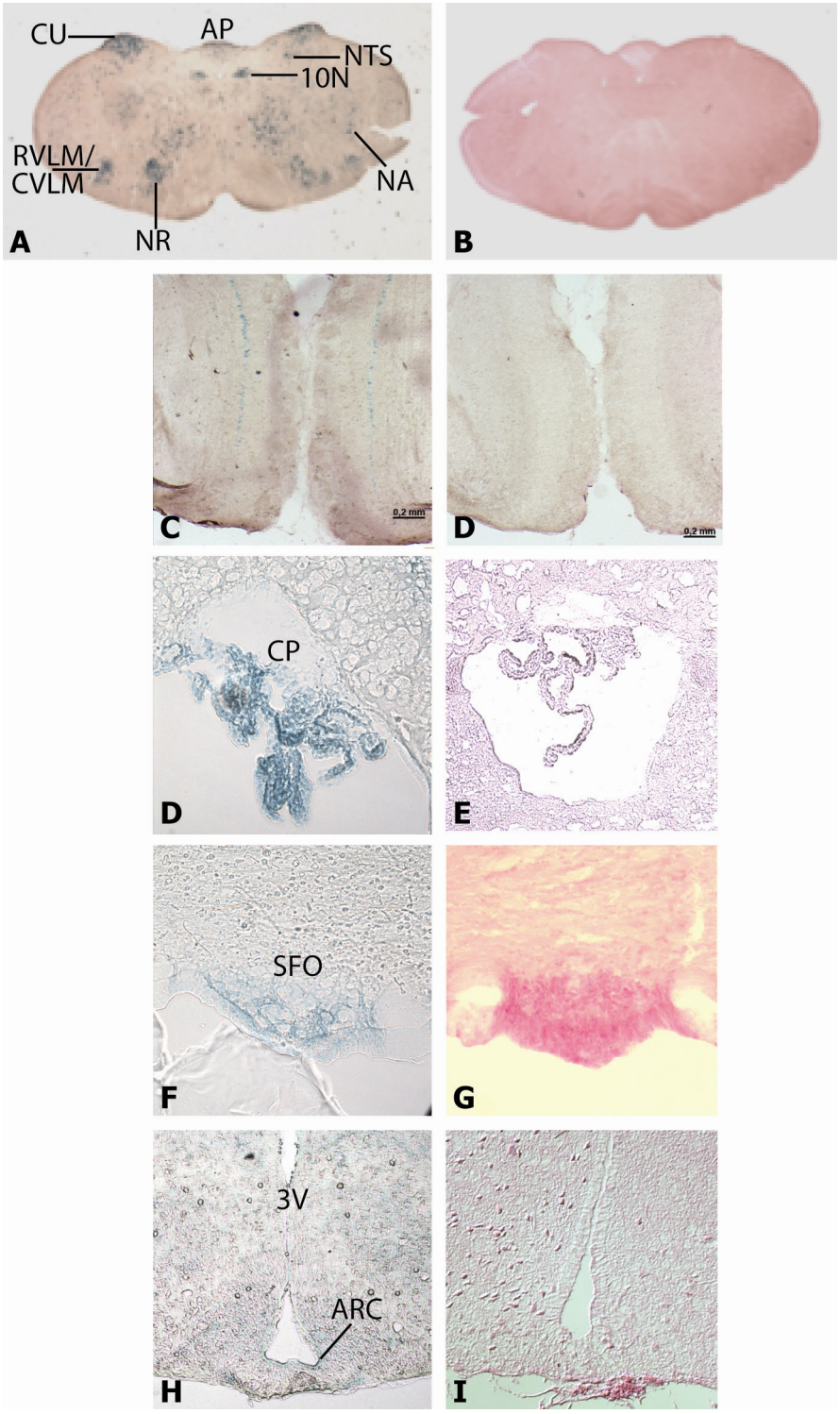

Figure 8: X-Gal staining of mouse brain slices.

Brain sections were incubated for 24 to 48 hours with X-Gal staining solution (blue), followed by 30 seconds EosinY counter staining (red). Left panel exhibits PRCP-/- brain slices, right panel PRCP+/+ controls. **A** and **B** are sections through the brain stem, **C** and **D** through the olfactorial bulb (2.5x magnification) and **D** to **I** are details taken from coronal slices of the telencephalon (20x magnification). Cu cuneate, AP area postrema, NTS nucleus of the solitary tract, 10N nervus vagus, RVLM/CVLM area of rostral- and caudal ventrolateral medulla, NR nucleus reticularis, NA nucleus ambiguus; CP choroid plexus; SFO subfornical organ; 3V 3rd ventricle, ARC arcuate nucleus

4.2 PRCP and Body Weight

Out of the list of potential PRCP substrates (Table 1) there are at least three peptides and small proteins, which play essential roles in the regulation of food intake and energy homoeostasis. These substrates include an N-terminal fragment of Agouti related peptide (AgRP), ghrelin (GHRL), and alpha melanocortin stimulating hormone (αMSH). Hence, body weight parameters and metabolic pathways were checked in the PRCP-/- mice.

4.2.1 PRCP-/- Mice are Leaner than Wild Type Controls

On the first view the body weight phenotype of the PRCP-/- mice is not clearly visible. But analyzing a large group of animals (n=23 to 36) revealed that they are leaner then wild type controls and this difference remained stable over the whole period measured but tended to be reduced with age (chapter 4.1.3). To further challenge this phenotype the mice were fed a 45% high fat diet (HD) for ten weeks (PRCP_C57Bl/6) or six months (PRCP_FVB/N). This diet increased the difference between wild type and knockout mice body weight independently of the background strain, finally showing that PRCP-/- mice stay lean while wild type mice gain weight as expected. Figure 9A is showing the body mass gain for mice on C57Bl/6 background.

Additionally a NMR-based body composition scan of male mice (C57Bl/6) before and after feeding three months a HD demonstrated wherein the differences in body weight consists off. The analysis of ten week old males fed a standard diet (SD) so far showed significant differences between the genotypes only in increased free liquid of PRCP-/- mice (6.52 $\pm$ 0.21% vs. 4.85 $\pm$ 0.44% in PRCP+/+, Figure 9B-D). The same analysis done after feeding ten weeks HD revealed that the main difference in body composition is characterized by less fat accumulation in the PRCP-/- (17.67 $\pm$ 1.04%) in contrast to wild type mice (21.08 $\pm$ 0.85%). Free water content and muscle mass were not different Figure 9E-G).

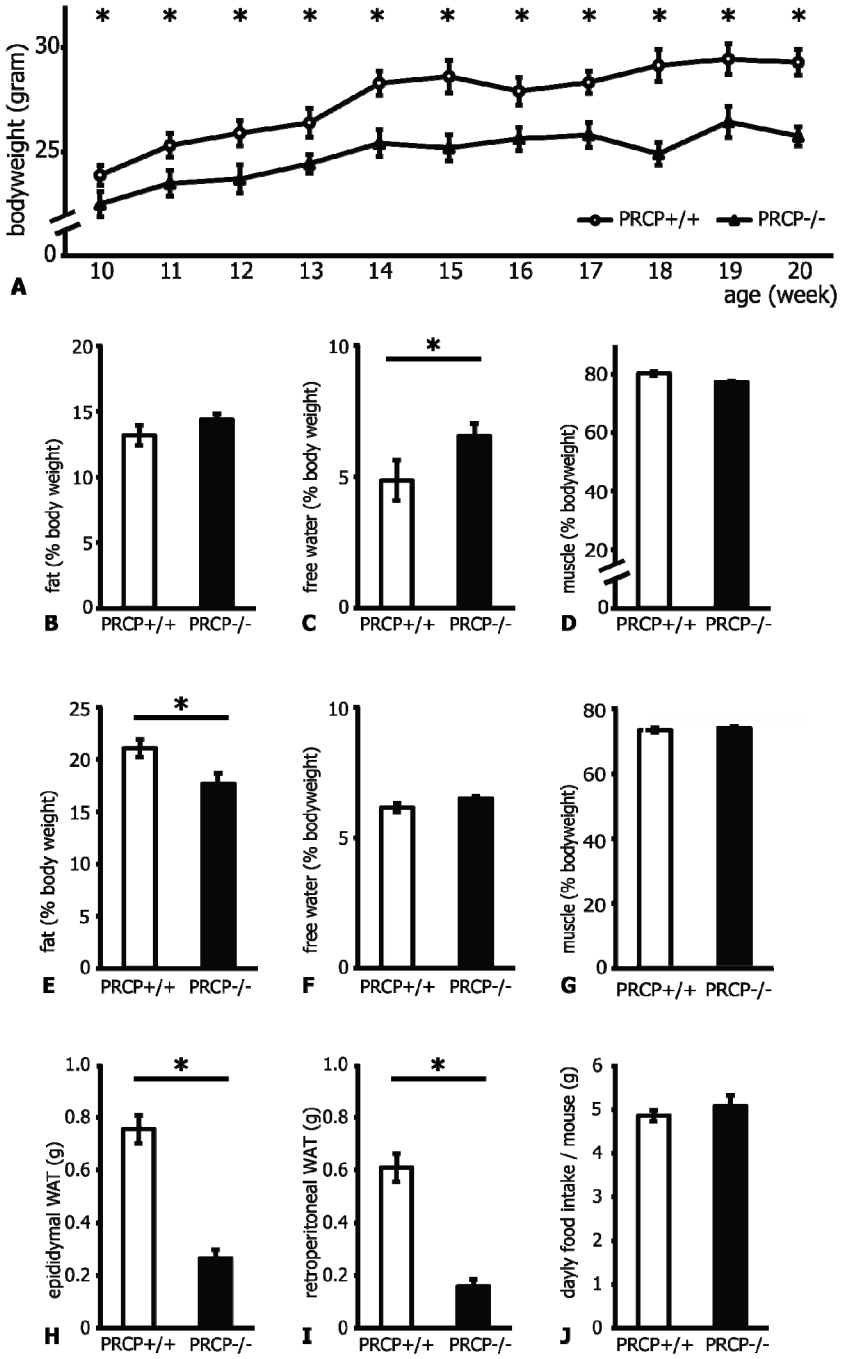

Figure 9: Body weight phenotype of PRCP-/- mice on C57Bl/6 background.

A development of body weight of PRCP+/+ and PRCP-/- (n=9 each group) when feeding 45% HD. **B** to **D** body composition scan of 10 week old male mice (PRCP+/+ n=8, PRCP-/- n=12). E to G body composition scan, **H** and **I** weight of particular fat depots of 20 weeks old male mice fed 45% HD over 10 weeks (n=9 each group). **J** Food intake of single housed 12 week old male mice (PRCP+/+ n=9, PRCP n=11). All data are mean ± SEM, *p < 0.05 vs. control

To see if fat depots are differentially affected in weight gain gonadal and retroperitoneal white adipose tissues from animals fed three months a HD were weighed indi-

vidually. As shown in Figure 9H and I both tissues displayed a significant reduction of weight in PRCP-/- mice.

4.2.2 Food Intake is not Reduced in PRCP-/- Mice

One mechanism by which hormones act to regulate body weight is by controlling appetite and food intake. Rising GHRL levels activate AGRP/NPX neurons of the hypothalamus to release AGRP, a potent orexigenic hormone. On the other hand αMSH was shown to signal satiety stimuli in the brain and to reduce leptin expression of rat adipocytes in culture [99]. But PRCP-/- mice do not show altered daily food intake when monitoring single housed animals in metabolic cages (Figure 9J).

4.2.3 Body Weight Related Hormones in PRCP-/- Mice

The reduced body weight in PRCP-/- mice gave strong evidence for changes in important metabolic pathways. Therefore potential PRCP candidate substrates as well as other hormones involved in weight control were tested for changes in expression and plasma content.

4.2.3.1 Ghrelin

Ghrelin is mainly produced in stomach mucosa and released into circulation. When reaching a specific threshold in the plasma, hypothalamic POMC neurons become activated to induce appetite. As described in the chapters above PRCP-/- mice exhibit a lean phenotype suggesting that if GHRL is involved in this phenotype plasma peptide content and gene expression levels at the tissue of origin could be changed in PRCP knockout mice.

The co expression of *prcp* and *ghrl* gene in wild type stomach presented in Figure 10A is showing that the enzyme is transcribed in the same tissue as the postulated substrate is produced. But neither the expression of *ghrl* nor the plasma content was found to be different in PRCP-/- mice (Figure 10B and C).

4.2.3.2 Agouti Related Peptide

As a counter player of αMSH agouti related peptide (AgRP), is a potent orexigenic hormone. Binding to the same receptors MC3R and MC4R like αMSH, AGRP blocks in hypothalamus the signal cascade normally activated by αMSH leading to increased food intake and lowered energy expenditure.

As the consequences of cleaving the last carboxy-terminal amino acid from the peptide are unknown yet, it can only be speculated whether an impact of PRCP is activating, degrading AGRP or has no effect at all. Postulating there is a change in peptide function seen by the lean phenotype of PRCP-/-, regulation of gene expression possibly changes in order to compensate the implications of lacking PRCP. Therefore *agrp* expression in knockout hypothalami was studied. But even though *prcp* gene expression is present in wild type hypothalami the expression level of *agrp* in PRCP-/- mice did not show any significant difference compared to their wild type controls (Figure 10D).

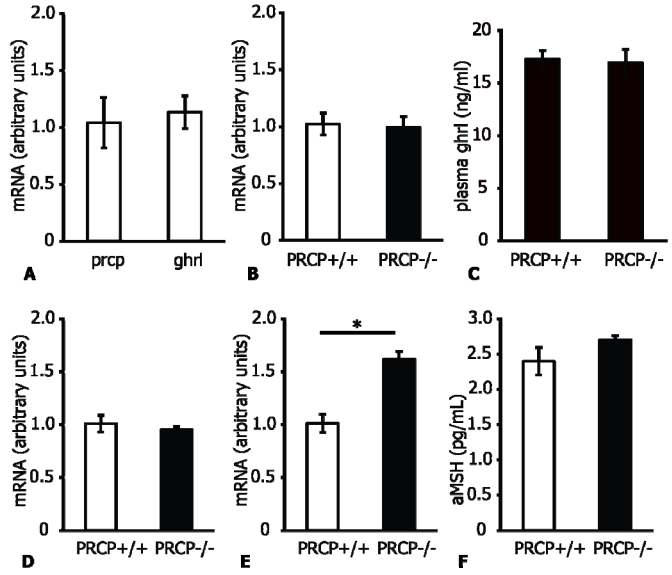

Figure 10: Measurement of potential PRCP substrates.

Quantitative realtime PCR showing **A** coexpression of *prcp* and *ghrl* in wild type stomach and **B** *ghrl* expression in PRCP-/- and wild type stomach (n=4 each group). **C** Plasma content of GHRL (n=10 each group). Expression of *agrp* **D** and *pomc* **E** in hypothalamus measured by qPCR. **F** αMSH plasma content (PRCP+/+ n=7, PRCP-/- n=9). All data are mean ± SEM, *p < 0.05 vs. control

4.2.3.3 α Melanocortin Stimulating Hormone

The peptide hormone αMSH is mainly produced within the intermediate pituitary lobe of rodents but also from POMC neurons in the ARC of hypothalamus, in monocytes, astrocytes, gastrointestinal cells and keratinocytes [100]. To measure peripherally circulating levels of αMSH an ELISA was used that was able to detect specifically αMSH but no similar *pomc* gene derived products like adrenocorticotropic hormone. As shown in Figure 10F plasma levels of αMSH are not different comparing PRCP-/- to wild type mice. But local expression of the *pomc* gene is two times increased in PRCP-/- hypothalami (Figure 10E). On the other hand immunohistochemical staining of the ARC in brain slices of PRCP-/- mice and controls did not show obvious changes of αMSH (data not shown).

4.2.3.4 Leptin

Leptin is the key activator of POMC neurons in hypothalamus leading to increased *pomc* gene transcription and release of αMSH from synapses when elevated levels in plasma are present. As seen by qPCR analysis shown in chapter 3.1.4., *prcp* is expressed in WAT nearly to the same extend as in brain, suggesting a role of PRCP in this tissue. Therefore the basic plasma level of leptin from twelve weeks old male mice was measured using a commercially available kit. Leptin levels in the knockouts were more than doubled (325.15 ± 45.58 pg/mL) compared to PRCP+/+ (155.69 ± 25.92 pg/mL). At the same time the expression of leptin in white adipose tissue (WAT) displays only a tendency to be increased (Figure 11A and B).

Utilizing a different ELISA approach leptin levels were analyzed again in 9 month old mice fed SD or HD (Figure 11C). As expected plasma leptin was found to be elevated in wild type mice on HD compared to SD (Δ 3154.28 pg/mL) as well as in PRCP-/- (Δ 3333.39 pg/mL). Of note, the basal hyperleptinemia discovered in young PRCP-/- mice is not significant in nine-month-old mice (SD) anymore.

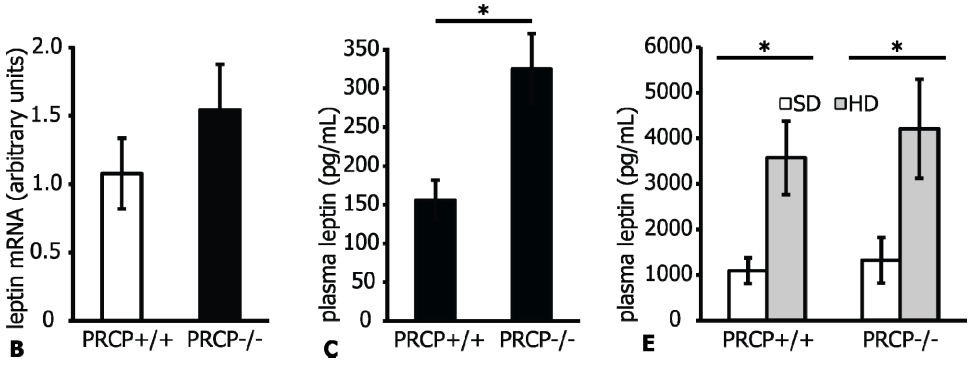

Figure 11: Leptin gene expression and plasma content.

Quantitative real time PCR for **A** *lep* in PRCP-/- and wild type WAT (n=4 each group) and **B** plasma leptin concentration (PRCP+/+ n=7, PRCP-/- n=8) of 12 week old mice. **C** plasma leptin content of 9 month old mice, fed a high fat diet (HD) or standard diet (SD) (PRCP+/+(SD) n=11, PRCP+/+(HD) n=10, PRCP-/-(SD) n=7, PRCP-/-(HD) n=10). WAT white adipose tissue. All data are mean ± SEM, $p < 0.05$ vs. control

4.2.3.5 Insulin

In the classical view of neurobiology the brain is considered a privileged organ that predominantly utilizes glucose for its metabolism. Glucose-sensing neurons were described decades ago but that POMC cells are taking over the role of glucose sensors in the ARC, was published just recently [101,102,103,104]. To test the influence of elevated *pomc* gene expression in hypothalamus and the hyperleptinemia in young PRCP-/- mice, blood glucose levels, peripheral glucose uptake and insulin sensitivity were examined in these animals.

Blood glucose was measured in 24 hours fasted male mice at the age of eight weeks. These mice did not show any basal changes in their glucose content (Figure 12C). In another group of twelve week old adult mice a glucose tolerance test was performed (Figure 12A). The basal blood glucose of these twelve hours fasted animals displayed again no differences between the groups (132.90 ± 8.25 mg/dL PRCP-/- vs. 134.33 ± 12.24 mg/dL in PRCP+/+). Following an injection of 2mg D-glucose per gram of body weight a peak level of blood glucose was reached after 30min, without revealing differences in the animal groups tested (424.30 ± 14.30 mg/dL PRCP-/- vs. 400.00 ± 40.56 mg/dL in PRCP+/+). Two hours later blood glucose levels returned to near basal levels for both groups.

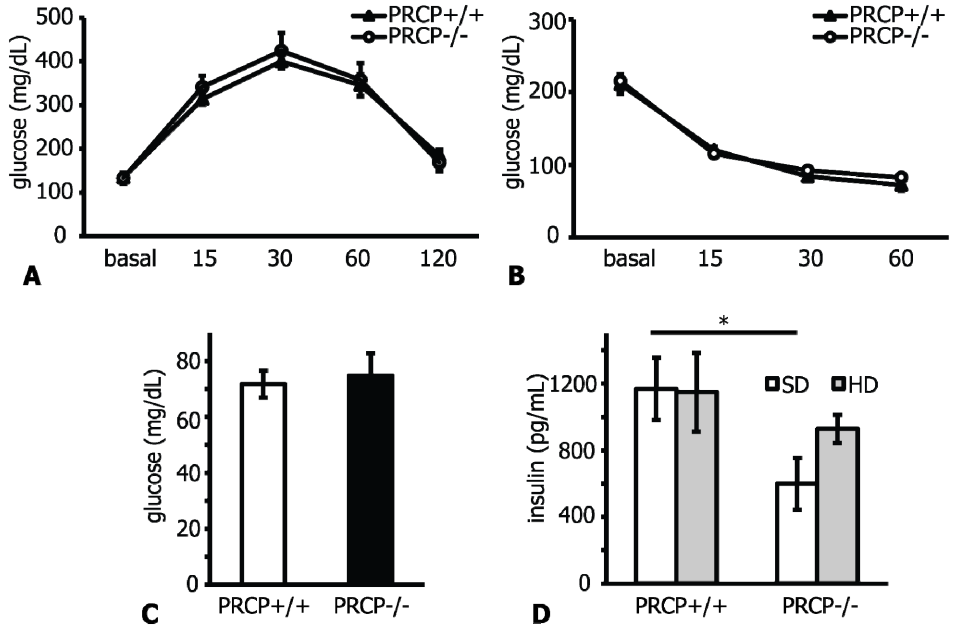

Figure 12: Glucose and insulin household in PRCP-/- mice.

A Glucose tolerance test injecting 2mg/kg D-glucose i.p. (PRCP+/+ n=9, PRCP-/- n=10). **B** Insulin sensitivity test injecting 0.75U/kg insulin. **C** basal blood glucose of 24 hours fasted mice (PRCP+/+ n=7, PRCP-/- n=6). **D** plasma insulin concentration of mice fed a high fat diet (HD) or standard diet (SD) (PRCP+/+(SD) n=11, PRCP+/+(HD) n=10, PRCP-/-(SD) n=7, PRCP-/-(HD) n=10). All data are mean ± SEM, *p < 0.05 vs. control

The same setup of experiment was used to perform an insulin sensitivity test (Figure 12B). A drop in blood glucose followed injection of 0.75U/kg insulin into these mice. The restoration process to reestablish normal blood glucose levels was monitored over 60 min for PRCP-/- (from 215.25 ± 13.61 mg/dL to 72.25 ± 7.60 mg/dL) and PRCP+/+ mice (from 210.75 ± 25.05 mg/dL to 82.50 ± 8.02 mg/dL) and was not found to be different over the period measured.

Quantifying plasma insulin concentrations in nine-month-old mice fed SD or HD revealed two interesting aspects (Figure 12D). While the groups of PRCP+/+ mice exhibited comparable insulin levels (SD 1168 ± 188 pg/mL and HD 1148 ± 237 pg/mL) plasma insulin is significantly decreased in the group of PRCP-/- mice on SD (599 ± 156 pg/mL) and a tendency of reduced insulin is also visible in HD fed knockouts (927 ± 86 pg/mL).

4.2.3.6 Activity of PRCP-/- Mice

Not only hyperphagia, but also behavioural adaptations have influence on body weight. In an experiment restricting food availability to MC4R-/- mice it has been shown that these mice develop obesity not only because of increased food intake but also due to lowered energy expenditure [105].

Therefore, single housed mice were monitored over three days in specialized cages to register their activity. Extracting the data with the ACTIMOT software (chapter 3.9.11) revealed no differences in basal activity or hyperactivity. Also circadian phases of resting and awake periods did not appear shifted or differentially pronounced (Figure 13).

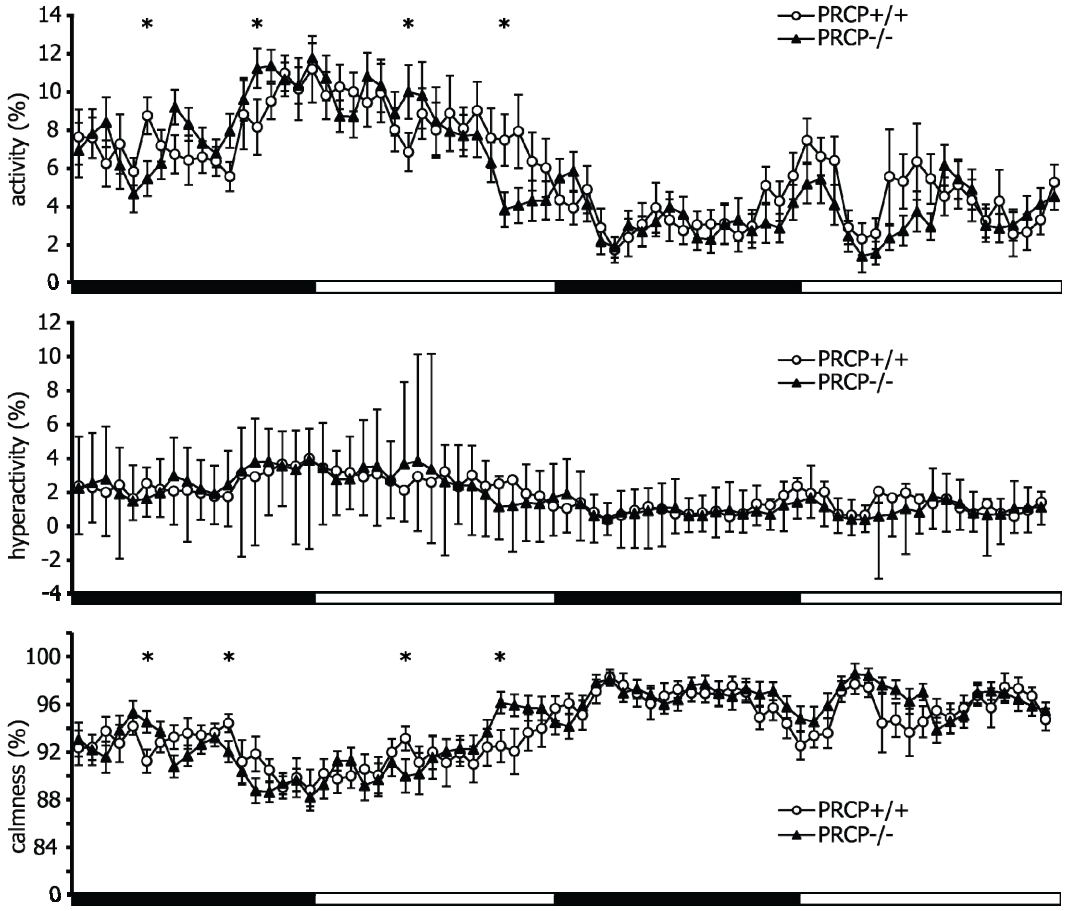

Figure 13: Activity of PRCP knockout mice.

The general activity **A**, hyperactivity **B** and calmness **C** was calculated by ACTIMOT® software. Displayed are 24 hours overviews of selected behaviours monitored (PRCP+/+ n=10, PRCP-/- n=11). Black and white bars stand for 6 hours starting with 3pm to 9pm (black), 9pm to 3am (white), 3am to 9am (black) until 9am to 3pm (white). All data are mean ± SEM, *p < 0.05 vs. control

4.3 PRCP and the Renin Angiotensin System

Initially, prolylcarboxypeptidase was named angiotensinase C when it was shown that it is cleaving AngII [1]. However, the exact role of the enzyme in cleaving this potent vasoactive hormone and at the same time generating the ligand Ang1-7 for the receptor Mas has never been clarified completely. Therefore, Ang peptides and known physiological consequences of a possible AngII overload were analyzed in the PRCP knockout mouse.

4.3.1 Angiotensin Peptides

Angiotensin peptides were measured using two different radioimmuno assays (RIA). First, protease inhibitor cocktail treated plasma samples were analyzed for AngI and AngII concentration. This study did not reveal any changes in peptide levels (Figure 14A and B). In a second approach AngII and its degradation product Ang1-7 were analyzed from SEP column extracts of blood and organs homogenized in GTC. Except a slight but insignificant AngII decrease in PRCP-/- kidneys no difference was present in the blood and selected organs tested (Figure 14C to G). But using the same extracts for Ang1-7 measurements revealed a 68% reduction of the peptide in knockout WAT (Figure 14H to L). In contrast the Ang1-7 concentrations in PRCP-/- kidneys were found to be 3-fold increased compared to the level found in wild type kidneys (Figure 14I).

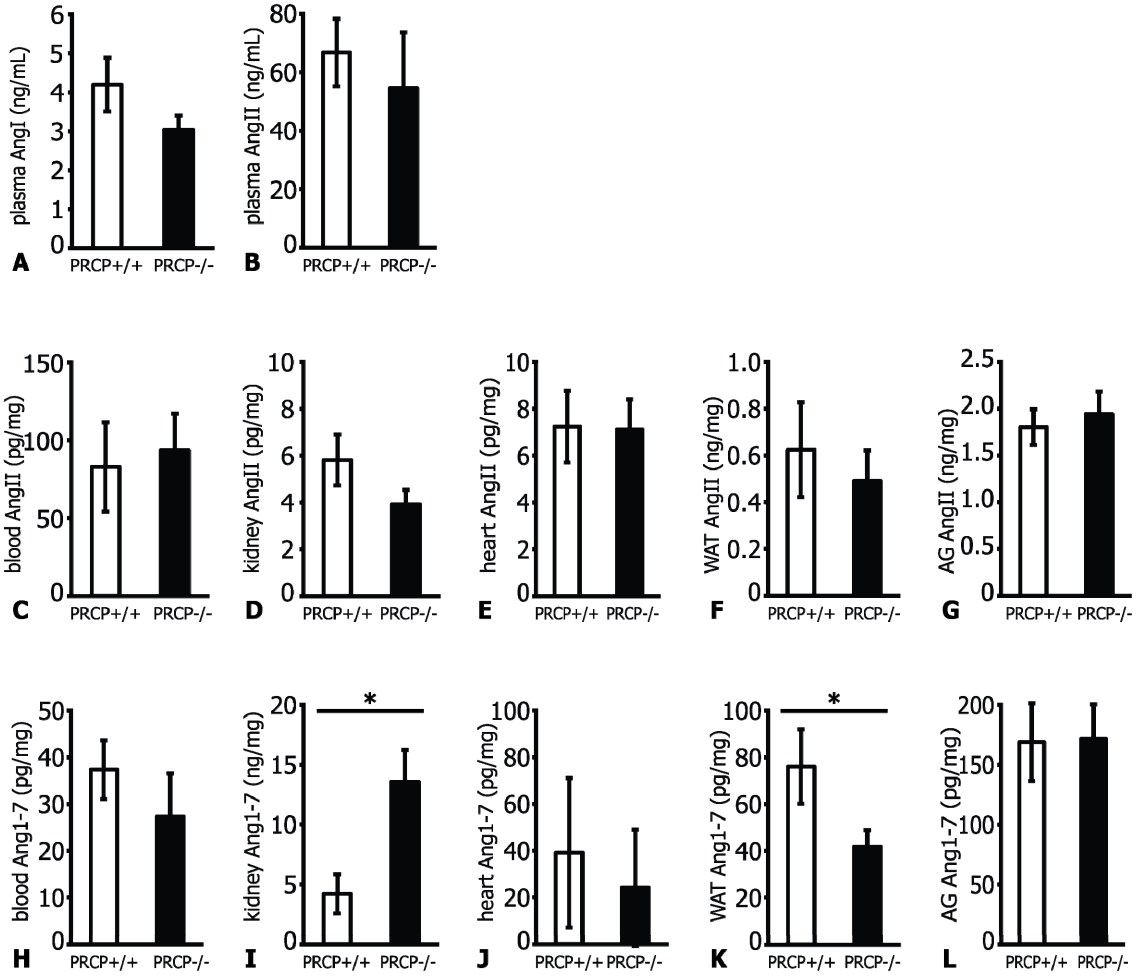

Figure 14: Angiotensin peptides measured by radioimmunoassay.

AngI **A** and AngII **B** measurement using protease inhibitor-treated plasma (n=7, each group). AngII **C** to **G** and Ang1-7 **H** to **L** measurement using extracted peptides from blood and organs (PRCP+/+ n=6, PRCP-/- n=9) all data are mean ± SEM, *p < 0.05, AG adrenal gland, WAT white adipose tissue

4.3.2 Enzymes Involved in Renin Angiotensin System

The concentration and activity of three enzymes important for RAS signaling were analyzed using two different assays. Renin, as the rate-limiting enzyme releasing AngI from its precursor AGT, is the key enzyme starting the RAS cascade. But the quantification of renin with RIA in plasma of PRCP-/- mice did not reveal any changes compared to wild type controls (Figure 15).

ACE2 and NEP activities were analyzed by assays utilizing peptide based enzyme substrates linked to a chromophor – here 2,4-Dinitrophenyl. Incubation of the NEP specific chromogenic substrate DALEK with tissue homogenates of kidney and small

intestine again did not show any abnormalities in PRCP-/- mice (Figure 15B). But using the ACE2 specific substrate MAPK, exhibited significantly increased activity in knockout kidneys (Figure 15C). At the same time ace2 expression in knockout kidney as well as ACE2 protein levels in the same tissue was not changed (Figure 15E and F).

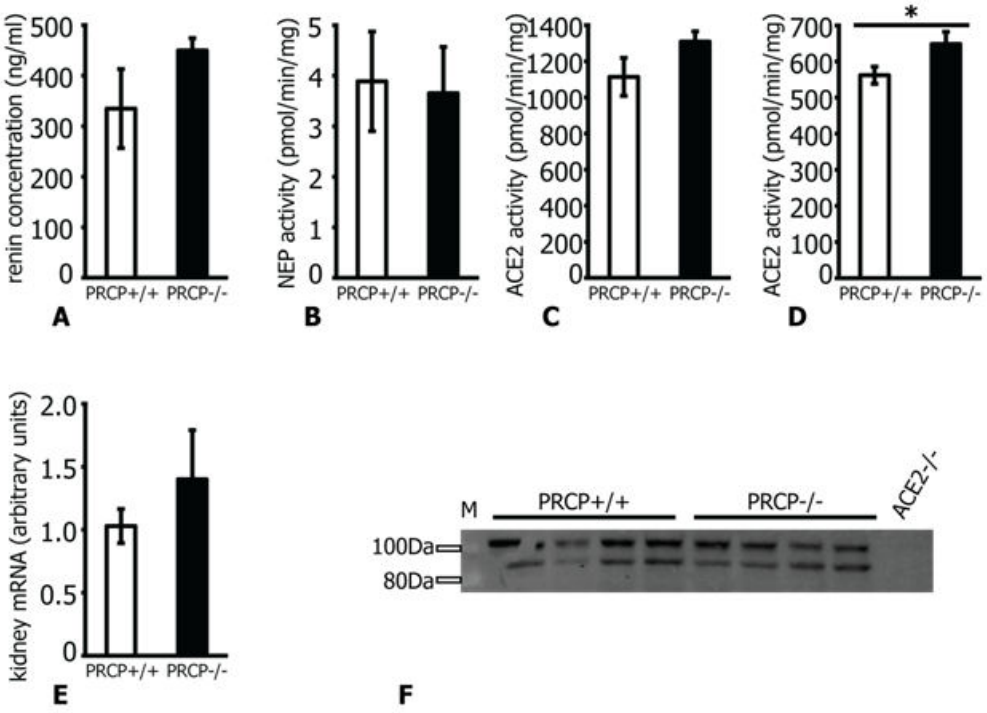

Figure 15: RAS enzyme activities.

Plasma renin concentration **A**, NEP activity in kidney extracts **B**, ACE2 activity in small intestine **C** and kidney extracts **D** (n=8 each group). Quantitative real time PCR measurements of *ace2* mRNA in kidney **E** and western blot detection of of ACE2 in kidney extracts **F** using a specific antibody (n=4 each group). All data are mean ± SEM, *p<0.05 vs. control, M marker, ACE2-/- protein extract from kidney of ACE2 knockout mice

4.3.3 Angiotensin Receptors

The AT1 receptor is mediating most of the actions of AngII while Ang1-7 was described to be responsible for counter balancing the actions of AngII via activation of Mas. Therefore a screen for these important RAS proteins was carried out using qPCR and western blot techniques. As the presence of both receptors has been demonstrated in kidney, heart and lung, these organs were chosen for analysis. The quantification of the expression levels of both receptors shown in Figure 16A and B

did not reveal significant differences. Western blot analyses confirmed that also protein levels of AT1 and Mas are not changed in the PRCP-/- mice (Figure 16C and D).

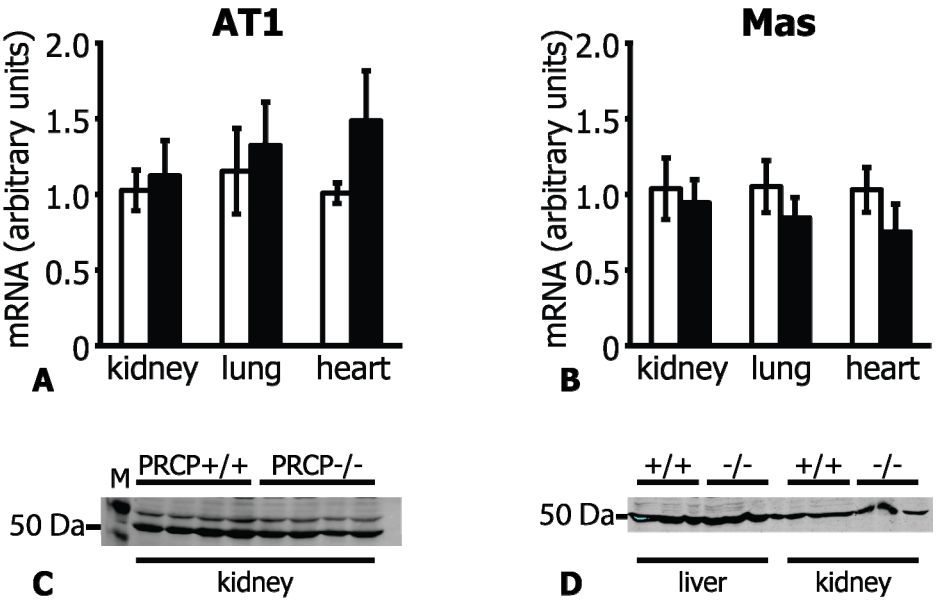

Figure 16: Angiotensin receptors.

AT1 receptor **A** and Mas expression levels **B** in selected organs. Western blot analysis using a AT1-specific antibody **C,** revealing the specific AT1 band at 50 kDa. Western blot analysis with a Mas-specific antibody **D** showing the specific band at 50 kDa. All data are mean ± SEM, n=4 each group, white bars indicate PRCP+/+, black bars PRCP-/- animals, M Odyssey® marker

4.3.4 Acute Infusion of Angiotensins and Bradykinin

The insertion of a femoral artery catheter is a standard method in cardiovascular research to measure blood pressure and heart rate response in reaction to an acute stimulus. In the following experiment, in which different dosages of AngI and AngII were applied to PRCP-/- mice backcrossed to FVB/N and C57Bl/6, are described. To rule out influences from the KKS on the RAS bradykinin (BK) was included into the list of injected compounds.

A first experiment was carried out using PRCP_FVB/N mice. Mean arterial pressure (MAP) and heart rate (HR) measured over a time of at least one hour before starting the experiment indicated no basal changes in the PRCP-/- mice (Figure 17A and C). Also the bolus injection of 1 μg/kg AngI, AngII and BK Figure 17A and C evoked only a typical response to every compound administered, but no difference between wild type and knockout mice was visible.

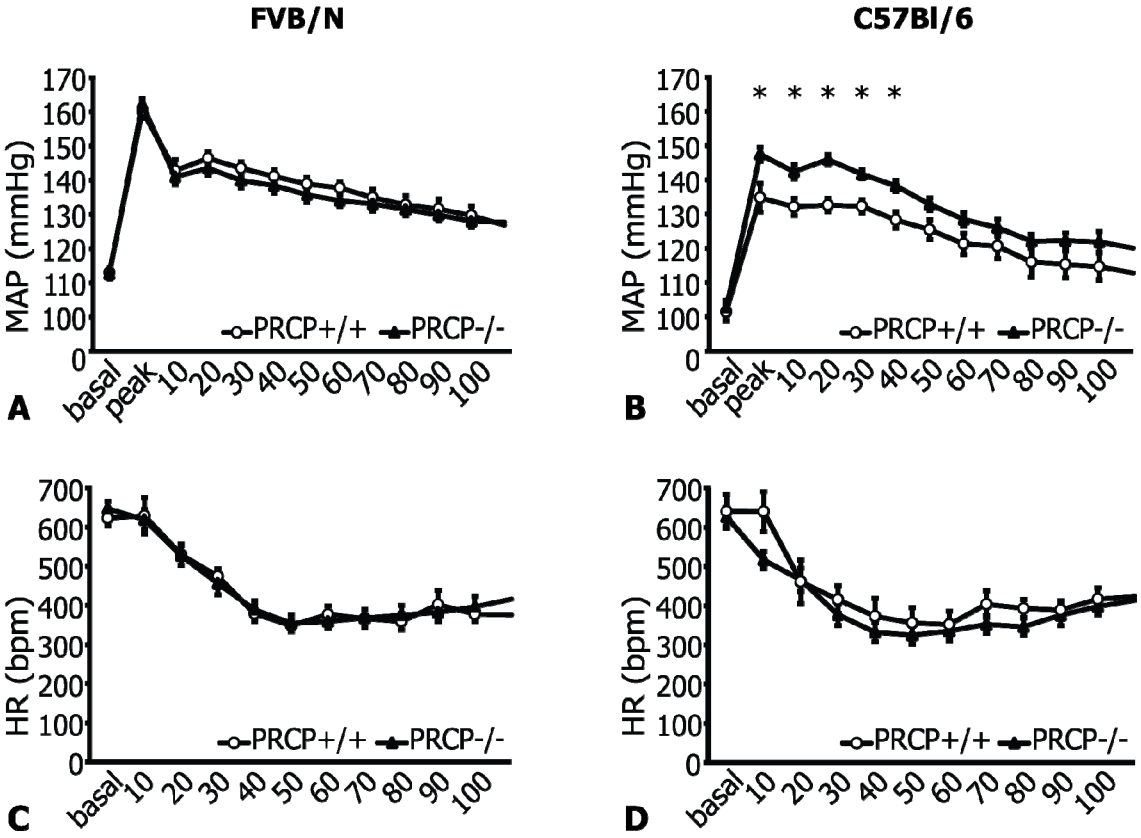

Figure 17: Acute angiotensin II injection (1μg/kg).

A Mean arterial pressure (MAP) and **C** heart rate (HR) of mice on FVB/N background (PRCP+/+ n=9, PRCP-/- n=11). **B** MAP and **D** HR of mice on C57Bl/6 background (PRCP+/+ n=6, PRCP-/- n=10). All data are mean ± SEM, *p < 0.05 vs. control

On the other hand, when repeating the experiment with PRCP_C57Bl/6 mice, one remarkable difference was discovered. An application 1 μg/kg of the vasoconstrictive peptide AngII revealed a 11.6 mmHg higher blood pressure response in PRCP-/- mice compared to controls while the fall in HR was not significantly changed (Figure 17B and D). The same response was monitored when using a lower dose (100 ng/kg) of AngII: Here, blood pressure rose 12.6 mmHg higher than wild type blood pressure, while heart rate was not found to react differently (not shown). Interestingly PRCP-/-_C57Bl/6 mice were able to catch up with wild type mice normalizing blood pressure to the same level (~110 mmHg) after three minutes.

4.3.5 Chronic Infusion of AngII

The increased response of knockout PRCP_C57Bl/6 mice to acute AngII injection (chapter 4.3.4) raised the question how these animals would react to a chronic AngII

overload. For this purpose telemetry transducers were inserted into a group of five PRCP-/- and six PRCP+/+ male mice (13 week old, FVB/N background). After ten days of recovery following the operation the basal MAP and HR was measured and both increased in PRCP-/- mice. Twenty-four hour average blood pressure went 8.7 mmHg beyond the basal wild type level, the HR was 36 bpm increased (Figure 18B and E). In parallel, activity data from telemetry revealed no changed activity of knockout mice indicating that the increased blood pressure and heart rate are activity independent.

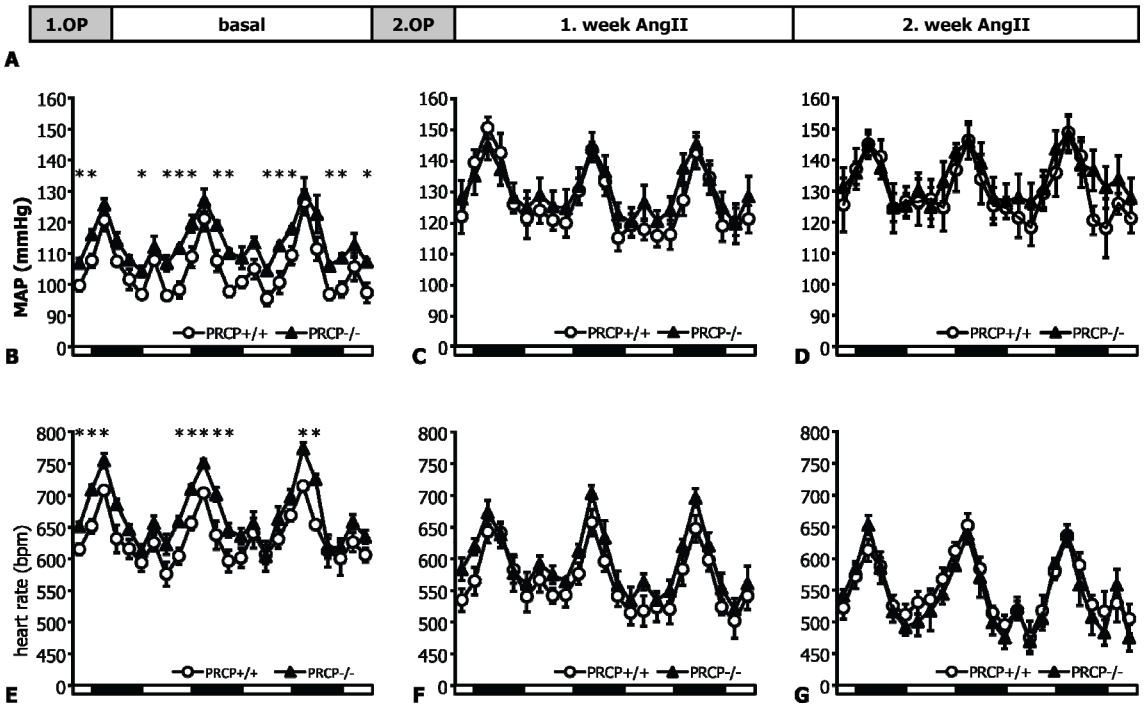

Figure 18: Telemetry and chronic AngII infusion.

A Scheme of experimental setup: The first operation (1.OP) indicates the starting point of experiment when telemetry transducers were inserted into mice followed by a period of basal mean arterial pressure (MAP) **B** and heart rate **E** monitoring (basal). A second operation (2.OP) was carried out to insert mini pumps filled with AngII to apply a constant dose of 1.4 mg/kg/d to the animals. From the measurement of MAP (**C** and **D**) and heart rate (**F** and **G**) following AngII treatment three representative days for each week are shown (n=5 each group). X-axis indicate periods of the day with white bars standing for the time between 3am to 3pm and black bars from 3pm to 3am. All data are mean ± SEM, *p < 0.05 vs. control

Infusing chronically 1.4 mg/kg/d AngII via mini pumps raised blood pressure and dropped heart rate of both groups over the whole period monitored. But neither heart rate nor MAP was significantly different in PRCP-/- mice (Figure 18C, D, F and G).

4.3.6 Echocardiography

Echocardiography was used to analyze changes in heart morphology in young adult PRCP-/- mice and after treating the mice three weeks with AngII (1.4 mg/kg/d).

Basal echocardiography was carried out using 13 weeks old male PRCP_FVB/N mice. This measurement revealed that young adult PRCP-/- mice already exhibit mild hypertrophy shown by increased LVPWd/LVD ratio compared to wild type hearts (Figure 19A). Fractional shortening and ejection fraction exhibited a tendency to be increased but were not significantly changed (Figure 19B and C).

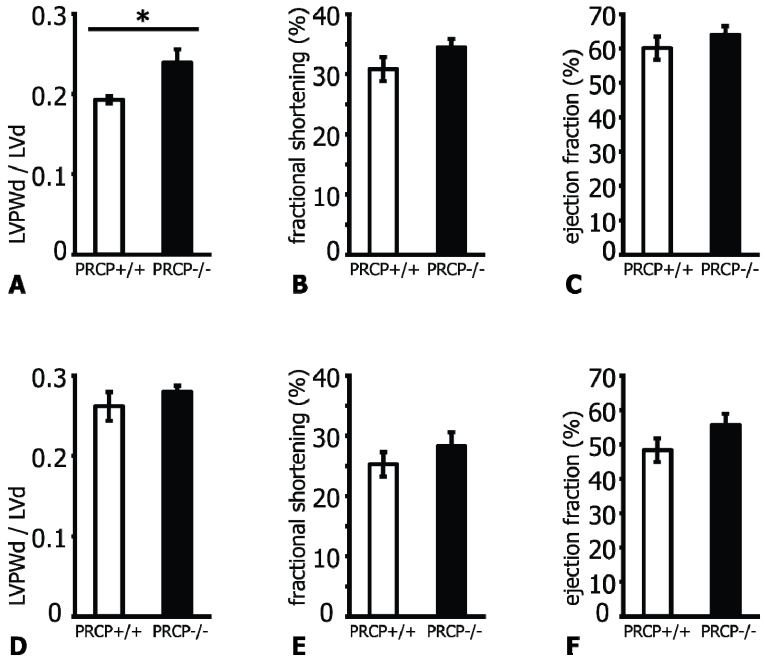

Figure 19: Echocardiography before and after chronic angiotensin II treatment.

A to **C** basal echocardiography of 13 week old male mice. **D** to **F** echocardiography after three weeks of chronic 1.4 mg/kg/day angiotensin II infusion. All data are mean ± SEM, *p < 0.05, n=5 each group, LVPWd diastolic left ventricular posterior wall dimension, LVd left ventricular dimension at diastole

The same groups of animals were reanalyzed by echocardiography after three weeks of chronic AngII infusion via mini pumps (chapter 4.3.5). Due to the permanent infusion of the vasoconstrictor AngII PRCP+/+ mice developed left ventricular hypertrophy and the already existing mild hypertrophy of PRCP-/- hearts worsened seen by comparison of basal to AngII treated LVPWd/LVd ratios (Figure 19A and D). On the other hand there were no significant difference between AngII treated PRCP-/- and

control mice in LVPWd/LVd, fractional shortening or ejection fraction (Figure 19D, E and F).

4.3.7 Water Balance and Ion Homeostasis

One of the first organs in which PRCP was described to be present was the kidney [9]. As the local AngII in the kidney is involved in controlling ion homeostasis and water balance daily drinking volume as well as urinary output of mice singly housed in metabolic cages was monitored. This procedure revealed that PRCP-/- mice drink approximately 1mL more per day than controls (**Figure 20**A). Consequently urinary output of the knockout mice was slightly but not significantly increased (Figure 20B). The analysis of urine taken from these mice did not show changes in sodium, potassium or albumine concentration (Figure 20C to E).

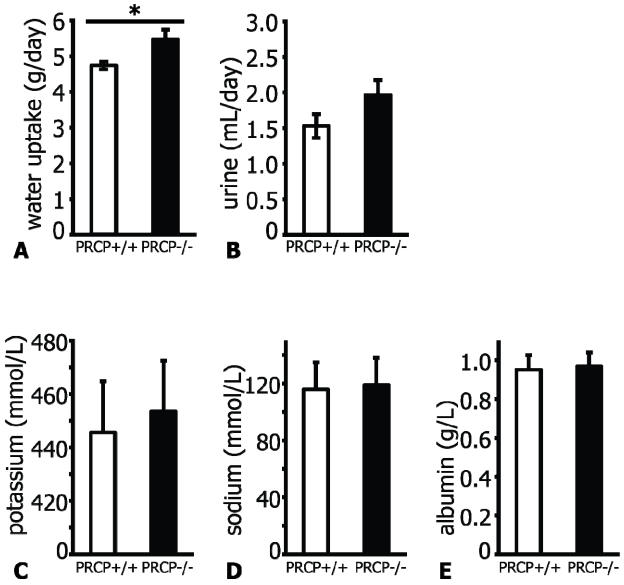

Figure 20: Water and ion homeostasis.

Daily water uptake **A** and urinary output **B** of single housed mice. Urinary potassium **C**, sodium **D** and albumin **E** levels (n=7 each group). All data are mean ± SEM, *p<0.05

5 DISCUSSION

The online database NCBI Pubmed counts 53 papers and reviews on PRCP. Thirty-three of them were published in the last decade indicating a rising interest in this enzyme and its possible substrates. The influence of PRCP on two of these peptides, αMSH and AngII, are in the focus of this study. The most powerful tool to analyse the involvement of the enzyme in the melanocortin system and in the RAS was the PRCP knockout mouse.

5.1 The Prolylcarboxypeptidase Knockout Mouse

The PRCP knockout mouse was generated using blastocyst microinjection of gene-trap ES cells and proven by RPA, showing that *prcp* mRNA was not present in tissues of PRCP-/- mice. To guarantee a pure genetic background, animals were first back-crossed for eight generations into two different background mouse strains creating two lines, PRCP_FVB/N (FVB/N) and PRCP_C57Bl/6 (C57Bl/6). While backcrossing the lines, the exact insertion site of the gene trap vector was identified and techniques to further analyze the knockout mouse were established.

Breeding mice homozygous for the *prcp* knockout allele, revealed that PRCP-/- mice are viable and show normal breeding performance. Even though PRCP has been described to be present in high concentrations in human placental microvilli and in vascular endothelial cells of the umbilical cord [3,17,20], litter size and birth rate of PRCP-/- mouse matings were in range of that of PRCP+/+. Therefore, the role of PRCP in these tissues cannot be essential, at least for mouse embryos. In contrast to these results, life expectancy of adult PRCP-/- mice presented a tendency to be reduced. Given that only a small number of animals could be included into this study, the Kaplan Meier survival analysis classified the tendency as insignificant ($p = 0.0578$). Nevertheless, a group of backcrossed PRCP_FVB/N mice showed the same trend of reduced life span in the knockout animals.

Looking at physical dimensions of the mice, no differences in terms of body length were detected. These data are in contrast to that published by Wallingford et al., who

described that PRCP knockout mice gained from KST302 (Baygenomics®) ES cells are significantly shorter than wild type controls [16]. This discrepancy is not explainable by background strains as for the study presented here, as well as in Wallingford et al. C57Bl/6 backcrossed mice were used. Whether or not the number of backcrosses into C57Bl/6 (Wallingford et al. 10x vs. 8x in the presented study) is able to produce such a difference is very speculative. On the other hand, the discovered body weight reduction of PRCP-/- is in accordance with Wallingford's findings as further discussed in chapter 5.2.

Expression of *prcp* in mouse tissues using qPCR was found in a variety of organs with highest expression in brain, white adipose tissue, kidney and heart. But to draw a final conclusion about expression levels in different tissues, qPCR seems not to be the optimal method. Besides being a powerful technique, qPCR suffers from certain pitfalls, with inappropriate data normalization as the most important problem (reviewed in de Jonge et al. [106], Dheda et al. [107], Pfaffl [98]). Due to this issue *actb*, showing highly different expression patterns when used in different tissues had to be excluded as a reference gene. *Tbp* turned out to be a better reference, even though expression in some tissue is still different. Therefore, the expression study remains incomplete concerning where in the wild type mo*use prcp* mRNA is produced the most, because organs with a different *tbp* C_t cannot be compared with each other. Thus, *prcp* expression was found in the heart and adrenal gland but their levels cannot put into relation to expression levels of other organs.

Therefore, western blot and immuno histostaining was used to clarify which organs contain highest or lowest PRCP protein concentrations. However, the commercially available antibodies T15 and Y15 were not able to produce a specific band in western blots under multiple conditions. Even though the manufacturer recommends antibodies for detecting mouse, rat and human PRCP, the original publication using these antibodies utilized only chromatographically purified proteins for western blot analysis [28]. Possibly, the purification process of the published protocol or the protein extraction procedure used in the presented study are changing the protein structure, enabling the antibodies to bind to chromatography purified PRCP but not to RIPA-buffer protein extracts. This may also explain why the immuno histostaining trials

utilizing the same antibodies were ineffective. Also X-Gal staining could not compensate for the missing tissue staining method, as endogenous *lacz* expression is present in most wild type tissues tested. Only the brain, with no detectable blue staining even after 48 hours X-Gal incubation was used to identify *prcp* promotor activity in particular brain structures.

X-Gal stainings of the brain led to a number of interesting discoveries. First of all, it confirmed qPCR expression analysis, showing that in all brain areas where qPCR mRNA was found, *prcp* promoter activity was also present. The highest qPCR expression was found in cortex, which is perfectly mirroring the intense blue staining of cortex in tissue slices. Then again, the clear staining of the hippocampus seems to be in contrast to qPCR data, which suggest a lower *prcp* expression than the house keeping gene *tbp*. Here, the difference in *tbp* C_t's, which is decreased in hippocampal compared to cortical samples, is probably masking a high *prcp* expression in hippocampus, demonstrating again that qPCR techniques are insufficient to perform organ screens.

Nevertheless, X-Gal staining finally provided a detailed overview about distinct nuclei with *prcp* promoter activity. For instance in so called circumventricular organs (CVO) like the SFO, SCO, AP and the ARC [108,109] *prcp* promotor activity was found. CVOs are small structures bordering the 3rd and 4th ventricle of the brain and lack a tight blood brain barrier. One of their unique characteristics is to connect the blood and cerebrospinal fluid by more loosely apposed glial cells. While the rest of the brain is normally covered by low-permeable capillaries these "windows of the brain" are believed to allow a crosstalk between peripheral blood born factors and ventricle fluid [109]. According to these findings the enzyme could be in an optimal position to function as a gatekeeper to control peptide availability to the brain. The diverse nuclei found, gave rise to theories in which mechanisms PRCP enzyme activity could be involved. One of them was the melanocortin system revealing its major actions in controlling food intake within the PVN and the ARC. In both areas *prcp* promotor activity was present. The second interesting system involved in central regulation of blood pressure is the brain RAS which was described to function via nervus vagus, NTS,

RVLM and nucleus ambiguus of the brain stem. Both systems are discussed in detail in the separate chapter 5.2 and 5.3.

5.2 Involvement of PRCP in the Melanocortin System

The idea to have a closer look at body weight and energy homoeostasis arose not only from the rising list of theoretically favourable substrates of PRCP which included candidates like αMSH, AGRP and GHRL. Also literature gave hints for an involvement of PRCP in obesity. In a study from McCarthy and colleagues a cohort of 305 patients with coronary heart disease, a population enriched in metabolic abnormalities, was surveyed for candidate genes that increase the risk of developing obesity. The authors described a SNP in the *prcp* gene that linked obesity only to male subjects of the cohort [110]. Just one year later another paper hypothesized multiple linked genes in a donor region on mouse chromosome 7 to be associated with obesity [111]. The genomic region described here includes the locus of the *prcp* gene, too.

Initially, the PRCP body weight phenotype was not obvious. Therefore a huge number of animals had to be analyzed, to find the basically reduced body weight in young mice. A HD aiming at challenging this phenotype finally confirmed that PRCP-/- mice significantly stay lean on a diet consisting of 45% fat. A body composition scan and individual weighing of distinct fat pads further supported the phenotype in revealing that PRCP-/- mice develop smaller fat depots than their wild type controls.

To understand the cause of the discovered body weight difference, activity as well as food and water intake was monitored. Established models of obesity in mice, like MC4R or MC3R knockout mice were reported to exhibit in addition to hyperphagia, also decreased locomotor activity [112,113,114,115]. However, activity of PRCP-/- was not changed compared to wild type controls neither in regard to time shifts of sleep and wakefulness phases nor in activity peaks, ruling out different activity levels to be responsible for the lean phenotype. Observation of single housed animals in metabolic cages revealed an increased water uptake of the knockouts, an interesting result that will be further discussed in chapter 5.3. But food intake was similar in wild type and knockout groups.

To find a mechanism explaining the involvement of PRCP in the maintenance of body weight the three potential substrates, GHRL, AGRP and αMSH were tested. Detecting

prcp expression in stomach and hypothalamus where synthesis and signalling of the candidate substrates is present, made an involvement of PRCP in the regulation of these hormones more likely. But neither ghrelin plasma contents, *ghrl* expression in stomach nor expression levels of *agrp* in PRCP-/- hypothalami were different from that found in wild type controls. On the other hand the up-regulation of *pomc* expression in knockout hypothalami was promising.

Focusing on *pomc*'s gene product αMSH, plasma contents of the hormone was analyzed. However, ELISA was not able to detect any differences in the circulating level of the peptide. But these results are not necessarily conclusive, as the methods base upon detecting αMSH with an antibody. The antibodies used here was not specific to the last carboxy-terminal amino acid of the peptide and cannot distinguish between the full length αMSH_{1-13} and its degradation product αMSH_{1-12}. Therefore, an imbalance between the two peptides is possibly masked.

Using X-Gal staining, prcp promotor activity was localized within the hypothalamus to the ARC and PVN. The ARC is located in the medio-basal hypothalamus and is thought to be a master player in the regulation of energy balance in adult mammals. The ARC is adjacent to the third ventricle, an area that is believed to lack the blood-brain barrier, thus placing it in an ideal location to be a putative brain sensor of humoral and metabolic factors originating in the periphery [116]. Because of its close proximity to the third ventricle, the ARC can also sense the levels of factors found in cerebrospinal fluid (CSF), which is the main pathway for the entrance of several peptides and hormones into the brain [31]. Other hormones entering the brain via CVOs need to be blocked or degraded to not disturb signaling of the same locally produced peptides in the brain. Thus, PRCP is in fact in the perfect location to degrade αMSH, originating in the periphery, in order to avoid an influence of blood αMSH on POMC neuron signaling in the PVN.

On the other hand, activated POMC neurons release αMSH to second order neurons within the PVN. Here the peptide exerts its strong anorexigenic function through binding to the melanocortin receptors MC3R and MC4R. Accordingly, POMC-/- [117] and MC4R-/- mice [118] develop obesity emphasising the importance of the melanocortin

system in the occurrence of obesity. Thus, looking at PRCP-/- mice the cleavage of the last carboxy-terminal amino acid valine from αMSH_{1-13} could change its receptor binding capability and therefore inactivate it. Consequently PRCP-/- mice stay lean. But the question left was, why is *pomc* expression up regulated in PRCP-/- mice while the inactivation of the peptide is impaired, therefore potentiating the action at its receptors?

The answer was found in the generally increased plasma leptin level of PRCP-/-. A high concentration of leptin is known to elevate *pomc* expression in hypothalamus and is leading in turn to a release of the gene product αMSH [33]. The increased leptin level in young PRCP-/- mice is surprising because at the same time these animals are lean and present smaller fat depots than their wild type controls. But a tendency of higher leptin levels was also found in nine-month old mice on SD as well as on HD indicating that leptin signalling in PRCP-/- might be impaired.

Similar to leptin, pancreatic β-cell derived insulin circulates at levels proportional to adiposity and signals the POMC and AGRP neurons in the ARC to regulate energy homoeostasis and satiety [119,120]. Furthermore, glucose metabolism was shown to alter serum leptin levels [121]. Therefore glucose and insulin levels were analysed.

General blood glucose levels as well as glucose tolerance and insulin sensitivity were found to be unaltered in young fasted mice, suggesting both parameters do not contribute to the elevated leptin level found in PRCP-/- mice. But insulin levels in old knockout animals seemed to be decreased. When PRCP-/- and wild type mice were fed a SD, insulin levels of knockout mice were found significantly decreased. These results mirrored the decreased body fat content as well as the low leptin level of PRCP-/- on SD. Insulin levels of aged PRCP-/- mice on HD tend to result in elevated insulin levels compared to SD fed mice, thereby reflecting the increased plasma leptin of this group.

On the other hand, insulin levels of aged wild type mice were increased independent of the diet and also independent of plasma leptin levels. The high plasma levels of insulin suggest that aged FVB/N mice developed insulin resistance. PRCP_FVB/N knockout mice on the contrary seemed to be protected against it. Interestingly,

αMSH has been shown to decrease insulin production in a pancreatic Langerhans cell line [122]. As PRCP was reported to be present on endothelial cell surfaces, regulating the activation cascade of prekallikrein and the cleavage of AngII (discussed in chapter 5.3), this localization enables the enzyme to cleave circulating αMSH. Certainly, the data presented here are not complete, but supposing PRCP responsible for αMSH degradation in hypothalamus, it can not be excluded that it degrades αMSH in the blood stream.

During the course of this study, in 2009 a paper by Wallingford and colleagues was published confirming most of the data gained here. The authors reported data from another PRCP knockout mouse line, which presented reduced body weight, reduced fat mass and up-regulated *pomc* expression in knockout hypothalami, as well as specific *prcp* expression in the ARC and the PVN [16]. They identified αMSH as a substrate of PRCP by mass spectrometry analysis showing that αMSH_{1-13} is degraded by recombinant PRCP, producing αMSH_{1-12}. Injections of αMSH_{1-12} intra peritoneal into wild type mice were shown to have no effect on food intake whereas the full length αMSH_{1-13} was able stimulate appetite.

On the contrary to results presented here, Wallingford et al. report a reduced body length and reduced food intake of PRCP-/- mice. The methods used to determine these parameters in this study were measurement of anal-nose-length and daily weighing of the food left in the cage. These methods are by nature error-prone and demand a higher number of animals per group. As only 7 to 11 mice per group were analyzed no difference was observed here.

Moreover, an antibody specific to the last carboxy-terminal amino acids of αMSH was able to show that αMSH_{1-13} is indeed increased in PRCP-/- hypothalami. Leptin and insulin levels have not been analysed by this group [16].

In summary the PRCP knockout mouse exhibited hyperleptinemia and increased hypothalamic expression of *pomc* resulting in a lean body weight phenotype even when fed a fat enriched diet. The carboxy-terminal structure of αMSH, which matches the PRCP cleavage characteristics, as well as the co-expression of *pomc* and *prcp* gene in hypothalamus makes αMSH a bona-fide substrate of the enzyme. Furthermore, leptin

levels in young mice were increased while insulin levels in aged mice were decreased in comparison to wild type controls. How PRCP participates in the regulation of leptin and insulin is not clear, yet. Given that *prcp* expression is high in brain and organs like WAT, peripheral as well as central actions of PRCP can be involved.

5.3 PRCP and the Renin Angiotensin System

The investigations focusing on a cardiovascular phenotype of PRCP knockout mice revealed that they are mildly hypertensive and react with a stronger blood pressure rise following acute AngII injection. These findings are likely due to the action of AngII. Since the discovery of PRCP in 1968 [1] AngII always belonged to the list of potential substrates of this enzyme. Localized at the surface of endothelial cells it was already described to activate circulating prekallikrein [28], but it would also be in ideal position to cleave AngII. The exact *in vivo* role of PRCP in degradation of plasma AngII is not clarified yet.

In the beginning of this study measurement of angiotensin peptides revealed that circulating levels of AngI, AngII and Ang1-7 were not different in mice lacking PRCP. In chapter 4.3.1 two individual measurements demonstrate that plasma and blood AngII in the knockout mice are unchanged compared to controls. These data question a major role of PRCP in the degradation of AngII in the blood stream.

On the other hand, bolus injection of AngII into PRCP-/- mice on C57Bl/6 background revealed that these animals are not able to adapt as fast as their wild type controls to the given stimulus. For more than 30 seconds PRCP-/- mice exhibited approximately 10 mmHg higher blood pressure than their wild type controls. But once the process of dropping the blood pressure to normal levels started, PRCP-/- already catch up with the wild type after 3 minutes reaching ~110 mmHg. The outcome of this experiment hint at a compensatory mechanism inactivating AngII in mice lacking PRCP. Furthermore, a study in hypertensive humans supports

Interestingly there is a difference between the two genetic background lines used, C57Bl/6 and FVB/N. While the PRCP_C57Bl/6 line is producing a significant difference in reaction to AngII stimulation, the response of knockout PRCP_FVB/N mice is not different compared to their wild type controls. A huge body of literature is available about background specific phenotypes of mice, including immune response to infections, wound healing, heart rate differences, glucose metabolism, development of

hypertension and thrombosis etc. [123,124,125,126,127,128,129]. The genetic causes underling these background differences are not clarified yet.

Further investigations of angiotensin peptides in selected organs uncovered that local peptide levels in kidney homogenates were changed. While AngII levels described a tendency to be decreased, Ang1-7 levels in kidney were more than 3-fold increased. One of the first descriptions of PRCP arose from monkey kidney studies [10] and also mice present *prcp* expression in kidney (chapter 4.1.4) suggesting a role of this enzyme in this tissue. But the peptide analysis revealed the opposite of what could be expected in PRCP-/- mice: instead of the substrate AngII, the degradation product Ang1-7 was found to be more than 3-fold increased in the absence of the enzyme.

These findings could be explained by the raised ACE2 enzymatic activity in PRCP-/- kidneys (chapter 4.3.2). Possibly, an increased ACE2 activity in kidney is clearing the excess AngII and therefore, is compensating the missing PRCP activity. Other RAS components like renin, NEP, AT1 and Mas did not turn out to be differentially expressed in knockout mice. Indeed, ACE2 is generally accepted to be the major enzyme responsible for cleavage of AngII to form Ang1-7 [78], making it a good candidate of compensating a possible AngII overload in PRCP-/- mice.

To check whether PRCP-/- mice under additional chronic AngII overload are affected differentially, telemetry transducers and mini pumps administering AngII constantly over three weeks, were inserted into the mice. This experiment revealed two new facts: First, blood pressure increased and heart rate decreased for knockout mice to the same level as in controls, showing that ACE2 hyperactivity may indeed be sufficient to compensate the lack of PRCP at least over the two weeks measured. Second, at basal level PRCP-/- mice are hypertensive. This finding is in accordance with a study linking a polymorphism in the human *prcp* gene with different responses of patients to an antihypertensive treatment [23].

The mild hypertension was further confirmed by echocardiography. The ratio of left ventricular posterior wall dimension and left ventricular diameter in diastole revealed a significant increase in the knockout group. At the same time ejection fraction and fractional shortening exhibited a trend to be elevated. These findings can be inter-

preted as mild hypertrophy of the heart in reaction to the chronically increased blood pressure seen in PRCP-/- mice.

The high expression of *prcp* in brains compared to other organs of the mouse finally provided a new possible explanation for the discovered hypertension: Disturbed central control of blood pressure. *Prcp* promotor activity visualized by X-Gal staining was present in the RVLM/CVLM area, nervus vagus, nucleus ambiguus and the NTS. These nuclei are known to be involved in cardiovascular regulation mechanisms, e.g. the baroreflex. When baroreceptors in vessels become stimulated the innervating vagus nerve transmits the signal to the NTS in the brain stem. The NTS confers the signal upon the CVLM which sends inhibitory fibers to the RVLM, thus inhibiting the RVLM and therefore inhibiting sympathetic nerve activity. The presence of *prcp* promotor activity in exactly these nuclei of the brain stem suggests an involvement of PRCP in processes controlled by these neuron populations, in particular since all of them express RAS components.

Furthermore, the SFO was suggested to transmit angiotensinergic input to the PVN [74,130,131,132,133]. The PVN is an essential hypothalamic nucleus not only by transmitting appetite and satiety signals, but also for the maintenance of cardiovascular parameters and the homeostasis of body fluids [74]. Intracerebroventricular injected, AngII is a potent stimulator of thirst [134]. Additionally, AT1 predominates in areas with established roles in control of body fluids including the SFO, NTS, PVN, supraoptic nucleus, AP and nucleus ambiguus [135,136,137,138]. The same list of brain nuclei showed *prcp* promoter activity, supporting the idea that the increased water uptake of PRCP-/- mice is mainly a central effect of lacking PRCP.

Interestingly AngII does not cross the normal blood-brain barrier [74] but the brain itself expresses all components of the RAS, creating a local RAS functioning independently of the peripheral RAS. Therefore, the role of central PRCP in degrading angiotensin peptides could be double sided, depending on its location. First, *prcp* promoter activity was found in CVOs like the SFO, SCO and AP. As explained in chapter 4.1 CVOs are structures that allow a limited contact of blood born factors with the cerebrospinal fluid. The SFO was already shown to transmit AngII signals to the PVN

[130,131,132,133]. According to this, PRCP in SFO and possibly in other CVOs, is in the right position to function as a kind of a gatekeeper to control AngII signaling within the SFO or modulate AngII amounts entering the brain.

A second regulatory role PRCP could play in brain areas producing local angiotensin peptides. Although, AngII is not fulfilling the classical criteria of a neurotransmitter, several publications hypothesize that AngII or one of its metabolites may function as one (reviewed in Grobe et al. [139], Ferguson et al. [74]). Therefore, the presence of PRCP in the synaptic cleft between defined neuron populations could be critical to control neurotransmitter availability in neuron signaling, like it was already suggested for the inactivation of αMSH by PRCP [16].

In summary, this study provides data supporting the theory of AngII being a major PRCP substrate. Although angiotensin peptide measurements in PRCP-/- mice did not reveal raised AngII levels, the mild hypertension, increased response to AngII bolus injection and increased drinking volume are indicating an involvement of AngII into the observed phenotypes. In parallel, compensatory mechanisms seem to be activated, shown by the elevation of kidney Ang1-7 levels as well as increased ACE2 activity. A contribution of the brain RAS is very likely, as centers of known brain RAS activity are also positive for *prcp* promotor activity.

In conclusion, the analysis of the PRCP knockout mouse model showed that this enzyme is involved in the control of metabolism and obesity by inactivating αMSH and in cardiovascular content by limiting the actions of AngII mainly in the brain.

REFERENCES

1 Yang, H. Y., Erdos, E. G. & Chiang, T. S. New enzymatic route for the inactivation of angiotensin. *Nature* **218**, 1224-1226 (1968).

2 Kakimoto, T., Oshima, G., Yeh, H. S. & Erdos, E. G. Purification of lysosomal prolycarboxypeptidase angiotensinase C. *Biochimica et biophysica acta* **302**, 178-182 (1973).

3 Tan, F., Morris, P. W., Skidgel, R. A. & Erdos, E. G. Sequencing and cloning of human prolylcarboxypeptidase (angiotensinase C). Similarity to both serine carboxypeptidase and prolylendopeptidase families. *Journal of Biological Chemistry* **268**, 16631-16638 (1993).

4 Mallela, J., Yang, J. & Shariat-Madar, Z. Prolylcarboxypeptidase: A cardioprotective enzyme. *The international journal of biochemistry & cell biology* (2008).

5 Cunningham, D. F. & O'Connor, B. Proline specific peptidases. *Biochimica et biophysica acta* **1343**, 160-186 (1997).

6 Fischer, G., Heins, J. & Barth, A. The conformation around the peptide bond between the P1- and P2-positions is important for catalytic activity of some proline-specific proteases. *Biochimica et biophysica acta* **742**, 452-462 (1983).

7 Yaron, A. & Naider, F. Proline-dependent structural and biological properties of peptides and proteins. *Critical reviews in biochemistry and molecular biology* **28**, 31-81 (1993).

8 Wilk, S. & Orlowski, M. Inhibition of rabbit brain prolyl endopeptidase by n-benzyloxycarbonyl-prolyl-prolinal, a transition state aldehyde inhibitor. *Journal of neurochemistry* **41**, 69-75 (1983).

9 Odya, C. E., Marinkovic, D. V., Hammon, K. J., Stewart, T. A. & Erdos, E. G. Purification and properties of prolylcarboxypeptidase (angiotensinase C) from human kidney. *Journal of Biological Chemistry* **253**, 5927-5931 (1978).

10 Skidgel, R. A. & Erdos, E. G. Cellular carboxypeptidases. *Immunological reviews* **161**, 129-141 (1998).

11 Soisson, S. M. *et al.* Structural definition and substrate specificity of the S28 protease family: the crystal structure of human prolylcarboxypeptidase. *BMC structural biology* **10**, 16 (2010).

12 Ollis, D. L. *et al.* The alpha/beta hydrolase fold. *Protein engineering* **5**, 197-211 (1992).

13 Kozarich, J. W. S28 peptidases: lessons from a seemingly 'dysfunctional' family of two. *BMC biology* **8**, 87 (2010).

14 Shariat-Madar, Z., Mahdi, F. & Schmaier, A. H. Assembly and activation of the plasma kallikrein/kinin system: a new interpretation. *International immunopharmacology* **2**, 1841-1849 (2002).

15 Schmaier, A. H. The kallikrein-kinin and the renin-angiotensin systems have a multilayered interaction. *American journal of physiology. Regulatory, integrative and comparative physiology* **285**, R1-13 (2003).

16 Wallingford, N. *et al.* Prolylcarboxypeptidase regulates food intake by inactivating alpha-MSH in rodents. *The Journal of clinical investigation* **119**, 2291-2303 (2009).

17 Skidgel, R. A., Wickstrom, E., Kumamoto, K. & Erdos, E. G. Rapid radioassay for prolylcarboxypeptidase (angiotensinase C). *Analytical biochemistry* **118**, 113-119 (1981).

18 Jackman, H. L. *et al.* Plasma membrane-bound and lysosomal peptidases in human alveolar macrophages. *American journal of respiratory cell and molecular biology* **13**, 196-204 (1995).

[19] Yang, H. Y., Erdos, E. G. & Levin, Y. A dipeptidyl carboxypeptidase that converts angiotensin I and inactivates bradykinin. *Biochimica et biophysica acta* **214**, 374-376 (1970).

[20] Kumamoto, K., Stewart, T. A., Johnson, A. R. & Erdos, E. G. Prolylcarboxypeptidase (angiotensinase C) in human lung and cultured cells. *Journal of Clinical Investigation* **67**, 210-215 (1981).

[21] Shariat-Madar, Z., Mahdi, F. & Schmaier, A. H. Recombinant prolylcarboxypeptidase activates plasma prekallikrein. *Blood* **103**, 4554-4561 (2004).

[22] Watson, B., Jr., Nowak, N. J., Myracle, A. D., Shows, T. B. & Warnock, D. G. The human angiotensinase C gene (HUMPCP) maps to 11q14 within 700 kb of D11S901: a candidate gene for essential hypertension. *Genomics* **44**, 365-367 (1997).

[23] Zhang, Y. *et al.* E112D polymorphism in the prolylcarboxypeptidase gene is associated with blood pressure response to benazepril in Chinese hypertensive patients. *Chinese medical journal* **122**, 2461-2465 (2009).

[24] Santos, R. A. *et al.* Angiotensin-(1-7) is an endogenous ligand for the G protein-coupled receptor Mas. *Proceedings of the National Academy of Sciences of the United States of America* **100**, 8258-8263 (2003).

[25] Silva, D. M. *et al.* Evidence for a new angiotensin-(1-7) receptor subtype in the aorta of Sprague-Dawley rats. *Peptides* **28**, 702-707 (2007).

[26] Ngo, M. L., Mahdi, F., Kolte, D. & Shariat-Madar, Z. Upregulation of prolylcarboxypeptidase (PRCP) in lipopolysaccharide (LPS) treated endothelium promotes inflammation. *Journal of inflammation (London, England)* **6**, 3 (2009).

[27] Palmeri, D., Zuo, F. R., Rosen, S. D. & Hemmerich, S. Differential gene expression profile of human tonsil high endothelial cells: implications for lymphocyte trafficking. *Journal of leukocyte biology* **75**, 910-927 (2004).

[28] Shariat-Madar, Z., Mahdi, F. & Schmaier, A. H. Identification and characterization of prolylcarboxypeptidase as an endothelial cell prekallikrein activator. *Journal of Biological Chemistry* **277**, 17962-17969 (2002).

[29] Pawluczyk, I. Z., Patel, S. R. & Harris, K. P. Pharmacological enhancement of the kallikrein-kinin system promotes anti-fibrotic responses in human mesangial cells. *Cell Physiol Biochem* **18**, 327-336 (2006).

[30] Hooley, E., McEwan, P. A. & Emsley, J. Molecular modeling of the prekallikrein structure provides insights into high-molecular-weight kininogen binding and zymogen activation. *J Thromb Haemost* **5**, 2461-2466 (2007).

[31] Dietrich, M. O. & Horvath, T. L. Feeding signals and brain circuitry. *The European journal of neuroscience* **30**, 1688-1696 (2009).

[32] Cowley, M. A. *et al.* Leptin activates anorexigenic POMC neurons through a neural network in the arcuate nucleus. *Nature* **411**, 480-484 (2001).

[33] Hakansson, M. L., Brown, H., Ghilardi, N., Skoda, R. C. & Meister, B. Leptin receptor immunoreactivity in chemically defined target neurons of the hypothalamus. *J Neurosci* **18**, 559-572 (1998).

[34] Ahima, R. S. & Osei, S. Y. Leptin signaling. *Physiology & behavior* **81**, 223-241 (2004).

[35] Ellacott, K. L. & Cone, R. D. The central melanocortin system and the integration of short- and long-term regulators of energy homeostasis. *Recent progress in hormone research* **59**, 395-408 (2004).

[36] Seeley, R. J. & Woods, S. C. Monitoring of stored and available fuel by the CNS: implications for obesity. *Nature reviews* **4**, 901-909 (2003).

[37] Chehab, F. F. The reproductive side of leptin. *Nature medicine* **3**, 952-953 (1997).

[38] Malendowicz, L. K., Rucinski, M., Belloni, A. S., Ziolkowska, A. & Nussdorfer, G. G. Leptin and the regulation of the hypothalamic-pituitary-adrenal axis. *International review of cytology* **263**, 63-102 (2007).

[39] Palou, M. *et al.* Induction of NPY/AgRP orexigenic peptide expression in rat hypothalamus is an early event in fasting: relationship with circulating leptin, insulin and glucose. *Cell Physiol Biochem* **23**, 115-124 (2009).

[40] Marti, A. *et al.* Leptin gene transfer into muscle increases lipolysis and oxygen consumption in white fat tissue in ob/ob mice. *Biochemical and biophysical research communications* **246**, 859-862 (1998).

[41] Snitker, S., Pratley, R. E., Nicolson, M., Tataranni, P. A. & Ravussin, E. Relationship between muscle sympathetic nerve activity and plasma leptin concentration. *Obesity research* **5**, 338-340 (1997).

[42] Gaja, A. *et al.* Bone marrow and peripheral blood leptin levels in lymphoproliferative diseases--relation to the bone marrow fat and infiltration. *Neoplasma* **47**, 307-312 (2000).

[43] Bouloumie, A., Drexler, H. C., Lafontan, M. & Busse, R. Leptin, the product of Ob gene, promotes angiogenesis. *Circulation research* **83**, 1059-1066 (1998).

[44] Sierra-Honigmann, M. R. *et al.* Biological action of leptin as an angiogenic factor. *Science (New York, N.Y* **281**, 1683-1686 (1998).

[45] Waelput, W., Brouckaert, P., Broekaert, D. & Tavernier, J. A role for leptin in the systemic inflammatory response syndrome (SIRS) and in immune response, an update. *Current medicinal chemistry* **13**, 465-475 (2006).

[46] Barsh, G. S. & Schwartz, M. W. Genetic approaches to studying energy balance: perception and integration. *Nat Rev Genet* **3**, 589-600 (2002).

[47] Wolff, G. L., Roberts, D. W. & Mountjoy, K. G. Physiological consequences of ectopic agouti gene expression: the yellow obese mouse syndrome. *Physiological genomics* **1**, 151-163 (1999).

[48] Ollmann, M. M. *et al.* Antagonism of central melanocortin receptors in vitro and in vivo by agouti-related protein. *Science (New York, N.Y* **278**, 135-138 (1997).

[49] Shutter, J. R. *et al.* Hypothalamic expression of ART, a novel gene related to agouti, is up-regulated in obese and diabetic mutant mice. *Genes & development* **11**, 593-602 (1997).

[50] Rosenfeld, R. D. *et al.* Biochemical, biophysical, and pharmacological characterization of bacterially expressed human agouti-related protein. *Biochemistry* **37**, 16041-16052 (1998).

[51] Shen, C. P. *et al.* Plasma agouti-related protein level: a possible correlation with fasted and fed states in humans and rats. *Journal of neuroendocrinology* **14**, 607-610 (2002).

[52] Hoggard, N. *et al.* Plasma concentrations of alpha-MSH, AgRP and leptin in lean and obese men and their relationship to differing states of energy balance perturbation. *Clinical endocrinology* **61**, 31-39 (2004).

[53] Li, J. Y. *et al.* Agouti-related protein-like immunoreactivity: characterization of release from hypothalamic tissue and presence in serum. *Endocrinology* **141**, 1942-1950 (2000).

[54] Wilson, B. D. *et al.* Physiological and anatomical circuitry between Agouti-related protein and leptin signaling. *Endocrinology* **140**, 2387-2397 (1999).

[55] Bicknell, A. B., Lomthaisong, K., Gladwell, R. T. & Lowry, P. J. Agouti related protein in the rat adrenal cortex: implications for novel autocrine mechanisms modulating the actions of pro-opiomelanocortin peptides. *Journal of neuroendocrinology* **12**, 977-982 (2000).

[56] Hoggard, N. *et al.* Localization of leptin receptor mRNA splice variants in murine peripheral tissues by RT-PCR and in situ hybridization. *Biochemical and biophysical research communications* **232**, 383-387 (1997).

[57] Kastin, A. J., Akerstrom, V. & Hackler, L. Agouti-related protein(83-132) aggregates and crosses the blood-brain barrier slowly. *Metabolism: clinical and experimental* **49**, 1444-1448 (2000).

[58] Coll, A. P., Farooqi, I. S., Challis, B. G., Yeo, G. S. & O'Rahilly, S. Proopiomelanocortin and energy balance: insights from human and murine genetics. *The Journal of clinical endocrinology and metabolism* **89**, 2557-2562 (2004).

[59] Hinney, A. *et al.* Prevalence, spectrum, and functional characterization of melanocortin-4 receptor gene mutations in a representative population-based sample and obese adults from Germany. *The Journal of clinical endocrinology and metabolism* **91**, 1761-1769 (2006).

[60] Larsen, L. H. *et al.* Prevalence of mutations and functional analyses of melanocortin 4 receptor variants identified among 750 men with juvenile-onset obesity. *The Journal of clinical endocrinology and metabolism* **90**, 219-224 (2005).

[61] Balthasar, N. *et al.* Divergence of melanocortin pathways in the control of food intake and energy expenditure. *Cell* **123**, 493-505 (2005).

[62] Inagami, T. The renin-angiotensin system. *Essays in biochemistry* **28**, 147-164 (1994).

[63] Guyton, A. C. & Hall, J. E. in *Textbook of Medical Physiology* (Elsevier Inc., 2006).

[64] Iwai, N. *et al.* Differential regulation of rat AT1a and AT1b receptor mRNA. *Biochemical and biophysical research communications* **188**, 298-303 (1992).

[65] Konishi, H., Kuroda, S., Inada, Y. & Fujisawa, Y. Novel subtype of human angiotensin II type 1 receptor: cDNA cloning and expression. *Biochemical and biophysical research communications* **199**, 467-474 (1994).

[66] Sasamura, H. *et al.* Cloning, characterization, and expression of two angiotensin receptor (AT-1) isoforms from the mouse genome. *Biochemical and biophysical research communications* **185**, 253-259 (1992).

[67] Burson, J. M., Aguilera, G., Gross, K. W. & Sigmund, C. D. Differential expression of angiotensin receptor 1A and 1B in mouse. *The American journal of physiology* **267**, E260-267 (1994).

[68] de Gasparo, M., Catt, K. J., Inagami, T., Wright, J. W. & Unger, T. International union of pharmacology. XXIII. The angiotensin II receptors. *Pharmacological reviews* **52**, 415-472 (2000).

[69] Touyz, R. M. The role of angiotensin II in regulating vascular structural and functional changes in hypertension. *Current hypertension reports* **5**, 155-164 (2003).

[70] Yayama, K. & Okamoto, H. Angiotensin II-induced vasodilation via type 2 receptor: role of bradykinin and nitric oxide. *Int Immunopharmacol* **8**, 312-318 (2008).

[71] Fyhrquist, F. & Saijonmaa, O. Renin-angiotensin system revisited. *Journal of internal medicine* **264**, 224-236 (2008).

[72] Kumar, R., Singh, V. P. & Baker, K. M. The intracellular renin-angiotensin system: a new paradigm. *Trends in endocrinology and metabolism: TEM* **18**, 208-214 (2007).

[73] Stock, P., Liefeldt, L., Paul, M. & Ganten, D. Local renin-angiotensin systems in cardiovascular tissues: localization and functional role. *Cardiology* **86 Suppl 1**, 2-8 (1995).

[74] Ferguson, A. V., Washburn, D. L. & Latchford, K. J. Hormonal and neurotransmitter roles for angiotensin in the regulation of central autonomic function. *Experimental biology and medicine (Maywood, N.J* **226**, 85-96 (2001).

[75] Carey, R. M. & Siragy, H. M. Newly recognized components of the renin-angiotensin system: potential roles in cardiovascular and renal regulation. *Endocrine reviews* **24**, 261-271 (2003).

[76] Albiston, A. L. *et al.* Evidence that the angiotensin IV (AT(4)) receptor is the enzyme insulin-regulated aminopeptidase. *The Journal of biological chemistry* **276**, 48623-48626 (2001).

[77] Keller, S. R., Scott, H. M., Mastick, C. C., Aebersold, R. & Lienhard, G. E. Cloning and characterization of a novel insulin-regulated membrane aminopeptidase from Glut4 vesicles. *The Journal of biological chemistry* **270**, 23612-23618 (1995).

[78] Rentzsch, B. *et al.* Transgenic angiotensin-converting enzyme 2 overexpression in vessels of SHRSP rats reduces blood pressure and improves endothelial function. *Hypertension* **52**, 967-973 (2008).

[79] Ferrario, C. M., Chappell, M. C., Tallant, E. A., Brosnihan, K. B. & Diz, D. I. Counterregulatory actions of angiotensin-(1-7). *Hypertension* **30**, 535-541 (1997).

[80] Stegbauer, J., Vonend, O., Oberhauser, V. & Rump, L. C. Effects of angiotensin-(1-7) and other bioactive components of the renin-angiotensin system on vascular resistance and noradrenaline release in rat kidney. *Journal of hypertension* **21**, 1391-1399 (2003).

[81] Tallant, E. A. & Clark, M. A. Molecular mechanisms of inhibition of vascular growth by angiotensin-(1-7). *Hypertension* **42**, 574-579 (2003).

[82] Santos, R. A., Brosnihan, K. B., Jacobsen, D. W., DiCorleto, P. E. & Ferrario, C. M. Production of angiotensin-(1-7) by human vascular endothelium. *Hypertension* **19**, II56-61 (1992).

[83] Yamamoto, K., Chappell, M. C., Brosnihan, K. B. & Ferrario, C. M. In vivo metabolism of angiotensin I by neutral endopeptidase (EC 3.4.24.11) in spontaneously hypertensive rats. *Hypertension* **19**, 692-696 (1992).

[84] Zini, S. *et al.* Identification of metabolic pathways of brain angiotensin II and III using specific aminopeptidase inhibitors: predominant role of angiotensin III in the control of vasopressin release. *Proceedings of the National Academy of Sciences of the United States of America* **93**, 11968-11973 (1996).

[85] Gammelgaard, I., Wamberg, S. & Bie, P. Systemic effects of angiotensin III in conscious dogs during acute double blockade of the renin-angiotensin-aldosterone-system. *Acta physiologica (Oxford, England)* **188**, 129-138 (2006).

[86] Sambrook, J. & Russell, D. W. *Molecular Cloning*. 3 edn, (Cold Spring Harbor Labaratory Press, 2001).

[87] Livak, K. J. & Schmittgen, T. D. Analysis of relative gene expression data using real-time quantitative PCR and the 2(-Delta Delta C(T)) Method. *Methods (San Diego, Calif* **25**, 402-408 (2001).

[88] Bradford, M. M. A rapid and sensitive method for the quantitation of microgram quantities of protein utilizing the principle of protein-dye binding. *Analytical biochemistry* **72**, 248-254 (1976).

[89] Velloso, E. P., Vieira, R., Cabral, A. C., Kalapothakis, E. & Santos, R. A. Reduced plasma levels of angiotensin-(1-7) and renin activity in preeclamptic patients are associated with the angiotensin I- converting enzyme deletion/deletion genotype. *Brazilian journal of medical and*

biological research = Revista brasileira de pesquisas medicas e biologicas / Sociedade Brasileira de Biofisica ... [et al **40**, 583-590 (2007).

90 Neves, L. A. *et al.* Pregnancy enhances the angiotensin (Ang)-(1-7) vasodilator response in mesenteric arteries and increases the renal concentration and urinary excretion of Ang-(1-7). *Endocrinology* **144**, 3338-3343 (2003).

91 Chappell, M. C., Brosnihan, K. B., Diz, D. I. & Ferrario, C. M. Identification of angiotensin-(1-7) in rat brain. Evidence for differential processing of angiotensin peptides. *The Journal of biological chemistry* **264**, 16518-16523 (1989).

92 Gembardt, F. *et al.* Organ-specific distribution of ACE2 mRNA and correlating peptidase activity in rodents. *Peptides* **26**, 1270-1277 (2005).

93 Winkler, A. *et al.* Gene expression and activity of specific opioid-degrading enzymes in different brain regions of the AA and ANA lines of rats. *Biochimica et biophysica acta* **1406**, 219-227 (1998).

94 Royer, A. *et al.* Mouse model of SCN5A-linked hereditary Lenegre's disease: age-related conduction slowing and myocardial fibrosis. *Circulation* **111**, 1738-1746 (2005).

95 Jankowski, V. *et al.* Mass-spectrometric identification of a novel angiotensin peptide in human plasma. *Arteriosclerosis, thrombosis, and vascular biology* **27**, 297-302 (2007).

96 Gross, V. *et al.* Autonomic nervous system and blood pressure regulation in RGS2-deficient mice. *American journal of physiology* **288**, R1134-1142 (2005).

97 Suzawa, Y., Hiraoka, B. Y., Harada, M. & Deguchi, T. High-performance liquid chromatographic determination of prolylcarboxypeptidase activity in monkey kidney. *Journal of chromatography* **670**, 152-156 (1995).

98 Pfaffl, M. W. in *A-Z of quantification PCR* Vol. no. 5 (ed S. A. Bustian) Ch. 3, 1-23 (International University Line, 2004).

99 Hoggard, N., Hunter, L., Duncan, J. S. & Rayner, D. V. Regulation of adipose tissue leptin secretion by alpha-melanocyte-stimulating hormone and agouti-related protein: further evidence of an interaction between leptin and the melanocortin signalling system. *Journal of molecular endocrinology* **32**, 145-153 (2004).

100 Catania, A., Airaghi, L., Colombo, G. & Lipton, J. M. Alpha-melanocyte-stimulating hormone in normal human physiology and disease states. *Trends in endocrinology and metabolism: TEM* **11**, 304-308 (2000).

101 Fioramonti, X. *et al.* Characterization of glucosensing neuron subpopulations in the arcuate nucleus: integration in neuropeptide Y and pro-opio melanocortin networks? *Diabetes* **56**, 1219-1227 (2007).

102 Ibrahim, N. *et al.* Hypothalamic proopiomelanocortin neurons are glucose responsive and express K(ATP) channels. *Endocrinology* **144**, 1331-1340 (2003).

103 Parton, L. E. *et al.* Glucose sensing by POMC neurons regulates glucose homeostasis and is impaired in obesity. *Nature* **449**, 228-232 (2007).

104 Wang, R. *et al.* The regulation of glucose-excited neurons in the hypothalamic arcuate nucleus by glucose and feeding-relevant peptides. *Diabetes* **53**, 1959-1965 (2004).

105 Ste Marie, L., Miura, G. I., Marsh, D. J., Yagaloff, K. & Palmiter, R. D. A metabolic defect promotes obesity in mice lacking melanocortin-4 receptors. *Proceedings of the National Academy of Sciences of the United States of America* **97**, 12339-12344 (2000).

106 de Jonge, H. J. *et al.* Evidence based selection of housekeeping genes. *PloS one* **2**, e898 (2007).

[107] Dheda, K. *et al.* The implications of using an inappropriate reference gene for real-time reverse transcription PCR data normalization. *Analytical biochemistry* **344**, 141-143 (2005).

[108] Ciofi, P. The arcuate nucleus as a circumventricular organ in the mouse. *Neuroscience letters* **487**, 187-190.

[109] Johnson, A. K. & Gross, P. M. Sensory circumventricular organs and brain homeostatic pathways. *Faseb J* **7**, 678-686 (1993).

[110] McCarthy, J. J. *et al.* Evidence for substantial effect modification by gender in a large-scale genetic association study of the metabolic syndrome among coronary heart disease patients. *Hum. Genet.* **114**, 87-98 (2003).

[111] Diament, A. L. & Warden, C. H. Multiple linked mouse chromosome 7 loci influence body fat mass. *Int. J. Obes. Relat. Metab. Disord.* **28**, 199-210 (2004).

[112] Butler, A. A. *et al.* A unique metabolic syndrome causes obesity in the melanocortin-3 receptor-deficient mouse. *Endocrinology* **141**, 3518-3521 (2000).

[113] Chen, A. S. *et al.* Inactivation of the mouse melanocortin-3 receptor results in increased fat mass and reduced lean body mass. *Nature genetics* **26**, 97-102 (2000).

[114] Elmquist, J. K. Hypothalamic pathways underlying the endocrine, autonomic, and behavioral effects of leptin. *Int J Obes Relat Metab Disord* **25 Suppl 5**, S78-82 (2001).

[115] Williams, D. L., Bowers, R. R., Bartness, T. J., Kaplan, J. M. & Grill, H. J. Brainstem melanocortin 3/4 receptor stimulation increases uncoupling protein gene expression in brown fat. *Endocrinology* **144**, 4692-4697 (2003).

[116] Norsted, E., Gomuc, B. & Meister, B. Protein components of the blood-brain barrier (BBB) in the mediobasal hypothalamus. *Journal of chemical neuroanatomy* **36**, 107-121 (2008).

[117] Yaswen, L., Diehl, N., Brennan, M. B. & Hochgeschwender, U. Obesity in the mouse model of pro-opiomelanocortin deficiency responds to peripheral melanocortin. *Nature medicine* **5**, 1066-1070 (1999).

[118] Huszar, D. *et al.* Targeted disruption of the melanocortin-4 receptor results in obesity in mice. *Cell* **88**, 131-141 (1997).

[119] Leibowitz, S. F. & Wortley, K. E. Hypothalamic control of energy balance: different peptides, different functions. *Peptides* **25**, 473-504 (2004).

[120] Riedy, C. A., Chavez, M., Figlewicz, D. P. & Woods, S. C. Central insulin enhances sensitivity to cholecystokinin. *Physiology & behavior* **58**, 755-760 (1995).

[121] Wellhoener, P. *et al.* Glucose metabolism rather than insulin is a main determinant of leptin secretion in humans. *The Journal of clinical endocrinology and metabolism* **85**, 1267-1271 (2000).

[122] Shimizu, H., Tanaka, Y., Sato, N. & Mori, M. Alpha-melanocyte-stimulating hormone (MSH) inhibits insulin secretion in HIT-T 15 cells. *Peptides* **16**, 605-608 (1995).

[123] Berglund, E. D. *et al.* Glucose metabolism in vivo in four commonly used inbred mouse strains. *Diabetes* **57**, 1790-1799 (2008).

[124] Campen, M. J., Tagaito, Y., Jenkins, T. P., Balbir, A. & O'Donnell, C. P. Heart rate variability responses to hypoxic and hypercapnic exposures in different mouse strains. *J Appl Physiol* **99**, 807-813 (2005).

[125] Hartner, A., Cordasic, N., Klanke, B., Veelken, R. & Hilgers, K. F. Strain differences in the development of hypertension and glomerular lesions induced by deoxycorticosterone acetate salt in mice. *Nephrol Dial Transplant* **18**, 1999-2004 (2003).

126 Hoover-Plow, J. L. *et al.* Strain and model dependent differences in inflammatory cell recruitment in mice. *Inflamm Res* **57**, 457-463 (2008).

127 Ma, L. J. & Fogo, A. B. Model of robust induction of glomerulosclerosis in mice: importance of genetic background. *Kidney international* **64**, 350-355 (2003).

128 Ryan, M. J., Didion, S. P., Davis, D. R., Faraci, F. M. & Sigmund, C. D. Endothelial dysfunction and blood pressure variability in selected inbred mouse strains. *Arteriosclerosis, thrombosis, and vascular biology* **22**, 42-48 (2002).

129 van den Borne, S. W. *et al.* Mouse strain determines the outcome of wound healing after myocardial infarction. *Cardiovascular research* **84**, 273-282 (2009).

130 Bains, J. S. & Ferguson, A. V. Paraventricular nucleus neurons projecting to the spinal cord receive excitatory input from the subfornical organ. *The American journal of physiology* **268**, R625-633 (1995).

131 Harding, J. W. *et al.* Release of angiotensins in paraventricular nucleus of rat in response to physiological and chemical stimuli. *The American journal of physiology* **262**, F17-23 (1992).

132 Li, Z. & Ferguson, A. V. Angiotensin II responsiveness of rat paraventricular and subfornical organ neurons in vitro. *Neuroscience* **55**, 197-207 (1993).

133 Tanaka, J., Kaba, H., Saito, H. & Seto, K. Electrophysiological evidence that circulating angiotensin II sensitive neurons in the subfornical organ alter the activity of hypothalamic paraventricular neurohypophyseal neurons in the rat. *Brain research* **342**, 361-365 (1985).

134 Crews, E. C. & Rowland, N. E. Role of angiotensin in body fluid homeostasis of mice: effect of losartan on water and NaCl intakes. *American journal of physiology* **288**, R638-644 (2005).

135 Aldred, G. P. *et al.* Distribution of angiotensin II receptor subtypes in the rabbit brain. *Regulatory peptides* **44**, 119-130 (1993).

136 Gehlert, D. R., Gackenheimer, S. L. & Schober, D. A. Autoradiographic localization of subtypes of angiotensin II antagonist binding in the rat brain. *Neuroscience* **44**, 501-514 (1991).

137 Phillips, M. I., Shen, L., Richards, E. M. & Raizada, M. K. Immunohistochemical mapping of angiotensin AT1 receptors in the brain. *Regulatory peptides* **44**, 95-107 (1993).

138 Song, K., Allen, A. M., Paxinos, G. & Mendelsohn, F. A. Mapping of angiotensin II receptor subtype heterogeneity in rat brain. *The Journal of comparative neurology* **316**, 467-484 (1992).

139 Grobe, J. L., Xu, D. & Sigmund, C. D. An intracellular renin-angiotensin system in neurons: fact, hypothesis, or fantasy. *Physiology (Bethesda, Md* **23**, 187-193 (2008).

ABBREVIATIONS

ACE /ACE2	angiotensine converting enzyme / -2
ACTH	adrenocorticotropic hormone
AGRP	agouti related peptide
AGT	angiotensinogen
Ang I / II / III / IV / 1-7	angiotensin I / II / III / IV / 1-7
αMSH	α melanocortin stimulating hormone
ARC	arcuate nucleus
AT1 / AT2	angiotensin receptor I / -II
AP	area postrema
Arg	arginin
bp / kbp	base pare / kilo base pare
BK	bradykinin
BSA	bovine serum albumin
CSF	cerebrospinal fluid
CVLM	caudal ventrolateral medulla
CVO	circumventricular organ
DALEK	(D-Ala2,Leu5)-enkephalin (NEP substrate)
DEPC	diethylpyrocarbonat
DMSO	dimethyl sulfoxide
DNA / cDNA	desoxyribonuclein acid / copy DNA
DNase	deoxyribonuclease
dNTP	deoxynucleotide triphosphate
ELISA	enzyme linked immunosorbend assay
ES cells	embryonic stem cells
GHRL	ghrelin (growth hormone release inducing)
HD	high fat diet
HPLC	high-performance liquid chromatography
HR	heart rate
HUVEC	human umbilical vein endothelial cells
KKS	kallikrein kinin system
LPS	lipopolysaccharide
MAP	mean arterial pressure
MAPK	Mca-APK(Dnp) (ACE2 substrate)
MCR3 / MCR4	melanocortin receptor 3 / 4
NEP	neutral endopeptidase
NO	nitric oxide
NPY	neuropeptide Y
NTS	nucleus tractus solitarius
PCR	polymerase chain reaction
Phe	phenylalanine
POMC	proopiomelanocortin
PRCP	prolylcarboxypeptidase
PRCP-/-	PRCP knockout mouse
PRCP+/+	PRCP wild type mouse
Pro	prolin
PVN	paraventricular nucleus
qPCR	quantitative realtime PCR
RAS	renin angiotensin system
RPA	ribonuclease protection assay
RT-PCR	reverse transcription PCR
RVLM	rostral ventrolateral medulla

SCO	subcommissural organ
SD	standard diet
SFO	subfornical organ
WAT	white adipose tissue

PUBLICATIONS

PUBLIKATIONEN

O. Martinez, I. Schadock, M. Gossmann, S. von Bargen, C. Buttner (2006) Investigation of pathogenity of different Fusarium spp. isolates originating form asparagus (Asparagus officinalis L.) and characterisation of fumonisin-genes from F. proliferatum. Mitteilungen – Biologische Bundesanstalt für Land- und Forstwirtschaft ISSU 400, pages 110

S. von Bargen, O. Martinez, I. Schadock, AM. Eisold, M. Gossmann and C. Buettner (2009) Genetic Variability of Phytopathogenic Fusarium proliferatum Associated with Crown Rot in Asparagus officinalis. J Phytopathol 157: 446–456

U. Schulze-Topphoff, A. Prat, T. Prozorovski, V. Siffrin, F. Schröter, I. Schadock, MA. Mori, I. Ifergan, I. Bendix, J. van Horssen, J. Herz, M. Bader, L. Steinman, O. Aktas & F. Zipp (2008) Activation of kinin receptor B1 limits encephalitogenic T lymphocyte recruitment to the brain. Nat Med. 2009 Jul; 15(7): 788-93

KONGRESSBEITRÄGE

I. Schadock, M. Todiras, L. Vilianovich, RAS. Santos, M. Bader (2009) Prolylcarboxypeptidase deficiency does not influence antiotensin II levels in vivo. XVII Congresso Brasileiro de Hipertensão / IASH Bello Horizonte - Poster

I. Schadock, F. Qadri, M. Todiras, L. Vilianovich, M. Bader (2010) Resistance to high-fat diet induced obesity in mice deficient for prolylcarboxypeptidase (angiotensinase C). 51. annual conference of the DGPT (German Association for experimental and clinical Pharmacology and Toxicology) Mainz - Poster

I. Schadock, M. Todiras, L. Vilianovich, F. Qadri, A. Heuser, M. Bader (2010) Prolylcarboxypeptidase deficient mice reveal its multiple functions. 15th Meeting of the European Council for Cardiovascular Research (ECCR), Nice (France) – Poster presentation price

I. Schadock, M. Todiras, L. Vilianovich, F. Qadri, A. Heuser, RAS. Santos, M. Bader (2009) Warum werden Mäuse ohne Prolylcarboxypeptidase (Angiotensinase C) nicht dick? DIB – Meeting 2009 (Deutsches Institut für Bluthochdruckforschung) Würzburg - Vortrag

I. Schadock, M. Todiras, L. Vilianovich, F. Qadri, A. Heuser, RAS. Santos, M. Bader (2010) A new possible role of prolylcarboxypeptidase in cleaving angiotensin II. HYPERTONY 34. Wissenschaftlicher Kongress der Deutsche Hypertonie Gesellschaft, Berlin - Vortrag

ERKLÄRUNG

Ich versichere hiermit, die vorliegende Arbeit mit dem Titel „Physiological Role of Prolylcarboxypeptidase" selbständig verfasst und nur die angegebenen Hilfsmittel und Hilfen in Anspruch genommen zu haben. Abbildungen, die anderen Quellen unverändert entnommen oder diesen entlehnt wurden, sind mit der Quellenangabe gekennzeichnet.

Ich versichere, dass ich mich nicht anderweitig um einen entsprechenden Doktorgrad beworben habe.

Die Promotionsordnung der Mathematisch-Naturwissenschaftlichen Fakultät I der Humboldt-Universität zu Berlin habe ich gelesen und akzeptiert.

Ines Claudia Schadock